Fakultät für Maschinenwesen

Name der promotionsführenden Einrichtung

Bio-Kinematic Design of Individualized Lift-Assist Chairs for the Support of Sit-to-Stand Movement

Titel der wissenschaftlichen Abhandlung

Samuel Mogens Friedrich Reimer

Vorname und Name

Vollständiger Abdruck der von der promotionsführenden Einrichtung
Fakultät für Maschinenwesen
der Technischen Universität München zur Erlangung des akademischen Grades
eines Doktor-Ingenieur (Dr.-Ing.)
genehmigten Dissertation.

Vorsitzende/-r: Prof. dr. ir. Daniel J. Rixen

Prüfende/-r der Dissertation:

1. Prof. Dr. rer. nat. Tim C. Lüth

2. Prof. Dr. phil. Klaus Bengler

Die Dissertation wurde am 08.12.2016 bei der technischen Universität München
eingereicht und durch die promotionsführende Einrichtung
Fakultät für Maschinenwesen am 07.07.2017 angenommen.

"*If I have seen further it is by standing on the shoulders of giants*"

Sir Isaac Newton

Abstract

Rising from a chair is a fundamental movement in daily life and a prerequisite for independent functional ability. Yet, it remains one of the most biomechanically demanding activities as it requires high levels of neuromuscular coordination, muscle strength and postural control. While standing up from a seated position is often implied to be a ubiquitous skill it becomes increasingly difficult with age. To prolong the independence of elderly a novel computational design procedure for lift-assist mechanisms is presented. This procedure individualizes the dimensions of a mechanism to the natural sit-to-stand movement of the patient while complying with the limited space given by the applicable furniture. Given marker-based sit-to-stand motion data task positions are defined to carry out a finite position synthesis of a four-bar linkage that provides patient-specific guidance of a seat. The four-bar linkage combined with the lower limb of a patient generates a biologically inspired six-bar linkage. Thus, accomplishing a bio-kinematic design of linkages where this thesis provides an exemplary design session.

Acknowledgments

While my name may be alone on the front cover of this thesis, I am by no means its sole contributor. Rather, there are a great many people behind this piece of work who deserve to be both acknowledged and thanked here: kind participants, committed colleagues, encouraging supervisors; supportive friends, inspiring grandparents, patient parents and heartwarming siblings.

I would like to express the deepest appreciation to my committed doctoral thesis supervisor, Professor Tim Lüth for his enthusiasm, guidance, overwhelming generosity to participate at international conferences and research facilities all around the world and unrelenting support throughout this process. Additionally, I would like to thank Professor Klaus Bengler and Professor Daniel Rixen for their candidness to partake in the supervision of my thesis; to the *Alfried Krupp von Bohlen und Halbach Foundation* for their generous financial support of my research and to Dr.-Ing. Kassim Abdul-Sater who introduced me to the exciting field of mechanisms and kinematics and whose enthusiasm for the 'geometric design of individualized linkages' had a lasting effect. He continually and convincingly conveyed a spirit of adventure in regard to research and scholarship, and an unrelenting excitement in regard to teaching. Without his guidance and persistent help this dissertation would not have been possible.

With deepest gratitude and appreciation, I humbly give thanks to all my colleagues, especially Konrad Entsfellner, Christina Hein and Joachim Kreutzer, who have routinely gone beyond their duties to support, debate and excel my research; to our secretary Renate Heuser and academic supervisor Dr.-Ing. Irlinger; to my determined and eager students Wiebke Pfeiffer, Maximilian Binder, Jonas Joachimmeyer, Carolin Stöckl, Kyra Kleine, Thao Nguyen and Corinna Eder with whom I have enjoyed working with so much; to Michael Pfitzer and Dr. Stefan Arend as well as the staff of the nursing home *KWA Luise-Kiesselbach-Haus* for their willingness to share and discuss their personal work life, their participation during numerous studies and their openness to share valuable insights during my clinical internship.

My heartfelt appreciation also extends to my colleagues abroad; to Go Nakamura, Dr.-Ing. Yuichiro Honda and Takaki Chin MD, PhD at the *Hyogo Rehabilitation Center* in Japan. Our cooperation and mutual encouragement has been especially valuable which extends to the greater foundation of this work.

On a more personal note I am forever indebted to my beloved parents, Donate and Morten Reimer for being the very foundation of what I have achieved and of who I am today; whose unprecedented support, love, patience and unremitting encouragement have carried me through the most challenging of times; to my gifted brother Leon and heartwarming sister Josephine who have always served as an inspiration to me, who keep on encouraging and believing in me and above all else whose company I will always enjoy and cherish.

I extend my special thanks to Dominik Baus, Lars Bergemann and Cornelius Holthöfer for such long-lasting and enduring friendships who have stayed in touch beyond great distances, who have fire fought my worries, concerns, anxieties and have worked to instill great confidence in both myself and my work.

Finally, but by no means least, this work is for my inspiring grandparents Ulla Lenz and Hans Reimer and in loving memory to Helga and Hermann Fischer-Hübner as well as to Siegfried Lenz who have paved the path before me and upon whose shoulders I stand.

This Dissertation is the culmination of a life-long passion for the natural sciences, medicine and engineering and has turned into as much a labor of love as a scientific contribution. I dedicate this piece of work to my grandfather Hans Reimer who as a great engineer himself has been an advocate of my academic and personal endeavors. He has been and still is the very inspiration of this decade long journey and of what I have become today. You are the very determination in every page.

Hamburg, December 2016

Samuel M. F. Reimer

Contents

List of Figures

List of Tables

Dedicated to my beloved Grandfather
Dr.-Ing. Hans Reimer

1. Introduction

To stand up from a chair is a prerequisite to carry out and sustain an independent life, to socialize with other people and to perform so-called ADL (activities of daily living). Not surprisingly, therefore, is the fact that many elderly have difficulties to partake in society due to natural age-related changes to the musculoskeletal system that impedes natural STS movement. The loss of independent STS movement leads to a mobility disorder which is the most common diagnosis leading to long-term care dependency in Germany. To rehabilitate and to maintain natural STS movement as well as to assist nursing professionals during patient transfers from a chair, this dissertation, a lift-assist mechanism integrated into a chair (LAD (lift-assist device)) is presented that is individualized to the biomechanics of the user. The individualization process aims to reduce the physical strain required to lift oneself at the very beginning of the stand-up process.

This thesis merges two research areas to produce user-specific LAD in order to allow a naturally perceived STS movement. This movement is based on a mechanical structure that is integrated into a chair and lifts the seat pan. In particular, the motion of the seat pan is based on data from natural STS movement and analyzed so as to transfer the user sitting on the chair into an almost upright position.

The first field of research is the fundamental biomechanical analysis of STS movement required to design individualized LADs. What biomechanical measurements of the human, i.e. the user are necessary in order to design an individualized LAD? What configurations of the LAD must be accessible to the user in order to adjust the force in the LAD or even adjust the entire structure to another person? The second area is the field of kinematic synthesis and analysis. What dimensions must the linkages hold in order to accomplish specific movements? How can the mechanism be designed in order to fit into a predefined workspace? These are questions answered in this thesis and in combination of biomechanical linkages it hopes to merge the field of biomechanics with kinematics to accelerate the field of bio-kinematic design. This is particularly interesting with respect to the growing physical human-machine interface, for example the research of wearable robotics. Biological joints such as the elbow are much more complex than simple hinges often found in robotics. Therefore mapping a mechanical structure based on hinges onto the biomechanical joints of the human leg can lead to sever injuries to the joints if mapped incorrectly.

At first, a general background on the loss of mobility and the demographic changes in Germany is presented and discussed. This is followed by a presentation of devices available on the market and technological solutions in research that aims to abrogate the aforementioned problem statement. The fundamental biomechanics of STS movement is discussed followed by the kinematic synthesis design procedure that creates planar linkages to the biomechanical parameters of a user. The fundamentals of kinematic synthesis and analysis are explained

and how these techniques have been manipulated in order to design individualized LADs. If a solution exists, this computational procedure allows a person to automatically find the correct dimensions of a LAD that fits into a specific type of chair and the measurements of the user.

The following chapter presents a prototype based on the individualization procedure and discusses and analyzes the forces and moments, i.e. the kinetostatics that are acting on the linkage, the user and the chair. For this chapter four prototypes have been realized that show a working example of an individualized LAD. It also discusses configuration possibilities that are user-friendly and how the system works in general.

In the experiments section the verification of both the computational individualization procedure as well as the mechanical design of the prototypes are presented and discussed. The individualization procedure is verified by applying biomechanical data from different male and female percentile groups and what linkages best fit the user. The mechanical prototypes were evaluated in a nursing home with elderly people who have difficulties with independent STS movement. A questionnaire was designed to be filled out by 50 participants to evaluate different aspects such as safety, adaptability, usability of the LAD and whether it can promote independent STS movement.

2. Problem Statement: The Downward Spiral of Mobility

Germany has one of the world's most rapidly aging and shrinking populations despite a strong current flux of immigration that has temporarily halted its overall decline. By 2060 it is estimated that the total number of Germans will have tumbled by 10 to 15 million depending on different modeled immigrations scenarios (Statistisches Bundesamt, 2015b). However, as was published by the German Federal Statistical Office in their 13th long term projection (Statistisches Bundesamt, 28.04.2015a), "[...] long-term population projections are no forecast. They provide 'if-then statements' and show how the population and its structure would change based on certain assumptions." For example this dramatic age decline is based on the assumption that the average annual birth rate will be 1.4 children per women while the life expectancy will increase by seven and six years for males and females respectively. Additionally, immigration is modeled in two different ways. The first scenario, called the 'continued trend based on lower immigration', assumes that the annual immigration rate will decrease from 500,000 to 100,000 per year over a period of six years while in the second scenario, called the 'continued trend based on higher immigration', the annual immigration rate is expected to fall to 200,000 by 2021 and subsequently remain at this level. These scenarios influence the expected population to be 67.6 and 73.1 million respectively in Germany.

"Population aging is a global phenomenon found in many industrial and developing countries, differing only in speed and extent. Not surprisingly, therefore, is the large number of studies covering a broad range of micro- and macroeconomic implications of population aging that have emerged in the last decades. (Hamm et al., 2008) offers a comprehensive overview of the German case who addresses the major impacts on economic growth, the labor and capital market, housing, fiscal policy, pensions and health care.

The most common issue addressed in the studies is that the current level of growth is not sustainable given a shrinking working age population, thereby negatively affecting pension funds as well as per capita income. In numbers, the working age population is expected to decrease by 23% and 30% depending on the two aforementioned scenarios, decreasing from 49 million people aged 20 to 64 (2013) to 38 and 34 million people respectively (Statistisches Bundesamt, 28.04.2015a). This in turn will impose a heavier fiscal burden on each working individual as the age dependency ratio continues to grow. This is a particularly pressing issue in countries with a pay-as-you-go system, where pensions are directly financed through social contributions of the working age population. The public pension scheme and the health insurance system will be responsible for a large part of future public debt that will drastically increase until 2060 (Werding, 2008). To assure the sustainability of the social insurance system, a gradual increase in the statutory retirement age might be inevitable.

While the total population in Germany decreases, the number of people aged 65 and over

will dramatically grow once the baby boomer generation will successively reach this age and make up for more than 20 million people by 2060 representing almost a third of the population (Statistisches Bundesamt, 28.04.2015a). Population aging is most dominantly noticeable and reflected by the number of the oldest seniors. In 2013, the number of people aged 80 and over amount to 4.4 million in Germany. In 2060, this number will be approximately twice as high as today, increasing the proportion of 5% to roughly 12% by 2060 (Statistisches Bundesamt, 28.04.2015a).

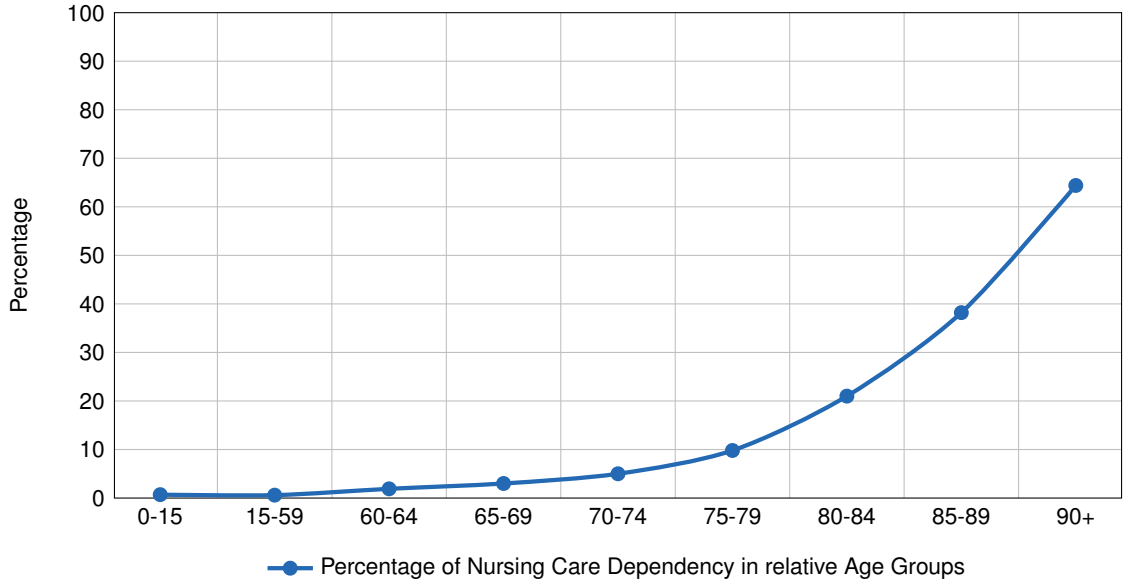

Figure 1 Long-term nursing care dependency in Germany (Statistisches Bundesamt, 2015b, p. 9)

Another implication of an aging society is the growing demand for nursing professions. Fig. 1 represents the long-term care dependency in percent for a certain age group in Germany for both males and females. While care dependency remains low up to the age of 80 it grows exponentially reaching 64.4% for the oldest seniors. (Maier and Afentakis, 2013) show that a shortage of fully qualified nursing professionals is already given. Counting fully-qualified and semi-skilled nursing professionals together and assuming an unchanged employment structure, the demand for nurses will be met through 2025 only." (Dmitry Chervyakov, DIW Berlin, 2015)

Currently 2.6 million people in Germany require some form of personal care, either ambulatory or in long-term care facilities such as nursing and retirement homes. This number represents a 35.8% and 48.3% increase of people requiring ambulatory and long-term care respectively since 1999. A steadily growing older population is bound to increase the need for nursing staff and infrastructure that can compensate for the expected lack of nursing professionals. An elder-friendly community should ensure the affordability and accessibility of public transportation, housing, safety and community involvement opportunities for the elderly, while also effectively maintaining a prolonged independence (Alley et al., 2007).

Nevertheless, population aging does have a bright side. Not only will longevity increase, but

the share of lifetime spend in good health will also rise. Due to progress in technology and health care the average man (woman) in 2050 will have spent 80 (70) percent of their lifetime in good health compared to 63 (60) percent today. Overall better health also means smaller expenditures for health care, which may partly compensate for the overall increased fiscal burden.

2.1. Loss of Physical Mobility with Age

Physical mobility is generally defined as the ability of humans to move and is further defined in health care as the 'ability to move independently'. This definition is further divided into 'active' (independent motion), 'assistive' (motion with technical support such as cranes or walkers), 'passive' (motion supported and carried out primarily by another human) and 'resistive' (supported motion carried out against the will of the subject) mobility. The degree of mobility complies with the ability to carry out tasks that are necessary to live an independent live. The thin threshold from mobility to immobility is crossed once the ability to move independently or to change postures and positions becomes impossible (Matolycz, 2016, p. 136).

Generally, the loss of mobility can be deduced as a consequence of human aging. Age-related changes in muscle tissue, tendons and joints lead to a continues reduction of muscle strength and therefore mobility. The sensory-motor system slows down and reaction times increase. Furthermore humans experience problems with their sleep cycle due to a lack of mobility.

The ability to access commodities, making use of nearby facilities, and participate in meaningful social, cultural, and physical activities is associated with freedom, independence and life quality. Not only does personal mobility allow us to carry out these so-called ADL but also promotes healthy aging as it stimulates and maintains a healthy balance of our musculoskeletal, cardio-respiratory as well as our sensory and neural system. With age, mobility naturally declines and becomes increasingly difficult to maintain while affecting the most complex and demanding tasks first. One of the most important and simultaneously physically demanding tasks is the capacity to rise from a seated position into a standing position. Not only does this movement require high levels of musculoskeletal strength but also neuromuscular coordination and stability. According to (Dall and Kerr, 2010) STS movement is carried out on average 60 times per day. Failure to stand up from a chair independently, especially in elderly, results in life altering changes such as reducing the frequency of ADL, thus avoiding manifest difficulties. This in turn, leads to further muscle strength deterioration and coordination and eventually leads to a full functional dependency, risking full institutionalization. To understand the fundamentals of STS movement, the risks involved and the motivation for this thesis different aspects of STS motion are described in detail in this section.

2.2. Fundamentals of Sit-to-Stand Movement

STS has been studied in many contexts such as (different age population, disabilities, musculoskeletal injuries) using various measuring techniques (i.e. kinematics, kinetics EMG (electromyography) and time characteristics).

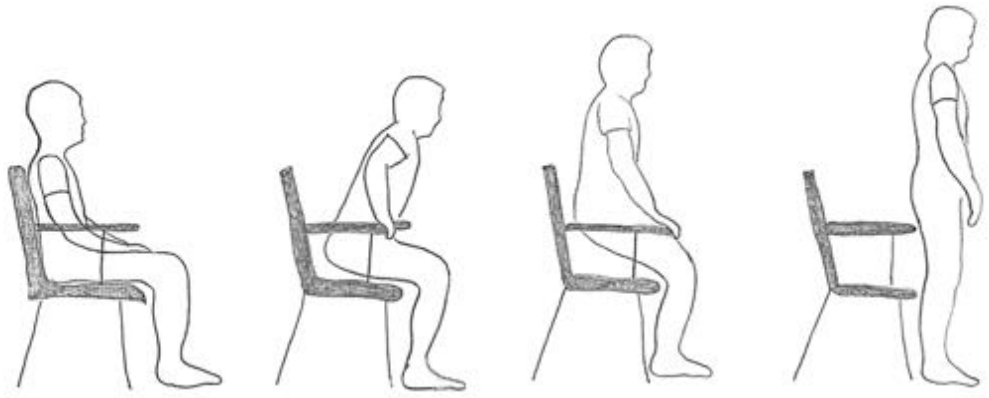

Figure 2 Qualitative view of the sagittal sit-to-stand movement split into four phases; sitting, hip flexion, chair rise and balance coordination (Taken from (Reimer et al., 2017))

The process of standing up requires a high degree of muscle strength, sensory-motor coordination and balance. In general this process can be divided into the following main movements in normal human beings: First the upper body bends towards the feet. this causes the center of mass to move horizontally until it is almost above the feet. The upper body then starts to rise shifting the center of mass into an almost vertical direction until a stable standing position is achieved. Section 4 describes STS movement in detail. In a study it was found that to subjects with difficulties of rising often make use of arm rests to support the stand up motion. This clearly highlights the challenge to find and maintain a stable standing position (Wheeler et al., 1985, p. 25 f.).

2.3. Causes of Decreased Independent Sit-to-Stand Movement

Rising from a seated position has been recognized as an ADL that becomes increasingly difficult with age. In fact, standing up requires forces and moments around the hip, knee and ankle joint that are much higher than compared to walking. It also results in contact pressures between femur and pelvis which are higher than during walking, jogging, even jumping.

“The STS transfer is one of the most demanding functional tasks that individuals undertake during daily life. At the hip joint, contact pressures between the femur and the pelvis are higher than during walking, jogging or jumping. At the knee joint, (Hughes et al., 1996) found that older individuals with functional impairments (i.e. inability to descend four stairs reciprocally or stand up from sitting at a 0.33 m seat height) utilized close to 78% available knee extensor strength to complete the STS transfer from a chair set to knee joint height whereas

younger individuals required approximately 34%. In addition, (Mizner and Snyder-Mackler, 2005) found knee extensor moments (internal moments) to be approximately twice the amplitude compared with walking in those individuals with knee osteoarthritis who received a total knee replacement. No other activities of daily living place this mechanical demand on the human body. given these demands, it is not surprising many individuals have difficulty with this task." (Rutherford et al., 2014, p. 158)

In a study with ten healthy male and four male subjects with partial walking disability an observation was carried out to compare different seat heights between 43 cm and 64 cm as well as with and without arm rests. It was found as expected that rising from a higher seated position and with arm rests requires less muscle activity. One can therefore conclude that the main difficulty in standing up lies within relocating the center of mass. Using a higher seated position or using arm rests lifts the center of mass initially therefore reducing the force and power required to lift the center of mass to the standing position (Burdett et al., 1985, p. 1179 ff.). Seat height, arm rests and leg position are critical determinants of the STS process (Janssen et al., 2002, p. 866).

2.4. Prevalence of Sit-to-Stand Weakness

The loss of muscle strength with age is a growing burden for each individual especially in conjunction with STS movement until independent rising from a chair is no longer possible. According to a study, elderly people require a higher percentage of their maximum muscle activity to lift themselves from a chair (Wheeler et al., 1985, p. 26). These findings have been reinforced in a chair-rise test, during which subjects had to stand up and sit down for five times as fast as possible. Results show that 4.4% of people aged between 65 and 79 years were not able to accomplish a single STS movement (Fuchs et al., 2013, p. 724, p. 728 f.).

In another study conducted in Australia and published in 1981 it was established that 42% of 379 elderly people had problems standing up. 48.5% of the subjects, however, were suffering from rheumatoid arthritis, a long-lasting autoimmune disorder that primarily affects joints (Munro et al., 1998; Munton et al., 1981). According to estimates some 2 million elderly over the age of 65 years have difficulties rising from a chair (Bashford et al., 1998).

A long-term study *LEILA75+* in 2000 assessed the mobility and independence of elderly people aged 75 and older in Leipzig, Germany. This study found that 61.8% of the participants had difficulties carrying out ADL. Even the execution of essential ADL such as personal hygiene, or walking proofed to be a challenge for 33% of the participants (Wilms et al., 2001, p. 348). Subjects were asked to carry out ADL within their own capabilities and afterwards assess their own behavior into three categories: 'without difficulties', 'with difficulties' and 'impossible'. 14.3% of the participants had difficulties with the essential task of rising from chair and for 5.3% this task was impossible. Subjects who assessed this task with difficulties or as impossible are henceforth combined as one category called 'participants with problems'.

21.5% of female participants with problems compared to 13.6% of males shows that female have much more difficulties compared to male subjects of the same age. Furthermore it was shown that with increasing age the percentage of participants with problems rose. 8.3% and 18.1% of people aged between 75-79 years and 80-84 years respectively had difficulties with STS movement while this share increased to 34.9% of people aged over 85 years (Wilms et al., 2001, p. 352).

1,584 million people in Germany suffer some form of musculoskeletal disorder. 42.99% of those are male, 57.01% are female (Statistisches Bundesamt, 2015b). This is particularly ominous considering the complexity of the aforementioned first two phases of STS movement in view of the relative amount of people with rheumatoid arthritis as was mentioned earlier. In conclusion STS movement is most dominantly influenced by the type of chair used. In particular with respect to seat height, armrests and leg position. Studies have shown that as we age naturally, STS movement becomes more difficult. In order to prolong the independence of elderly therefore one must look at factors that simplify STS movement in order for the subject to carry out ADL independently for a longer period of time.

2.5. Medical Objective: Stopping the Downward Spiral of Mobility

The prevalence of STS weakness as well as the correlating risk of falling are core triggers to employ services of nursing staff. 16.9% of the people in outpatient care compared to 43.8% of elderly living in nursing homes had deficits with the motion sequence STS as was found in the study *LEILA75+*. Etiological factors of course are that people living in nursing homes are often much more fragile and less independent than those able to live at home (Wilms et al., 2001, p. 353 f.). This frailness partially originates from an “accustomed dependency” through which passive behavior of elderly is indirectly encouraged since active participation is rarely appealed with positive response. Influencing factors such as time pressure play a key role in the promotion of active participation of elderly. Passive participation, however, results in the continued degeneration of muscle tissue, thereby increasing the dependency during STS movement and in turn decreasing the independence of elderly (Heidenblut and Zank, 2015, p. 322).

Another negatively influencing factor are psychotropic drugs. *“In dem Bemühen, Stürze in Krankenhäusern und Pflegeeinrichtunen zu verhindern, versuchen Fachkräfte in Gesundheitssituationen nach wie vor, Patienten oder Bewohner durch Einschränkung ihrer Mobilität vor Stürzen zu bewahren. Dafür bleibt ihnen häufig nichts anderes übrig, als auf Fixierungsmaßnahmen und Psychopharmaka zurückgreifen.”* (Tideiksaar, 2008, p. 16) (Nursing staff try to limit the mobility of patients in certain health situations in an effort to protect patients from falling in hospitals and nursing homes. Often the only choice that remains is to resort to fixation measures and the utilization of psychotropic drugs.). Despite the questioned effects of psychotropic drugs to lower the risk of falling (Tideiksaar, 2008, p. 16) has mentioned that relative to their dosage psychotropic drugs can possibly worsen the physical and psy-

chological state of the patient, thereby decreasing the active mobility and increasing care dependency.

Nursing staff stand in the middle of a major economical conflict. Providing carefully planned and coordinated care and welfare for those in need of care on the one hand and complying with the continuously rising economical challenges of health care on the other side has become a rising concern to health care specialists. This conflict of aims at this point are only met by strictly regulating and standardizing care procedures resulting in higher physical and psychological stress for nursing staff ((Rabe-Kleberg et al., 1991) in (Stagge, 2014, p. 91)). Maintaining such standards has proven to be counterproductive as the increase in workload over decreasing time frames can have extreme consequences on physical and psychological health (Zimber, 1998, p. 418). Therefore nursing staff suffer from a much higher risk of work related injuries as well as suffering from the so-called 'burnout syndrome'. In particular, nursing staff are said to be six-times more likely to incur a lumbar disc herniation or other forms of lumbosciatica compared to employees of other physically demanding industries (Cohen-Mansfield et al., 1996; Leiter and Harvie, 1996, p. 98 f.).

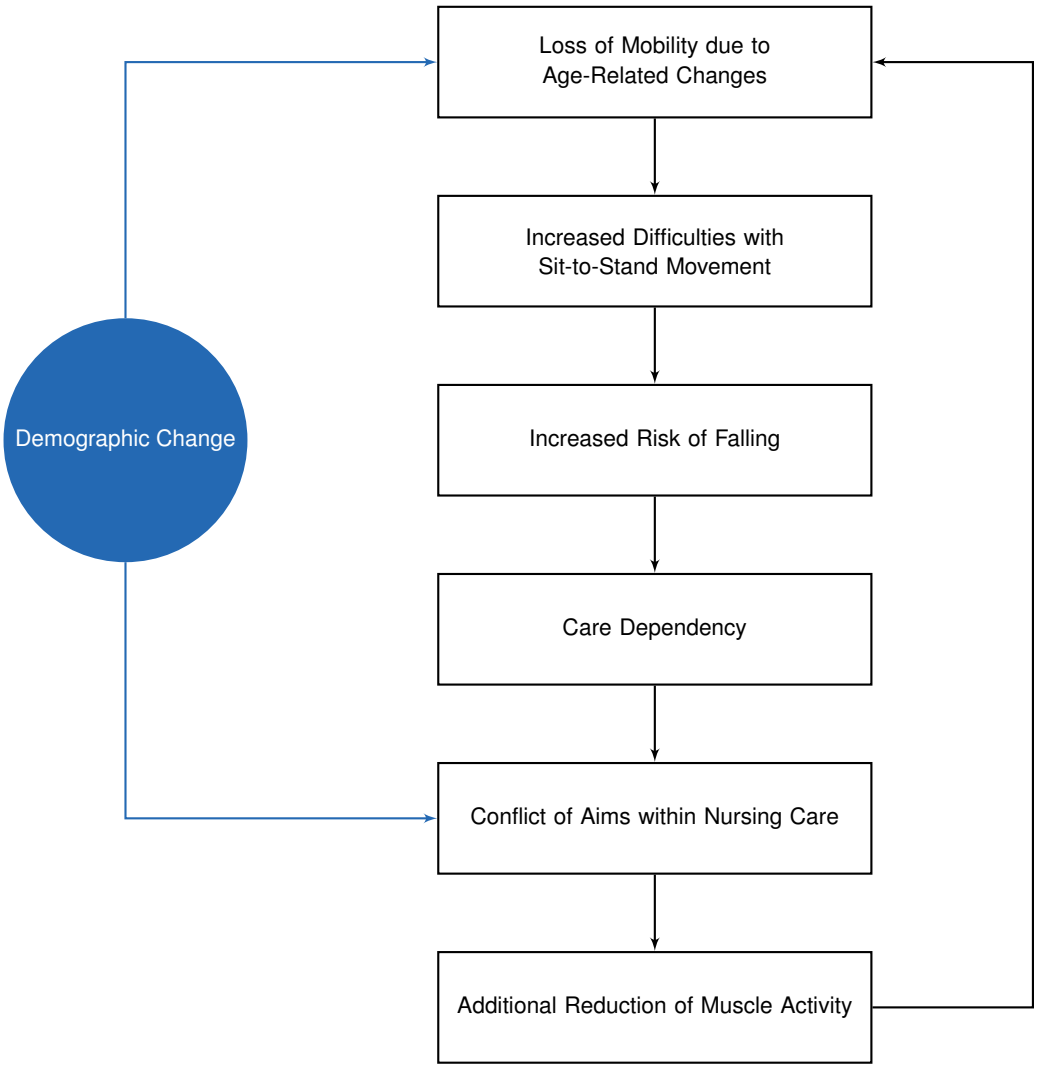

Figure 3 The downward spiral of mobility

TNS Infratest released results of a study in 2009 where only 26% of the staff in nursing homes haven't changed their jobs compared to 39% in 1997 (TNS Infratest Sozialforschung, 2011). Furthermore it was observed that nursing staff remain an average time of 8.4 years in their work profession only (Hackmann, 2010). Thus the congestion of work for nurses is expected to dramatically increase upon major economical establishments such as a continued high demand for professionally trained nursing staff and an increasing shift of full-time to part-time positions due to cost-cutting measures (Simon, 2012, p. 53; Stagge, 2014, p.83)

All these factors that influence STS movement are mostly interconnected as seen in Fig. 3. The 'Loss of Mobility due to Age-Related Changes' is responsible for a decreased independence and thus 'Increased Difficulties with STS Movement' which in turn is accountable for an 'Increased Risk of Falling'. At some point it becomes inevitable to support ADL via nursing staff. However, the aforementioned 'Conflict of Aims within Nursing Care' leads to a considerable neglect ion of personal mobility and therefore in turn is responsible for the continued 'Loss of Mobility due to Age-Related Changes'. This downward spiral of mobility is accelerated due to the socio-economical challenge of demographical change.

3. Background and State-of-the-Art

Sitting down and standing up is a transfer motion is a fundamental movement that is carried out countless times during the day to conduct other ADL. It is a prerequisite at home as well as in nursing homes to live an independent life and therefore also influences social interactions with others. Numerous technological solutions exist as will be discussed in this section that assist in the STS transfer motion. The right choice of device ought to be chosen on the degree of disability and independence and should always try to rehabilitate normal STS movement. The state-of-the-art is split into three distinct sections. The first sections will discuss the ubiquitous manual transfer as carried out from person to person. This is followed by technological solutions as well as patents that exist on the market. Last but not least technological research and development in this field will be analyzed. The following Fig. 4 represents the most distinct technological solutions which try to intervene with the downward spiral of mobility.

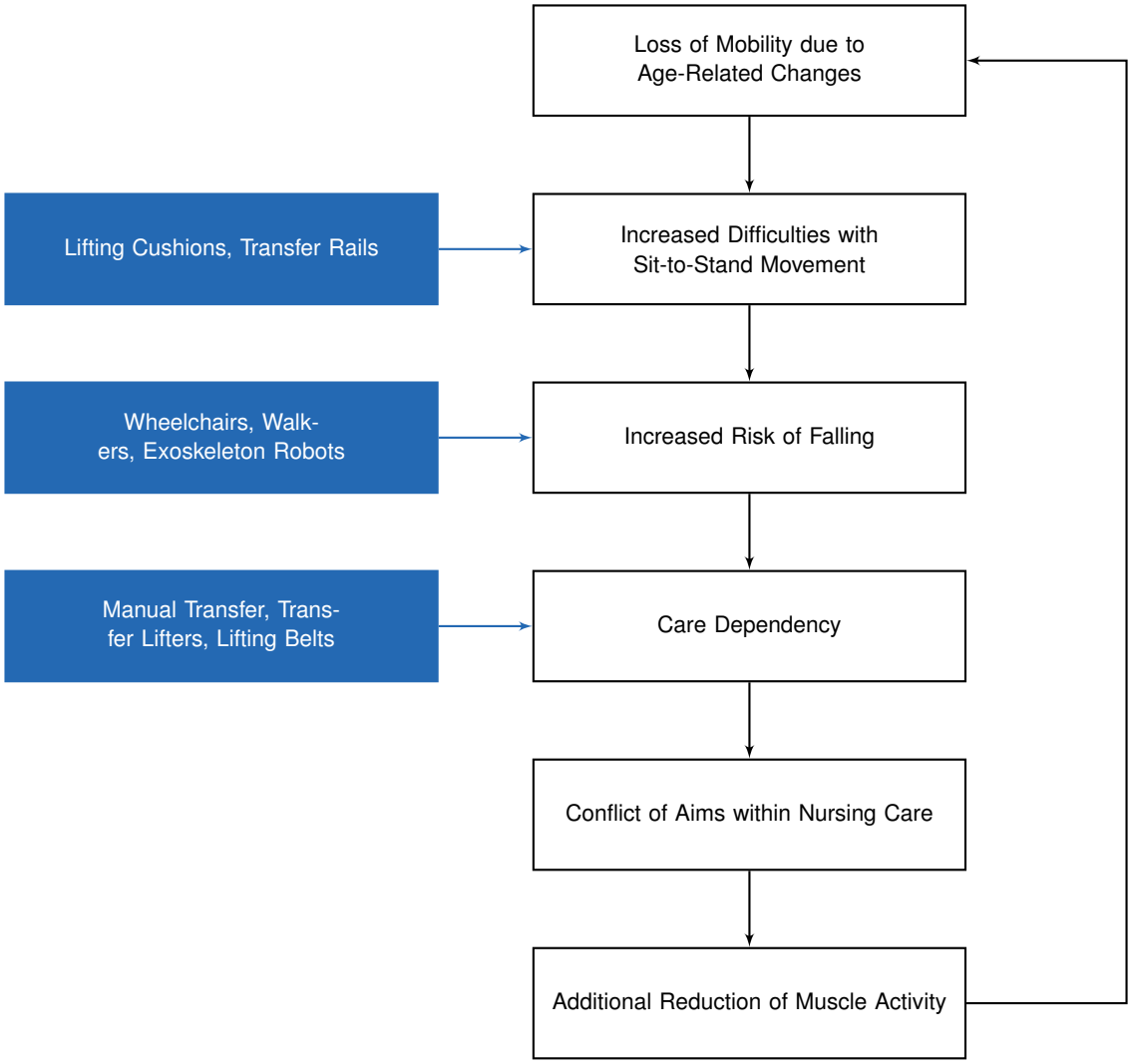

Figure 4 Intervention of technological solutions to impede the downward spiral of mobility

3.1. Manual Sit-to-Stand Transfer

The choice of assistive technologies for the STS transfer of patients depend on a number of criteria. First and foremost it depends on the physical capabilities of the patient. This is followed by pain resistance, and personal will. The transfer carried out by a caregiver or nurse is usually carried out in one of two ways. The patient is lifted while the nurse stands in front of the patient and embraces the patient underneath his arms. The patient is being lifted in parallel to the upward movement of the nurse. The second method integrates a spiral movement to the side. For both methods supportive technologies are available such as slide plates (Steigele, 2013). The spiral movement consists of rotations around two axes which reduces the overall force required for the patient. However it increases the space required to perform this transfer. The parallel movement consists of a single rotation while increasing the difficulty of the bend and stretch movement (Lektorad Pflege and Menche, 2014).

During a manual STS transfer nurses and caregivers ought to support the patient in such a way that the patient is able to perform the movement almost independently. Therefore the supportive movement mustn't interfere with the movement of the patient. Every patient uses a different combination of parallel and spiral movement to stand up and therefore has an individual STS transfer method. It is the aim of the nursing profession to incorporate the patient's movement into their STS transfer (Lektorad Pflege and Menche, 2014).

This individual activity of the patient is paired with individual effort. In turn this effort is split into either pressure or pull exertion with respect to different body parts. The result is a complex movement of the patient's body. Maximum support is achieved by a nurse or caregiver if the support works in parallel to the movement of the patient and not against that movement, e.g. it is counterproductive if a nurse tries to lift a patient underneath his arms while the patient tries to use the arm rests to stand up (Lektorad Pflege and Menche, 2014).

The initial position of the STS transfer is considerably easier if the patient sits at leading edge of the chair. This simplifies the weight transfer above the feet. The position of the feet plays a key role during STS transfers. Positioning the feet slightly further back to the leading edge of the chair reduces the effort to stand up. However, when the feet are positioned too far back the stability of the STS movement suffers. In a study consisting of two groups of 10 women each with an average age of 24 and 75 respectively it was found that the older group of women positioned their feet 4.2 cm further back compared to the younger group of women (Wheeler et al., 1985). Another crucial factor during STS movement is the speed at which a supported STS transfer is carried out. Slow speeds are preferable in elderly as it gives the patient enough time to stabilize and abort the transfer to avoid a fall (Steigele, 2013).

There are different methods of carrying out a manual STS transfer while the most profound influence on the technique depends on the independence and capabilities of the person in need of care. Patients with a smaller impairment are often helped by a nurse pressing down

the knee with one hand and shifting the lower back to the front while standing next to the patient.

Patients who need active support during the STS movement are often lifted using the aforementioned parallel lifting method. The nurse stands in front of the sitting patient. While using the knees the nurse bends down to the patient and wraps the arms around the trunk of the patient. In a similar fashion the patient holds his arms at the hips of the nurse to stabilize the transfer. Giving clear vocal instructions to the patient the STS is carried out in harmony of both parties until the weight of the patient is distributed above the feet.

3.2. Existing Lift-Assist Devices on the Market

To support the STS movement there exist a number of technologies and supportive materials to help both patient and nurses which will be described in detail below. The most basic supportive materials are often passive aids that make the manual STS transfer a little easier. These include lifting belts worn around the hip of the nurse such that the person can hold tight to the nurse, and transfer pads made out of a material with a low friction coefficient. The pads are placed underneath the patient's buttocks so that the patient can slide to another chair or bed more easily without having to stand up at all.

Here are the most profound and dominating technologies that have been used in hospitals and nursing homes to assist people that are not able to perform a STS movement independently. This is the current state of the art of lift-assist devices on the market.

Transfer Rails

Transfer Rails are handrails commonly positioned in front of a piece of furniture or in the bathroom. They consist of a rigid rod structure for the user to hold on to while performing transfer motions such as standing up or sitting down (Lektorad Pflege and Menche, 2014). There exist a great many handrail solutions for different areas and these can be divided into two categories:

- Structures that consist of a single handrail (see Fig. 5a) that exist as a mobile walking cane or are fixed to the walls or furniture comparable to armrests of a chair.
- Structures consisting of two handrails on either side while the user stands in the middle as seen in Fig. 5b. These structures are often used as walking aids as their U-like structure stabilizes the user in all directions.

Stand Assist Lifts

The stand assist lift is a device that lifts a person from a seated position to a stable standing position. It consists of a crane like structure where a lever holds a sling that must be wrapped around the patient's back. The lever is equipped with handles for the patient to hold on to. The device is stands on four wheels and can therefore be moved freely. During the STS transfer

(a) (b)

Figure 5 Conceptual design of handrails based on (Razon, 2004) (Drawing by Kyra Kleine)

the device is positioned in front of the sitting patient. The patient must lift the feet such that the foot plate of the device can be positioned underneath the feet. Next the transfer sling is wrapped around the back and underneath the arms of the patient. An electric motor actuates a piston that raises or lowers the lever. The legs are fixed to the foot plate such that the legs do not slip away during the lift process of the lever. Once the stand position is achieved the patient can either be released from the slings or transfered to another seating position such as the bed or wheelchair. In this case the device is also used as a transfer lift while lowering the patient to a seated position (Hakamiun et al., 2001).

Similar devices exist that are either mounted to a floor base or even to a ceiling. These devices carry slings that can lift the entire body. This is especially useful for obese and bedridden patients, who entail a higher risk of back problems for nurses and caregivers alike. These lifts have the power to transfer a patient from one room to another into a seated or lying position (Lektorad Pflege and Menche, 2014).

Lifting Cushion

A lifting cushion is a lifting device in form of a cushion that is placed onto a seating furniture. The purpose of this device is to help users to sit down more comfortably and help the user to stand up easily. This is achieved by an integrated mechanism that lifts part of the cushion upwards and forwards mimicking the natural STS movement of a human. By means of actuation the device can compensate for muscle weakness in the user.

The lifting cushion is designed as a modular addition to any kind of seating furniture. It is therefore always between the user and the actual seat, thereby increasing the height of the chair, which is between 5 - 8 cm. The weight of the device is between 4 kg and 6 kg which allows for easy transportation of the lifting cushion. The mechanism of the lifting cushion can be divided into two plates. The base plate which is placed onto the seat and a lifting plate

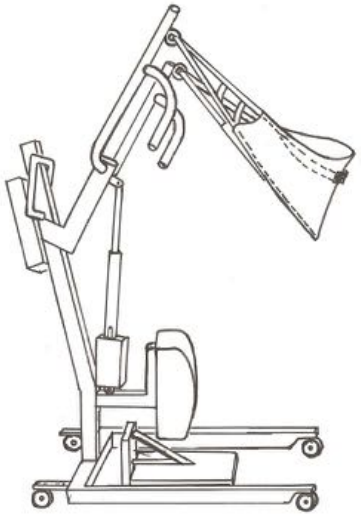

Figure 6 Conceptual design of a stand assist lift based on (Hakamiun et al., 2001) (Drawing by Kyra Kleine)

that is lifted by a linkage and an actuator. The lifting plate is hinged at the front edge of the cushion thereby creating a convex shape when the mechanism lifts the plate. Two devices of this kind exist on the market which distinguish themselves by the method of actuation:

- The first device is a passive lifting cushion called the *UpLift Premium Seat* it actuates the lifting plate via a gas spring strut as seen in Fig. 7. The head of the gas spring strut can be fixed to different configurations thereby changing the lever. This in turn allows the device to be configured to different weights of the user. According to technical details provided with this product this device can support 70-80% of the users weight. The gas spring strut is intended for a user weight of 35 kg to 105 kg.

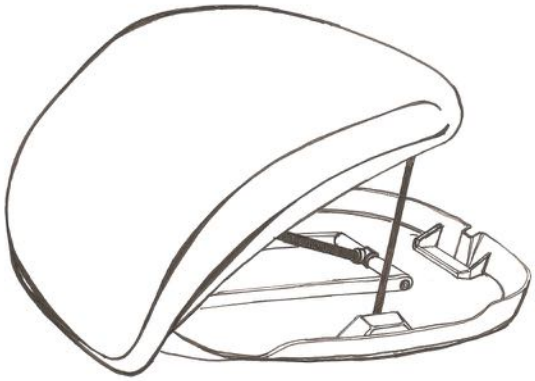

Figure 7 Conceptual design of a stand assist lift based on (Hakamiun et al., 2001) (Drawing by Kyra Kleine)

- The second device is called the *UpLift Premium Power Seat* and it replaces the gas spring strut with an electric motor. It is an electric seat assist device where the lift plate is also pivotally secured to the base plate. A controller connected to the drive member initiates the raising or lowering process of the seat. The electric power must be provided by a

220-240 V wall socket and therefore the device is not necessarily as independent as the *UpLift Premium Seat*. However the electric power provides the user with enough power to lift a user weight of up to 136 kg.

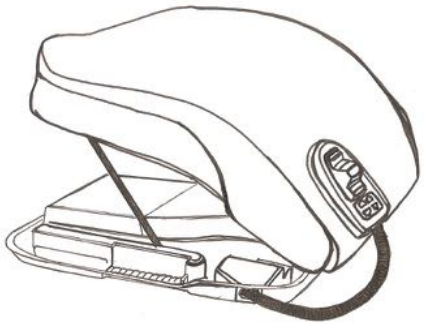

Figure 8 Conceptual design of an electric lifting cushion based on (Newman and Knappers, 2004) (Drawing by Kyra Kleine)

- A third concept exists in form of a US patent. It is a portable seat lift that consists of a seat mounted on a base with two levers, which are powered by a drive unit as seen in Fig. 9. The invention is described as “a portable seat lift that can help physically impaired individuals lower themselves to a sitting position or raise themselves to a standing position. This seat lift consists of a seat mounted with two levers to a base. The levers are powered by a drive unit that can completely lift the weight of a user without any assistance from the user. When the drive unit actuates the two levers, both the front and back of the seat are raised in a manner that coincides with how the backs of the thighs normally approach or leave a chair when a person sits or stands, respectively. As a result, the physically impaired person can sit or stand with more ease and much more naturally” (Weddendorf, 1994).

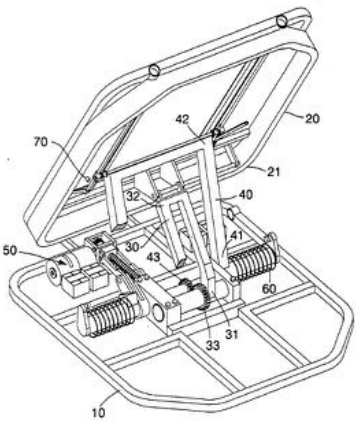

Figure 9 Conceptual design of a portable seat lift based on (Weddendorf, 1994)

Lifting Seats

Another device that helps users to stand up are armchairs with an integrated lift assist mechanism. Rather than lifting only the seat pan the entire chair is lifted including the back rest and the armrests. This is achieved through an electrically driven motor that must be powered via a wall socket. Often these chairs allow a range of configurations for the seat thereby including

leg rests and declining of the back rest to an almost horizontal position. The lift assist mechanism can commonly hold a weight of up to 130 kg and has a weight of approximately 60 kg depending on the manufacturer. The chair is lowered and raised via a remote controller.

Figure 10 Conceptual design of a stand assist lift based on (Curdija et al., 2010) (Drawing by Kyra Kleine)

A similar concept exist as a modular lift assist mechanism that can be placed between the floor and the legs of a chair as seen in Fig. 11. The device increases the height of the chair by 4.5 cm and is actuated by an electric motor also powered via a wall socket. The device is controlled with a remote.

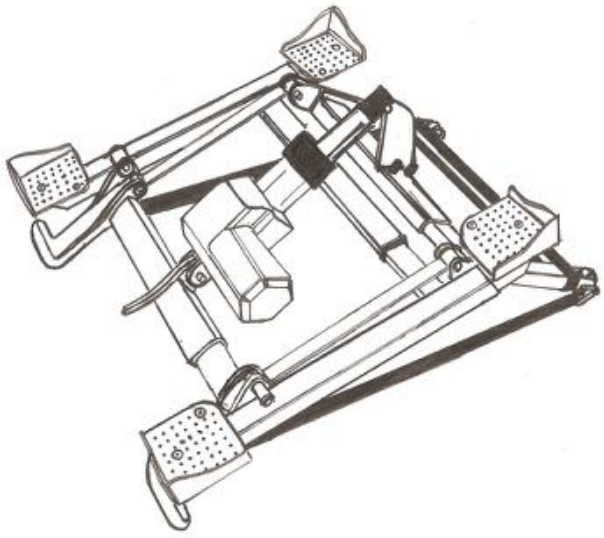

Figure 11 Conceptual design of an electric lifting cushion based on (Newman and Knappers, 2004) (Drawing by Kyra Kleine)

Sit-to-Stand Wheelchairs

Sit-to-stand wheelchairs gives users the possibility to rise into an almost vertical standing position with the wheelchair. Usually the seat and the backrest are slowly moved upwards while the user is attached to the wheelchairs with seat belts. The user is able to rest his hands on armrests that stabilize the user and hence gives that person some feeling of stability. Actuation methods range from purely passive mechanisms as well as electrically driven actuators that move the chair up and down via remote control.

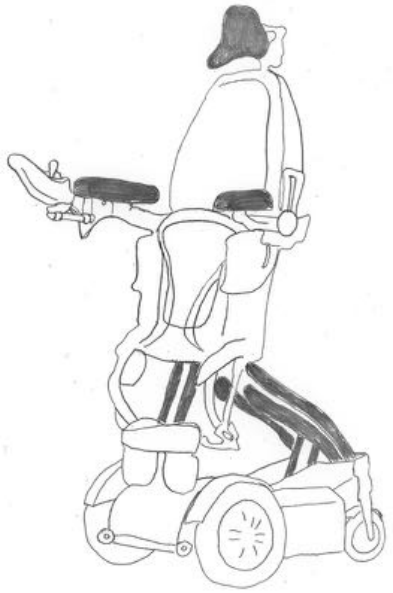

Figure 12 Conceptual design of an electrically powered sit-to-stand wheelchair

Companies such as *LEVO AG*, *Permobil GmbH*, *Invacare GmbH* and *PARAVAN GmbH* offer a broad range of sit-to-stand wheelchairs as seen in Fig. 12. This wheelchair in particular consists of a four-bar linkage that lifts the seat pan from the wheelchair base. Four-bar linkages at either end of the seat pan align the leg- and backrest with the seat pan into an almost vertically line. The linkages are called biomimetic designs according to the manufacturer that aim to mimic natural STS movement of the user. However, to our knowledge no experimental evidence has been published.

3.3. Existing Lift-Assist Devices in Research

Wearable Robots

Wearable robots also known as exoskeleton robots are mechanical structures that can be worn by a human being (Reimer, Lueth and D'Angelo, 2014). The purpose of this wearable robot is to support the movement as to strengthen certain body parts to restore or even exceed the strength of a normal human being. Therefore there is a high-level of communication between robot and human as compared to master-slave configurations. The robot must communicate to the human if it requires more strength and the human must be able to communicate to the robot what to do (Pons, 2008).

Exoskeletons for the elderly have been introduced in (Kong and Jeon, 2006) which consist of ortheses placed around the lower extremities of the user and an electric walking frame for stabilization purposes. The ortheses are actuated by electrical drive units which actuate the wearable structure. The purpose of this wearable structure is to compensate the loss of muscle strength and to allow elderly to walk independently for a longer period of time. Different sensor types come into play such as pressure sensitive sensors, EMG sensors that measure the electrical activity of muscles and EEG (electroencephalography) sensors. Sensors that measure the nerve activity. A whole body exoskeletons known as *HAL - Hybrid Assistiv Limb* suit (Sankai, 2006) is equipped with EEG sensors. This structure picks up specific stimuli by the brain and interprets them as actuation signals for the exoskeleton motors.

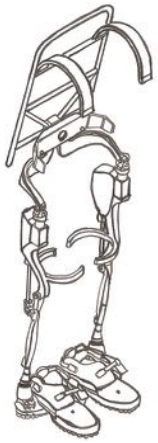

Figure 13 Conceptual design of a lower extremity exoskeleton based on (Kazerooni et al., 2011) (Drawing by Kyra Kleine)

Wheelchairs with Integrated Transfer-Assistance Device

(D'Angelo et al., 2015) has published a journal paper that has introduced two concepts of transfer-assistance devices that are integrated into a standard wheelchair. Aim of these devices are to relieve nursing professionals in their daily routines of lifting patients from and to the wheelchair without the need of an additional external lift device. Each design consists of a mechanical linkage actuated by a passive gas spring strut. Passive actuation was chosen in order to compensate for the weight of the user as well as to stimulate the user to participate in the transfer. Rapid prototyping techniques were used to prepare and evaluate 1:10 models.

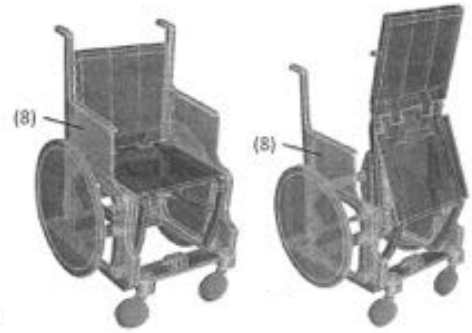

Figure 14 Conceptual design of the sit-to-stand wheelchair based on (D'Angelo et al., 2015, p. 011012-2)

The first concepts consist of a planar linkage that lifts the seat and backrest of the chair into an almost vertical configuration. The linkage consists of two coupled four-bar linkage. The fixed pivot points are installed into the frame of a standard wheelchair. In fact, the entire structure is designed in such a way that in sit configuration the entire linkage fits into the workspace of a standard wheelchair is in accordance with the DIN EN 12183 regulations.

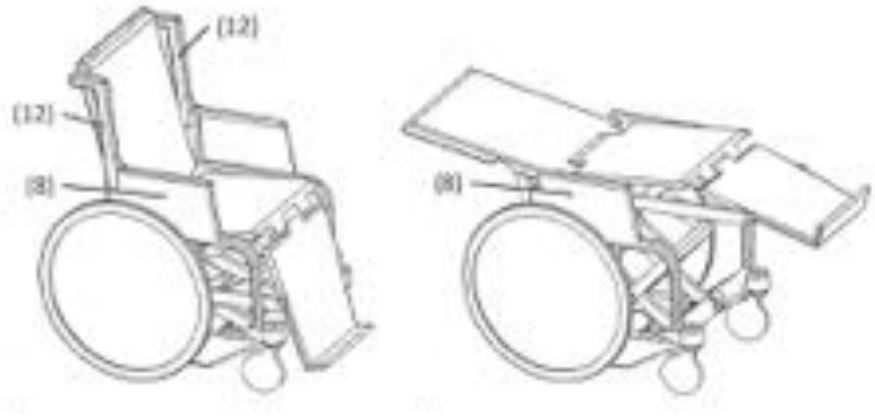

Figure 15 Conceptual design of the sit-to-horizontal wheelchair based on (D'Angelo et al., 2015, p. 011012-4)

The sit-to-horizontal concept consists of a scissor like mechanism that lifts the seat, declines the backrest and inclines the leg-rest in order to reach an almost horizontal position of the patient. The seat experiences a translational movement only consisting of a dominating vertical and slightly anterior position change. The anterior transition is necessary in order for the center of mass of wheelchair and user to stay within the horizontal limits of the wheelchair chassis The goal of the vertical climb is necessary such that the patient can be comfortably pushed onto a bed at the same height without the arm rest being impeding this motion. Again the linkage is designed to comply with DIN EN 12183 standards. The entire structure consists of one DOF (degree of freedom) only which is actuated by a gas spring strut that connects the frame of the wheelchair and the seat.

Individualized Bio-Kinematic Design Approach

In particular the aforementioned sit-to-stand wheelchair concept by (D'Angelo et al., 2015) was examined more closely in respect to the kinematics of the mechanism. A 1:1 prototype was constructed using rapid prototyping and rapid manufacturing techniques such as 3D printed bearings and laser-cut linkages for experimental purposes only. On behalf of this thesis further functional specification to the mechanism were made. How could we design a linkage such that is would fit densely fit into a small working space below the chair and secondly how could the mechanism be designed such that it would fit to an individual person, yet be configurable to be applicable by a range of users easily.

3.4. Disadvantages of existing Lift-Assist Devices

Table 1 illustrates the advantages and disadvantages of the major technical devices that are currently available on the market. Devices that in some form assist a user to stand up and sit down more easily. Each device is assessed in different categories either positively, neutral or negatively. These categories range from the space the devices take up, the amount of assistance they province during STS movement, stability, time consumption and applicability within nursing homes and at home.

Table 1 Advantages ($+$), disadvantages ($-$) or neutral effect ($\circ$) of the state-of-the-art for assisting STS movement

Device	**Method**	**Lift Assistance**	**Time Consumption**	**Required Space**	**Stability**	**Availability**
Manual Transfer	Nurse, caregiver	$+$	$+$	$+$	$\circ$	$+$
Transfer Rails	Stabilization and grip support	$-$	$+$	$+$	$\circ$	$+$
Lifting Belts	Stabilization and grip support	$-$	$+$	$+$	$\circ$	$+$
Stand Assist Lifts	Crane-like stand-up support	$+$	$-$	$-$	$+$	$-$
Transfer Lift	Crane-like transfer support	$+$	$-$	$-$	$+$	$-$
Lifting Chair	Chair with integrated lift mechanism	$\circ$	$-$	$\circ$	$\circ$	$-$
Lifting Cushion	Cushion with integrated lift mechanism	$\circ$	$+$	$+$	$\circ$	$+$
Stand-Up Wheelchair	Wheelchair with integrated lift mechanism	$+$	$\circ$	$\circ$	$+$	$\circ$
Exoskeleton Robot	Wearable device that assists limb movement	$+$	$-$	$\circ$	$\circ$	$\circ$
STS Wheelchairs	Wheelchair integrated STS mechanism	$+$	$+$	$+$	$+$	$\circ$

Work overload in Nursing Homes

Work overload is a conspicuous predicament nursing homes are facing in Germany as was shown in a study in Saxony-Anhalt. In this survey 92.7% of nurses complained about rare, frequent or permanent dorsal pain. Additionally, 90.8% of nurses suffered from rare, frequent or permanent neck pain (Hirsch and Lindenberg, 2013, p. 138). Similar results were shown in the aforementioned study by (Stagge, 2014, p. 138) conducted by the University of Vechta. Here, 73.2% of the interviewees disapproved about their workload showing physical symptoms such as dorsal pain and sleeping disorders. The *BGW-DAK Health Report*

2013 showed that 44.3% of caregivers in nursing homes suffer from psychosomatic problems (Stagge, 2014, p. 85).

The underlying cause of work overload finds itself in the frequent repetition of lifting, transferring and rearranging of patients in a bend position (Hirsch and Lindenberg, 2013, p. 139). It was shown that lifting weights between 5 and 35 kg numerously over a short period of time can have negative consequences on the physical health of the subject. The fact, that the average amount of sick days in the nursing profession lies at approximately 17.8 compared to 11.8 days in other professions illustrates the indispensable problem (Behrens et al., 2008, p. 52ff.). For this reason many nurses quit their job prematurely (Stagge, 2014, p. 84f.).

Labor costs represent the most significant share of nursing home expenses which. To relief this high cost pressure the staff is bound to conduct their workload over a shorter period of time. This lack of time is a core problem when it comes to assistive devices for the transfer of patients (Reimer, Pfeiffer, Kreutzer, Lueth and D'Angelo, 2014). The lack of time impedes many nurses to apply the use of technological solutions such as the lifter as it requires too much time and effort.

Refusal of Transfer Belts and Lifters among Nursing Staff

The aim of the project *Arbeitsschutz in der Altenpflege* (Protection of labor in nursing care) was to find improvements in work and health care of nurses and caregivers, especially handling topics such as patient transfer, organization and work schedules. During this project it was found that 25.3% of the nurses and caregivers did not make use of any kind of assist device to carry out patient transfers. The three most common justifications not to use any assistive device, next the argument that they have accustomed themselves to the manual procedure, are:

- 56% of nurses and caregivers suffer from immense an workload and time pressure. Using assistive devices requires significantly more time compared to the manual transfers as they need to be brought to the patient due to often limited availability. In addition the devices such as transfer lifters commonly must be set-up and removed from the patient.
- 48% of nursing staff mentioned that space is a frequent limitation to use LAD.
- 25% of nurses and caregivers do not feel a physical relief when applying devices such as lifting belts.

The disadvantages of acquisition and space requirements are particularly oriented at transfer lifters and lifters a like. Furthermore they often very difficult to store without taking up valuable space. Meanwhile 68.4% of the nursing staff implied that they would be willing to use assistive devices during every day routines if they were easy to use and available at all times.

Lack of Customization in Lifting Seats

There are generally two types of devices available for helping a physically impaired individual go to carry out STS movements as has been described in (Weddendorf, 1994): "[...] while being totally sufficient with respect to sitting and standing assistance, (a lifting seat) has the disadvantage of not being readily portable for the individual who requires help with sitting and standing in many places." Additionally, lifting chairs are powered via an electric power that must be connected to a wall power socket. Not only does this limit the location of the device, it also increases the danger of tripping over the wire. Such electric drives are also included in lifting cushions. The speed at which the lift process is carried out, however, can take more than 30 seconds which compared to a normal STS transfer is significantly slower.

Increased Seat Height with Lifting Cushions

In this thesis, individuals with lower limb impairments are unable to perform a safe and effective STS transfer from a fixed-seating system. Studies have shown that raised seat heights reduce the mechanical demands (i.e. lower sagittal plane hip and knee moments and reduced quadriceps activation amplitudes) when compared with a normal seat height, but having a fixed-raised seat is not always practical for many environments of daily living. Systems have been designed to provide assistance to elevate the height. Early work on these designs focused on booster or spring-loaded flap seats, although it was argued that these designs challenge balance, forcing the patient to stand up using abnormal movement mechanics. Positive experiences, however, have been reported and largely comprise the evidence of lifting-seat effectiveness. (Bashford et al., 1998) found that 75% of the individuals rated easier transfers as a result of using an ejector mechanism, a result similar to that presented by another study. Health care professionals, scientists, and industry have joined together to develop advancements in adaptive seating systems that aim to assist the STS transfer. These designs include systems without mechanical assists (e.g. adding arm rests, increasing seat height), systems with mechanical assists (e.g. Booster or ejector chairs), and those systems that can lift, tilt, recline or rock.

"To our knowledge, while investigations exist to support the use of non-mechanical assist techniques, extrapolated from the determinants of STS (Janssen et al., 2002), few studies have investigated the mechanical demands (i.e. biomechanics and muscle activation) of using seating devices to mechanically assist the STS transfer. (Munro et al., 1998; Munro and Steele, 2000) analyzed both the mechanics (angular kinematics and kinetics) and muscle activation patterns of individuals with *rheumatoid arthritis* as they transferred from STS using an ejector chair. In general, participants rated their perceived exertion much lower when the ejector mechanism was employed. Trunk and knee angular displacement was significantly reduced but knee joint moments at seat off were not with the ejector mechanism compared with standard height (Munro et al., 1998). Earlier *quadriceps* and *tibialis anterior* muscle activation onsets and longer activity durations (*quadriceps*) were found with ejector mechanism use as well. In addition, either no change or increased muscle amplitudes were found when rising with ejector assistance (Munro and Steele, 2000). In contrast, (Wretenberg et al.,

1993) found that the use of spring-loaded flap seat reduced both external hip and knee flexion moments and *vastus lateralis* muscle activity. While comprehensive, how these findings translate to other lifting-seat designs, such as those that do not provide a horizontal thrust (eject or boost), remain unknown." (Rutherford et al., 2014, p. 159)

4. Analysis of Sit-to-Stand Movement

Section 2.2 has partially introduced the biomechanics of STS and how this motion can be divided into characteristic phases. In this chapter, STS movement is further analyzed by looking at past research papers that have investigated STS motion in different contexts and measuring techniques.

4.1. Phases of Sit-to-Stand Movement

According to a review paper by (Janssen et al., 2002, p. 867) on STS movement: "The manner in which the STS movement is defined depends to some extent on the aim of the study. (Roebroeck et al., 1994), for example, defined the STS movement as moving the body's center of mass upward from a sitting position to a standing position without losing balance. (Vander Linden, 1994) defined the STS movement as a transitional movement to the upright posture requiring movement of the center of mass from a stable position to a less stable position over extended lower extremities. The STS movement also can be described using kinematic or kinetic variables, with definitions supplied for phases and events during the movement (Schenkman et al., 1990)." These phases are illustrated once more in Fig. 16 and explained in detail below.

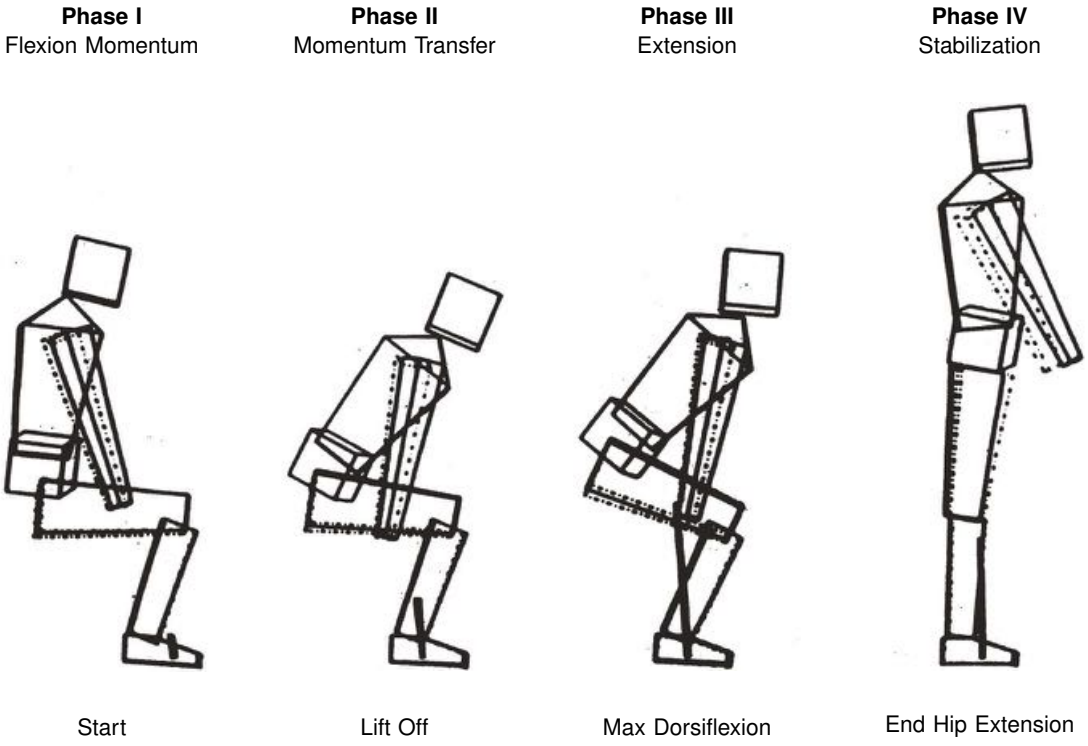

Figure 16 Four phases of rising marked by four key events. Pictures taken from (Schenkman et al., 1990)

STS is commonly divided into four phases (Schenkman et al., 1990, p. 638 ff.):

Phase I: The first phase is called the 'flexion-momentum phase'. Here the upper body is accelerated horizontally and rotated around the hip joint therefore causing a flexion of the upper body. In this phase maximum rotational speed and therefore angular momentum are achieved during STS movement.

Phase II: During the 'momentum transfer phase' maximum dorsiflexion is achieved. The upper body moves forward and starts to rise upwards. During this phase the hip starts to rise from the seat. This momentum uses the build up momentum from phase I and transfers it into a general upwards movement of the human body. The center of mass moves forward and upwards.

Phase III: After phase II the 'extension' phase starts which sees an extension of the hip and knee joint and an upright posture of the human body. The extension phase starts with the tilting of the upper body from phase II and ends with hip extension.

Phase IV: The final phase starts when the human body is fully extended and therefore standing up right. This final phase stabilizes the body such that the subject doesn't fall. This is particularly important as the human body moves from an intrinsically stable seated position onto a unstable standing position.

However, other studies have described STS movement slightly differently such as (Roebroeck et al., 1994, p. 239): "STS movement is defined as a sequence of two phases. The first phase is called the acceleration phase in which the upper body accelerates horizontally. The second phase is called the transition phase, in which the center of mass decelerates horizontally and accelerates vertically. Thus the transition from forward motion to upward motion is made. Finally, the deceleration begins, where the user decelerates. This phase is defined from maximal vertical velocity of the center of mass until the end of the movement. During this phase the horizontal velocity shows only slight fluctuations about zero."

According to (Vander Linden, 1994, p. 653), STS movement is a "Transitional movement to the upright posture", which "requires movement of the center of mass from a stable to a less stable position over extended lower extremities." (Vander Linden, 1994, p. 656) also describes STS movement as a three phase movement "Phase 1 (flexion-momentum phase) began with initiation of head movement in the horizontal direction and ended with seat-off. Phase 2 (momentum-transfer phase) began with seat-off and ended with maximum ankle dorsiflexion. Phase 3 (extension phase) began with maximum ankle dorsiflexion and continued until erect stance had been obtained."

The determinants that influence STS movement, whether they are subject-related (e.g. age, disease, muscle force, etc.), chair-related (e.g. height, with armrests, etc.) or strategy related (e.g. speed, foot position, trunk movement, etc.) are independent of the phase description. Here, the description by (Schenkman et al., 1990) will be used.

4.2. Kinematics and Kinetcis of Sit-to-Stand Movement

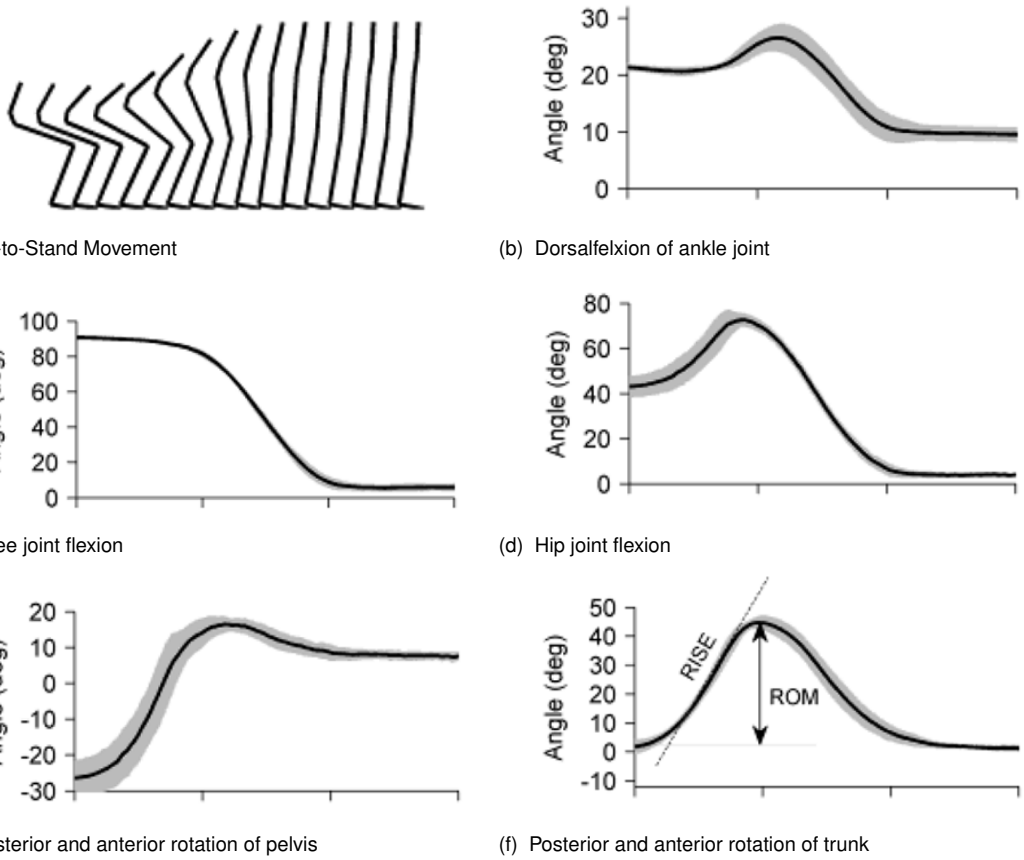

(a) Sit-to-Stand Movement

(b) Dorsalfelxion of ankle joint

(c) Knee joint flexion

(d) Hip joint flexion

(e) Posterior and anterior rotation of pelvis

(f) Posterior and anterior rotation of trunk

Figure 17 Flexion/extension of ankle (b) , knee (c) and hip (d) joint as well as anterior/posterior rotation of pelvis (e) and trunk (f) during Sit-to-Stand movement (a). Pictures taken from (Matjacic et al., 2016)

The aforementioned phase observation follows the mentioned STS strategy in which velocity and angular momentum from the upper body of phase II is transfered into an upward movement of the human body. Fig. 17 illustrates the movement and angle patterns of normal STS movement. At the beginning of STS movement ankle, knee and ankle hip are flexed represented by relatively large angles as seen in Fig. 17b, 17c and 17d respectively. After phase I pelvis and trunk start to lift and rotate into the anterior direction. Knee and hip angles drop sharply as seen in Fig. 17c and 17d until trunk and pelvis reach an almost vertical orientation.

According to (Rutherford et al., 2014, p. 162) at the beginning of phase II, i.e. the initial lifting of the hip from the chair, the highest forces are found in the muscle ‘Vastus Lateralis’ a dominating muscle in the thigh that causes knee extension. Further it was shown that the percentage of the maximum force required varies with age. In Elderly the percentage of the maximum force is higher than in younger subjects. When exactly this part of lifting from the chair is supported by a device or another person, one can deduce that the proportion of the maximum force is reduced, i.e. in converse argumentation the movement of phase II is most challenging during STS movement. This is one of the reasons why elderly have difficulties

standing up. The challenge lies within the force required that a person must raise within the lower extremities (Schenkman et al., 1990, p. 645).

“STS mechanics differ very little between older and younger adults when no significant impairments exist (Hughes et al., 1996; Akram and McIlroy, 2011; Ikeda et al., 1991); however, various populations of individuals have been studied to understand the limitations on STS ability imposed by aging and/or disease. Despite numerous studies that examine external and internal constraints on STS movement characteristics in individuals with limitations in this activity, investigations of adaptive seating designs to overcome these constraints have been lacking. Specifically there is minimal information on how these devices change the mechanical demands (i.e. joint loading and muscle activation) associated with standing up.” (Rutherford et al., 2014, p. 159).

4.3. Chair-Related Influences on Sit-to-Stand Movement

Review papers such as by (Kerr et al., 1991; Janssen et al., 2002) categorized studies according to chair related, subject related or strategy related experiments. Here, with regard to this thesis, chair related influences on STS movement are explained as has been well documented in (Janssen et al., 2002): “The literature indicated that the chair has an influence on the performance of the STS movement (e.g. the height of the seat can make an STS movement impossible). Most research has been focused on the height of the seat, and few studies tried to clarify the influence of the armrest position, use of armrests, or the type of chair on the STS movement.” (Janssen et al., 2002, p. 868ff.)

Seat height

“Lowering the height of the seat makes the STS movement more demanding or even unsuccessful according to the literature we reviewed (Munton et al., 1981; Schenkman et al., 1990; Munro et al., 1998; Hughes et al., 1996; Burdett et al., 1985). The minimum height for successful rising for elderly people (community-dwelling and nursing home residents 64-105 years of age) with chair rise difficulties appears to be 120% of lower leg length. A lower seat apparently leads to increased angular velocity of the hip in order to stand and to more repositioning of the feet (also called the “stabilization strategy”). In young subjects (25-36 years of age) without impairments, lowering the seat of the chair from 115% to 65% of knee height results in an increase in trunk flexion angular velocity of almost 100% in order to stand. A lower seat has been shown to increase trunk, knee and ankle angular displacement. Changing the seat height affects the maximum moment needed at the hip and knee. Differences for hip and knee moments can be as large as 50% to 60%, with seat height can result in changing biomechanical demands (e.g. the need to move the body’s center of mass over a large distance) or in an altered strategy (e.g. “stabilization strategy”, due to the imposed biomechanical demands by a different foot, trunk, or arm position).” (Janssen et al., 2002, p. 874)

Armrests

“Issues related to the armrests use include positioning of the hands on the armrests, height of the armrests, and the moments exerted. There is no research on the relationship among the height of the armrests, seat height, hand positioning, and their cumulative effect on performance of the STS movement.

Using armrests, according to the articles we reviewed, results in lower moments at knee and hip; at the hip, a reduction of about 50% of the extension moment needed to perform the STS movement has been calculated. (Burdett et al., 1985) found no influence of the use of arms on joint angles in subjects without impairments (24-41 years of age). In a study by Alexander et al., young and old subjects without impairments used a hand bar positioned in front of them to perform the STS movement. They found no differences in body segment rotations in the young subjects (19-31 years of age). A difference in trunk rotation was observed in the old subjects (63-86 years of age), although this movement was analyzed only at the moment of maximum anterior head displacement.” (Janssen et al., 2002, p. 874)

Chairtype

“We found only three studies on the influence of specially designed chairs. Different types of chairs designed to “ease” the STS movement were studied. (Wheeler et al., 1985) suggested a negative influence of seat posterior slant because of tilting the body’s center of mass farther backward. use of an ejector mechanism lowered vertical impulses applied to the armrests by 47% in patients with arthritis, but no differences were found for knee and ankle moments.” (Janssen et al., 2002, p. 874)

Backrests

“We found no experimental studies concerning the influence of backrests of STS movement. In only eight studies was a chair with a backrest used. When a backrest was used, it was to standardize the STS movement starting position. The influence of trunk position has been studied; however, this influence cannot necessarily be related to backrest use or backrest position, because the trunk position studied was not comparable to the trunk position using a backrest.” (Janssen et al., 2002, p. 874)

5. Individualized Computational Bio-Kinematic Design Procedure

In this chapter a computational design procedure is described that calculates the dimensions of a lift-assist mechanism to fit to the dimensions of the user with respect to a limited workspace in which the mechanism must fit inside. An overview of the process is seen in Fig. 18. At first the biomechanical structure of the human is analyzed and different kinematic models that aim to represent the kinematics of the human are compared. This is followed by forming individualized task positions with respect to a kinematic structure of the LAD. The third step consists of finite position synthesis given the task positions of the user as well as the workspace restrictions of the chair. If a solution exists, a kinematic analysis of the total structure, i.e. LAD and user combined, is carried out in the final step.

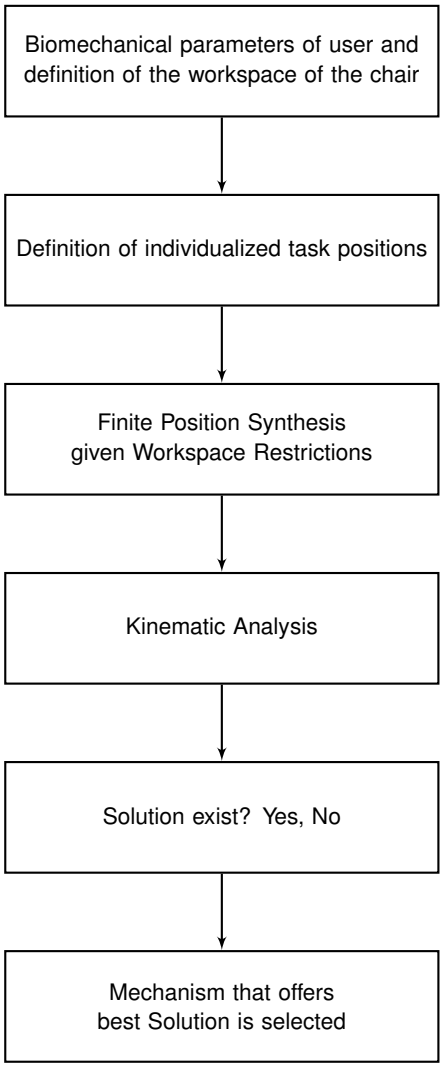

Figure 18 Overview of the computational bio-kinematic design procedure

5.1. Bio-Kinematic Representation of Lower Limb and Lift-Assist Device

STS movement has been analyzed extensively. It shows that the motion can be generally split into four phases within the sagittal plane (see Fig. 2). At the beginning the human body is in a stable sitting position. Next, hip flexion occurs which lifts the feet from the ground slightly decreasing ground reaction force. Phase two ends when the body begins to stand up. The final phase lasts until a stable standing position is reached. The kinematic behavior of the lower limb is frequently modeled as a serial kinematic chain which describes shank, thigh and trunk as rigid links connected by revolute joints that mimic ankle, knee and hip joint. Note, that this clearly defines a particularly simplified view point, which, however will be sufficient for our purposes. Linkages studied in this thesis are build from two elementary joints, the rotary hinge, called a *revolute* joint (denoted by R), and a linear slider, or *prismatic* joint (denoted by P).

In order to individualize the LAD to the user's leg geometry and movement we investigated possible simplified kinematic representations that connect the human leg (blue) with the four-bar structure (black) of the LAD as seen in Fig. 19.

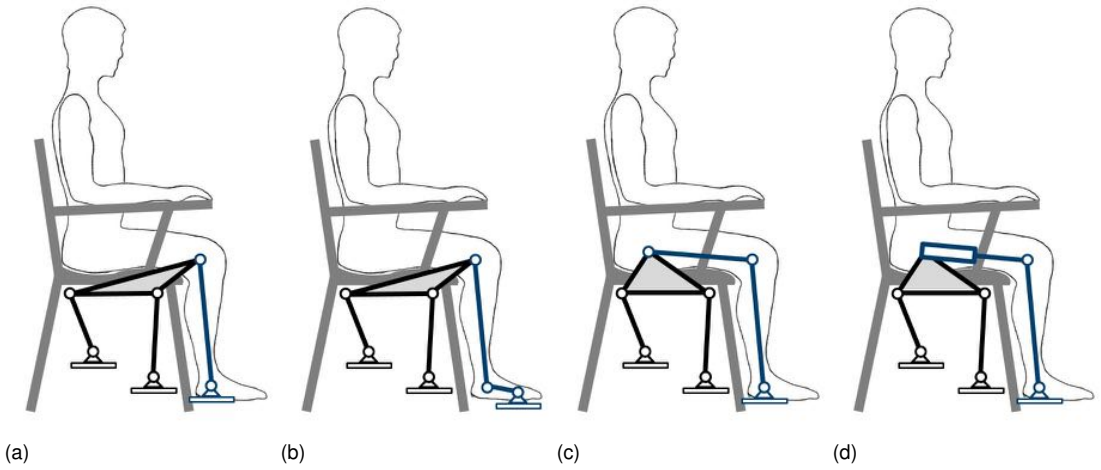

Figure 19 Kinematic representations of the lower limb (blue) and lift-assist device (black) as a five-bar (a), six-bar ((b) and (c)) and six-bar with prismatic joint (d) linkage structure

Thus, the thigh is considered to be in continuous contact with the seat, i.e. the coupler of the four-bar linkage (see Fig. 19a). However, in this case one can immediately deduce that the structure cannot move because applying the *Chebychev-Grübler-Kutzbach criterion* yields a DOF of $F = 3(n - 1 - g) + \sum_{i=1}^{g} b_i = 3(5 - 1 - 6) + 6 = 0$, where g and n are the number of revolute joints and links respectively. b_i represents the number of DOF for the ith joint. Hence, to obtain a suitable linkage we must integrate another link and joint either into the LAD or into the human model to achieve 1 DOF.

Increasing the complexity of the LAD is generally unfavorable as this has ramifications on

workspace, actuation, weight and cost of the kinematic assembly. However, there exist several scenarios how to implement a suitable joint into the lower limb model. Implementing a joint at the toe as seen in Fig. 19b would imply that there is continuous movement between heel and ground while the user rises from the chair. This is often the case for people whose leg length is shorter than the height of the chair. During STS movement they touch ground first with their toes before their heel is lowered to ground. However, the majority of the STS transition occurs after the person has reached a stable foot position on the ground rendering any further movement of the LAD impossible.

Alternatively, Fig. 19c displays a linkage model with a modeled hip joint. The leg is now modeled as a 3R chain connected to the coupler of the four-bar linkage. The revolute joint situated at the hip is a logical modification as there is generally some rotary movement about the hip when the seat lifts the individual.

Fig. 19d replaces the revolute joint at the hip with a prismatic joint. This imitates linear sliding of the hip on the seating surface during STS movement. Hip sliding occurs when the persons pelvis gradually moves forward during seating. Sliding on the seat is generally more uncomfortable and ought to be avoided. Hence, we continue with the 7R linkage configuration as shown in Fig. 19c.

The three different approaches from Fig. 19b - 19d may all be seen as valid models, if the joint movement in the corresponding R or P joint approximately vanishes during STS motion. This is possible if appropriate kinematic dimensions of the four-bar LAD can be synthesized. Once a four-bar synthesis is completed, kinematic analysis of the six-bar linkage must detect, whether the considered joint motion stays approximately constant.

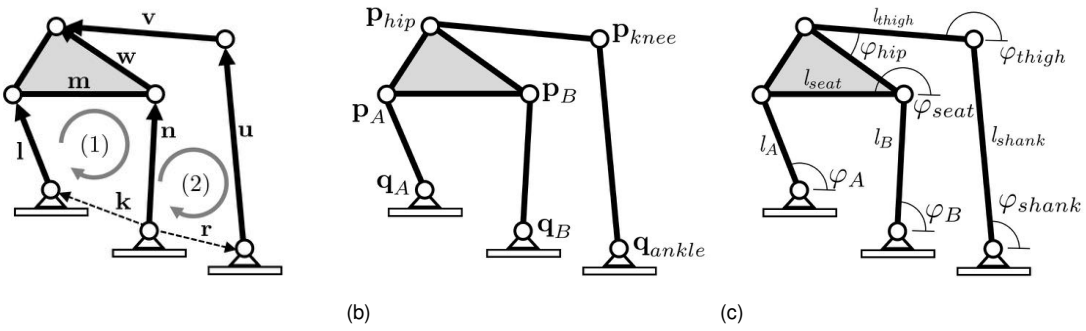

Figure 20 Nomenclature of links and two closed loops (1) and (2) (a), joints (b) and link length and angles of a 7R kinematic interpretation of lift-assist device and lower limb (taken from (Reimer et al., 2017))

The system from Fig. 19c is also known as a *Stephenson III* linkage (see Fig. 20). The lower limb model consists of a fixed pivot point at the ankle, $\mathbf{q}_{ankle}$, and two moving pivots each with one DOF representing the knee, $\mathbf{p}_{knee}$, and hip joint, $\mathbf{p}_{hip}$. The hip joint is attached to a coupler of the four-bar linkage which represents the LAD. The LAD consists of two 2R chains, link A which consists of two revolute joints $\mathbf{q}_A$ and $\mathbf{p}_A$ and link B which consists of $\mathbf{q}_B$ and $\mathbf{p}_B$. The length of link A and B is yet to be determined. Once suitable parameters for the two

links are found, the movement of the linkage and in particular the movement between lower limb and LAD can be analyzed. In fact, the angle φ_{hip} between the coupler described by $\mathbf{p}_A$, $\mathbf{p}_B$ and $\mathbf{p}_{hip}$ and the thigh described by $\mathbf{p}_{knee}$ and $\mathbf{p}_{hip}$ will be of interest in this approach. Since rotary movement between human leg and seating surface is inevitable, the four-bar link dimensions should satisfy

$$\varphi_{hip} \approx const. \tag{5.1}$$

within a user-specific range of motion so as to allow a smooth transition of the user from sit-to-stand.

5.2. Dimensional Finite Position Synthesis

The simplest planar structure that has one DOF is a four-bar linkage. Four-bars consist of two 2R diads. These diads are connected by a third link which is called the coupler as it couples the two diads. Four-bar linkages have numerous applications as it is advantages when certain movements must be repeated precisely as is the case with STS movement.

In this section we examine the design of 2R planar open chains that reach a specified set of task positions. A constraint equation is defined for each chain that characterizes the set of positions that it can reach. This relationship is inverted by considering the positions as known and the fixed and moving pivots of the chain as unknowns. The result is a set of design equations that are solved to design the chain.

Two of these chains can be connected to the moving body to form a one-DOF planar four-bar linkage. This closed chain can be used as a function generator which provides coordinated movement of the input and output links. such a connection, however, limits the movement of the two chains and can interfere with the smooth travel of the workpiece through the task positions. Techniques used to avoid this problem are known as solution rectification.

The very foundation of this work builds upon *Burmester's theory* on a geometric technique for synthesis of linkages. What linkage is required in order to create an ergonomic STS movement? What dimensions must the linkage have in order for the LAD to lift the user as well as to fit inside of the chair? To answer the questions we examine the geometric design of linkages.

"A linkage is a collection of interconnected components, individually called links. The physical connection between two links is called a joint." - (McCarthy and Soh, 2011, P. 1) In this work we limit our attention to joints that consist of either a rotary movement, called a *revolute* joint (denoted by R) or joints that slide linearly, called a prismatic joint (denoted by P).

To define a moving body in planar kinematics, we need to know its translation along the x- and y-axis as well its rotation or orientation relative to a fixed coordinate frame. Let's consider

a coordinate frame M fixed to the moving body. The body and therefore the coordinate frame is initially aligned with the fixed world coordinate frame W. A vector in the moving coordinate frame is defined by ${}^{M}\mathbf{p}$. When translating M to a new position, say M' by a constant displacement $\mathbf{t} = [x_t, y_t]^T$. The new position of ${}^{M}\mathbf{p}$ becomes

$$ {}^{W}\mathbf{p}' = {}^{M}\mathbf{p} + \mathbf{t}. \tag{5.2}$$

Rotation of M creates an angle φ around between the x-axis of W and the x-axis of the roated moving body M'. Let $\vec{i} = [1, 0]^T$ and $\vec{j} = [0, 1]^T$ define the unit vectors of M and $\mathbf{e}_x$ and $\mathbf{e}_y$ be the unit vectors along the x- and y-axis of M', then

$$ \mathbf{e}_x = \vec{i}\cos\varphi + \vec{j}\sin\varphi \text{ and } \mathbf{e}_y = -\vec{i}\sin\varphi + \vec{j}\cos\varphi. \tag{5.3}$$

Thus the rotation a vector in M, ${}^{M}\mathbf{p}$ by φ can be written in matrix form as

$$ {}^{W}\mathbf{p}' = \mathbf{R}(\varphi)\ {}^{M}\mathbf{p} = \begin{bmatrix} \cos\varphi & -\sin\varphi \\ \sin\varphi & +\cos\varphi \end{bmatrix} \begin{Bmatrix} x \\ y \end{Bmatrix} \tag{5.4}$$

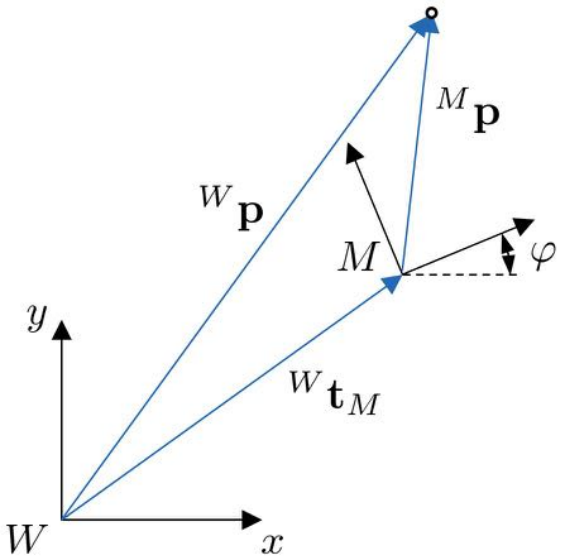

Figure 21 Planar displacement of a fixed point within a moving coordinate frame M with respect to a fixed world coordinate frame W

Eq. 5.2 - 5.4 define the general planar displacement as seen in Fig. 21 of the coordinate frame M to M^i. This consists of an initial rotation followed by a translation which is commonly expressed as the *displacement* equation

$$ {}^{W}\mathbf{p}^i = {}^{W}\mathbf{R}^i_M \cdot {}^{M}\mathbf{p} + {}^{W}\mathbf{t}^i_M \tag{5.5}$$

It is convenient to assemble the rotation matrix and translation vector into a single 3×3 matrix

$[T]$, called a homogeneous transformation matrix which takes the form

$$\begin{Bmatrix} x_{\mathbf{p}^i} \\ y_{\mathbf{p}^i} \\ 1 \end{Bmatrix} = \begin{bmatrix} \cos\varphi & -\sin\varphi & x_{\mathbf{t}^i} \\ \sin\varphi & \cos\varphi & y_{\mathbf{t}^i} \\ 0 & 0 & 1 \end{bmatrix} \begin{Bmatrix} x_{\mathbf{p}} \\ y_{\mathbf{p}} \\ 1 \end{Bmatrix} \tag{5.6}$$

Let i task positions be specified by the transformations $[\mathbf{T}^1] = [\mathbf{R}(\varphi_1), \mathbf{t}_1]$ up to the ith transformation $[\mathbf{T}^i] = [\mathbf{R}(\varphi_i), \mathbf{t}_i]$. Similarly to Eq. 5.5 $[\mathbf{T}^1]$ can be expressed as *displacement* equations

$${}^W\mathbf{p}^1 = {}^W\mathbf{R}^1_M \cdot {}^M\mathbf{p} + {}^W\mathbf{t}^1_M \;\leftrightarrow\; {}^M\mathbf{p} = ({}^W\mathbf{R}^1_M)^T \cdot ({}^W\mathbf{p}^1 - {}^W\mathbf{t}^1_M) \tag{5.7}$$

Solving Eq. 5.7 for ${}^M\mathbf{p}$ and substituting into Eq. 5.5 yields

$${}^W\mathbf{p}^i = \underbrace{{}^W\mathbf{R}^i_M \cdot ({}^W\mathbf{R}^1_M)^T}_{{}^W\mathbf{R}^{1i}_M(\varphi^{1i})} \cdot {}^W\mathbf{p}^1 + \underbrace{{}^W\mathbf{t}^1_M - {}^W\mathbf{R}^i_M \cdot ({}^W\mathbf{R}^1_M)^T \cdot {}^W\mathbf{t}^1_M}_{{}^W\mathbf{t}^{1i}_M}, \; i = 2, ..., n. \tag{5.8}$$

Note that in Eq. 5.8 all M-frame coordinates have been eliminated. Therefore for simplicity the top left suffix is ignored for all future coordinates as they contain W-frame coordinates unless specified otherwise. Eq. 5.8 is the first significant equation in the design procedure since it calculates the pivot points in a reference configuration based on specified movement of the set of task positions.

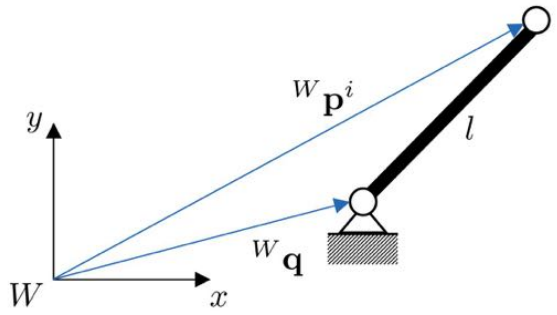

Figure 22 Characteristics of the *constant constraint equation* which characterizes the 2R chain

The second equation is represented by the geometric constraint of each 2R diad as seen in Fig. 22, which is the fixed length between the two revolute joints. This is known as the *constant distance constraint*

$$l^2 = (\mathbf{p}^i - \mathbf{q})^T(\mathbf{p}^i - \mathbf{q}), \qquad i = 1, ..., n. \tag{5.9}$$

Subtracting Eq. 5.9 for $i = 1$ from Eq. 5.9 eliminates l.

$$(\mathbf{p}^i - \mathbf{q})^T(\mathbf{p}^i - \mathbf{q}) - (\mathbf{p}^1 - \mathbf{q})^T(\mathbf{p}^1 - \mathbf{q}) = 0, \qquad i = 2, ..., n \tag{5.10}$$

Rearranging Eq. 5.10 and simplifying yields

$$(\mathbf{p}^i)^T\mathbf{p}^i - (\mathbf{p}^1)^T\mathbf{p}^1 - 2(\mathbf{p}^i - \mathbf{p}^1)^T\mathbf{q}, \qquad i = 2, ..., n. \tag{5.11}$$

Applying the third binomial theorem to Eq. 5.11 yields

$$(\mathbf{p}^i - \mathbf{p}^1)^T \cdot (\frac{\mathbf{p}^i - \mathbf{p}^1}{2} - \mathbf{q}), \qquad i = 2, ..., n. \tag{5.12}$$

Finally substituting the relative displacement equation Eq. 5.8 into Eq. 5.12 and rearranging yields

$$(\mathbf{p}^1)^T \cdot (\mathbf{E} - \mathbf{R}_M^{1i})^T \cdot \mathbf{q} + (\mathbf{t}_M^{1i})^T \cdot \mathbf{R}_M^{1i} \cdot \mathbf{p}^1 - (\mathbf{t}_M^{1i})^T \cdot \mathbf{q} + \frac{1}{2}(\mathbf{t}_M^{1i})^T \cdot \mathbf{t}_M^{1i} = 0 \tag{5.13}$$

for $i = 2$,...,n and where $\mathbf{E}$ is the 2×2 identity matrix. By solving this set of equations we can calculate the coordinates of each link's pivot points in reference configuration 1 of the linkage. Eq. (5.13) is known as the algebraic *design* equation of planar 2R chains, where motion quantities $\mathbf{R}_M^{1i}$ and $\mathbf{t}_M^{1i}$ are given and $\mathbf{q} = (x_\mathbf{q}, y_\mathbf{q})^T$ and $\mathbf{p}^1 = (x_{\mathbf{p}^1}, y_{\mathbf{p}^1})^T$, are four unknown W-frame coordinates. Hence, the maximum number of task positions of the thigh is $n = 5$, since then there are four equations in four unknowns.

Eq. (5.13) is often simplified such that the known parameters are represented by one variable respectively

$$(\mathbf{p}^1)^T \cdot \mathbf{M}^{1i} \cdot \mathbf{q} + (\lambda^{1i})^T \cdot \mathbf{p}^1 + (\mu^{1i})^T \cdot \mathbf{q} + \epsilon^{1i} = 0 \tag{5.14}$$

where $\mathbf{M}^{1i} = (\mathbf{E} - \mathbf{R}_M^{1i})^T$, $(\lambda^{1i})^T = (\mathbf{t}_M^{1i})^T \cdot \mathbf{R}_M^{1i}$, $(\mu^{1i})^T = -(\mathbf{t}_M^{1i})^T$ and $\epsilon^{1i} = \frac{1}{2}(\mathbf{t}_M^{1i})^T \cdot \mathbf{t}_M^{1i}$.

```
1   M_12 = (E - R_12)';
2   M_13 = (E - R_13)';
3
4   lambda_12_transp = (t_12)'*R_12;
5   lambda_13_transp = (t_13)'*R_13;
6
7   mue_12_transp = -(t_12)';
8   mue_13_transp = -(t_13)';
9
10  epsilon_12 = 0.5*(t_12)'*t_12;
11  epsilon_13 = 0.5*(t_13)'*t_13;
```

Given two task positions we receive one *design* equation, which can only be solved when three of the four unknown parameters are defined. Similarly, when three task positions are defined two unknown parameters must be set to solve the pair of equations $i = 2$ and $i = 3$. Say that the $\mathbf{p}$ of a 2R diad was defined such that $\mathbf{p} = (x_\mathbf{q} y_\mathbf{q})^T$ are known. Rearranging Eq.

5.14 for $\mathbf{p}$ yields

$$\underbrace{(\mathbf{q}^T \cdot (\mathbf{M}^{1i})^T + (\lambda^{1i})^T)}_{(a^i(\mathbf{q})\ b^i(\mathbf{q}))} \cdot \underbrace{\mathbf{p}^1 + (\mu^{1i})^T \cdot \mathbf{q} + \epsilon^{1i}}_{r^i(\mathbf{q})} = 0 \qquad i = 2, 3. \tag{5.15}$$

Now a linear system of equations can be constructed

$$\underbrace{\begin{bmatrix} a^2(\mathbf{q}) & b^2(\mathbf{q}) \\ a^3(\mathbf{q}) & b^3(\mathbf{q}) \end{bmatrix}}_{\mathbf{K}} \underbrace{\begin{bmatrix} x_\mathbf{q} \\ y_\mathbf{q} \end{bmatrix}}_{\mathbf{q}} = \underbrace{\begin{bmatrix} r^2 \\ r^3 \end{bmatrix}}_{\mathbf{v}} \tag{5.16}$$

Therefore

$$\mathbf{q} = \mathbf{K}^{-1} \cdot \mathbf{v} \tag{5.17}$$

Which can be solved in MATLAB using the following

```
1   hor_12 = q'*M_12' + lambda_12_transp; %hor stands for horizontal
2   hor_13 = q'*M_13' + lambda_13_transp; %transp stands for transposed
3
4   a_12 = hor_12(1,1);
5   b_12 = hor_12(1,2);
6   a_13 = hor_13(1,1);
7   b_13 = hor_13(1,2);
8
9   r_12 = mue_12_transp*q + epsilon_12;
10  r_13 = mue_13_transp*q + epsilon_13;
11
12  K = [a_12 b_12; a_13 b_13];
13  v = [-r_12; -r_13];
14
15  q = K\v;
```

5.3. Number and Definition of Task Positions

The aforementioned algebraic synthesis is able to determine the coordinates of $\mathbf{q}_A$, $\mathbf{q}_B$ $\mathbf{p}_A^1$ and $\mathbf{p}_B^1$. However, it does not necessarily comply with the prerequisite that all coordinates in configuration 1, i.e. the *sit* configuration of the LAD, lie within the dimensions of the chair. From Fig. 19c it is apparent that the workspace for $\mathbf{p}^1$ and $\mathbf{q}$ must lie underneath the seat and between the chair legs. While $\mathbf{q}$ can be located anywhere within this space $\mathbf{p}^1$ is further limited by the fact that it acts as the rotary joint of the seat and therefore $\mathbf{p}^1$ should ideally be attached as close to the seat as possible.

Earlier it was described that a maximum number of $n = 5$ task positions can be defined in

order to ensure a continuous user-specific STS movement. When specifying the maximum number of task positions the four-bar linkage will be more likely to follow the movement of the user. In turn, however, we receive four *design* equations in four unknowns. Therefore, none of the parameters of $\mathbf{p}^1$ and $\mathbf{q}$ can be specified such that they are within the workspace of the chair.

Decreasing the number of task positions to $n = 4$ results in three *design* equations. Hence, one of the four unknown parameters can be confined within the workspace of the chair. $\mathbf{p}^1$ is more limited than $\mathbf{q}$. Therefore $x_{\mathbf{p}^1}$ or $y_{\mathbf{p}^1}$ may be preallocated within a particularly narrow space while the three remaining parameters are obtained from solving the three design equations, see (McCarthy and Soh, 2011). However, this still means that we cannot ensure, whether $\mathbf{p}^1$ lies within the given space. For these reasons we consider $n = 3$, which yields two *design* equations. Thus, we are unrestricted to specify $\mathbf{p}^1$ in regard of the desired space and may solve for $\mathbf{q}$ linearly (see (McCarthy and Soh, 2011)).

5.3.1. Definition of Task Positions based on the Individual User

Each task position is defined by its position and orientation. To define these variables for each of the three task positions we analyze STS movement of the individual using a motion tracking system or applying statistical values of anthropometric data. While the former method provides data that supports an individually designed mechanism the former method could be used to define categories such as shoe sizes that could fit to a cluster of users in a certain range of height. The former method will be illustrated in

STS movement of the individual can be recorded using marker-based motion capturing cameras which emit infrared light to detect reflective passive markers attached to the human. Markers are positioned at the hip, knee and ankle joint of the lower limb and a reference marker placed onto the chair. This allows for capturing discrete three-dimensional motion data of $\mathbf{p}^i_{hip}$, $\mathbf{p}^i_{knee}$ and $\mathbf{q}_{ankle}$.

Task positions of the seat are derived from captured motion data. Given vector $\mathbf{p}^i_{hip}$ and $\mathbf{p}^i_{knee}$, we can determine the translation $\mathbf{t}^i_M$ and orientation $\mathbf{R}^i_M(\varphi^i_{thigh})$ where $\mathbf{t}^i_M = \mathbf{p}^i_{knee}$ and φ^i_{thigh} is measured from the x-axis of W to the vector from $\mathbf{p}^i_{knee}$ to $\mathbf{p}^i_{hip}$.

The third task position defines the *end* configuration of the supported movement, which could, for example, be assessed by a doctor or physiotherapist depending on the support that the individual requires. The second task position is in between the first' and last'. Repetitions of the STS movement produce a range of possible $\mathbf{p}^i_{hip}$ and $\mathbf{p}^i_{knee}$ values, and therefore a set of different $\mathbf{t}^i_M$ value for $i = 2$ and 3. Note, that the first position is not considered to vary here. Each set defines an upper and lower boundary of possible values for $\mathbf{t}^i_M$ defined by x^i_{min}, x^i_{max} and y^i_{min}, y^i_{max}. Discrete values in this range can be inserted into $\mathbf{t}^i_M$ and $\mathbf{R}^i_M(\varphi^i_{thigh})$ for $i = 2$ and 3. The result is a set of task positions that will yield a set of four-bars each of which may be analyzed with regard to Eq. (5.1).

5.3.2. Definition of Task Positions based on Anthropometric Data

The second method to define task positions is to use statistically determined anthropometric data. The dimensions of human beings are normally distributed and can be found in tables such as the DIN 33402-2:2005-12 Ergonomie - Körpermaße des Menschen. This document provides the mean human body measurements such as height, length and width of lower limb, etc. of the user for females and males in Germany for the 5th, 50th and 95th percentile. The 50th percentile represents the mean which means that 50% of the population are either below or above the mean. Similarly the 5th percentile represents the number for which 5% of the population are below that value and 95% are above. The 95th percentile is analogues to the 5th percentile in which 5% are larger than this value.

Given the biological model of the user as seen from Fig. 19c we can simulate the movement of the lower limb and determine the information required from DIN 33402. Fig. 24 represents the user in a seated position. To define this as well as the other two task position we need to determine the body measurements required to calculate the task positions for each user.

The first task position is defined as the *sit* task position. The second task position will be called as the transitional task position, while the final task position is defined as the stand *stand* task position. Each task positions is characterized by its orientation φ^i and position ${}^W\mathbf{t}^i_M$. Since it is our aim to create an ergonomic movement of the seat that is identical to the movement of the human thigh it is convenient to attach the coordinate frame M rigidly to the knee $\mathbf{p}_knee$ joint of the user which is also defined as the moving rotational joint $\mathbf{p}^i_{knee}$. Thus the translation of M in the xy-plane of W is measured using the 2×1 translation vector $\mathbf{t}^i_M = \mathbf{p}^i_{knee}$. Orientation of M with respect to W shall be measured using the angle φ^i_{thigh} and shall be described using a proper 2×2 rotation matrix $\mathbf{R}^i_M(\varphi^i_{thigh})$ as seen in Fig. 23.

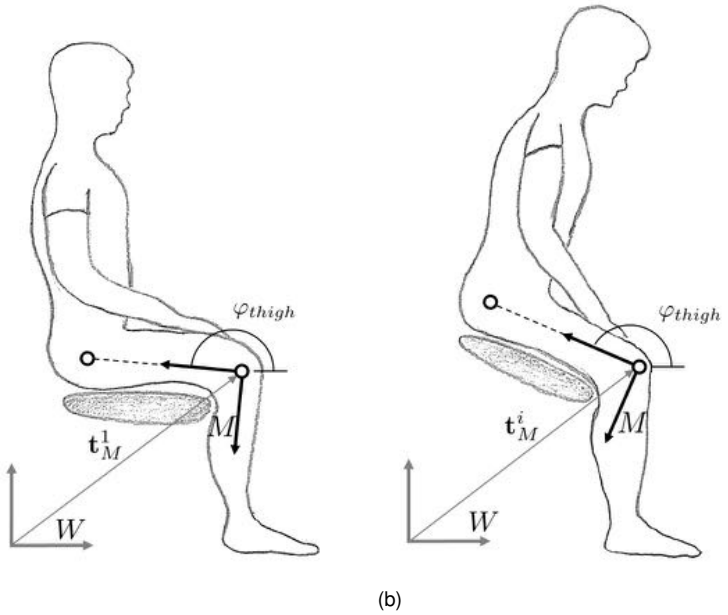

(a) (b)

Figure 23 Task positions of frame M in configuration 1 (a) and configuration i (b) with respect to a world coordinate frame W (Pictures taken from (Reimer et al., 2017))

Task Position: Sit

Geometrically the user is expected to sit on the chair such that his back rest gently against the backrest of the chair. In that case the hip joint, modeled as $\mathbf{p}^1_{hip}$ is located at half the body width along and half the thigh width along the x-axis and y-axis respectively as seen in Fig. 24. The thigh and shank will be positioned such that the shank is oriented perpendicular to the ground, i.e. the x-axis. Given the height of the chair one can compute the angle φ^1_{thigh}

$$\varphi^1_{thigh} = \pi - \arcsin\left(\frac{c_{height} + \frac{1}{2} \cdot h - l_{shank}}{l_{thigh}}\right) \tag{5.18}$$

where c_{height} is the height of the chair. The position of the M coordinate frame is therefore located at

$${}^W\mathbf{p}^1_{knee} = \begin{pmatrix} l_{thigh} \cdot sin(\varphi^1_{thigh} - 90°) \\ \\ l_{shank} \end{pmatrix} \tag{5.19}$$

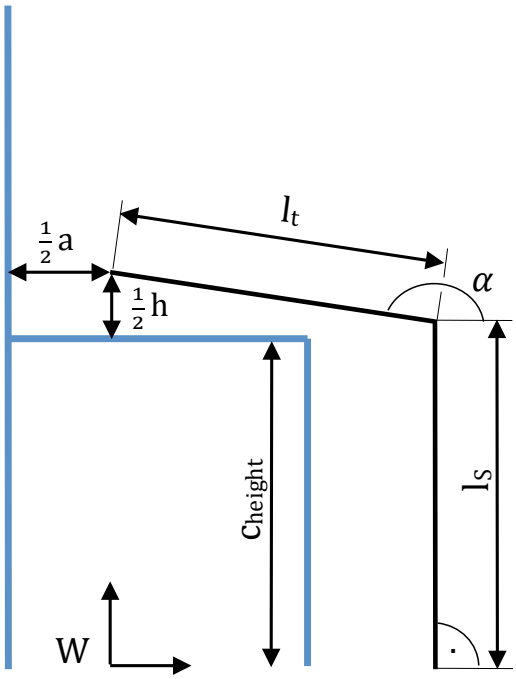

Figure 24 Schematic view of the first task position (Drawing by Corinna Eder)

Task Position: Transition

The second task position is the transitional task position between the *sit* and *stand* configuration. The transitional task position was characterized arbitrarily at a knee flexion of 60° as seen in Fig. 25 which implies that φ^2_{thigh} = 130° and φ^2_{shank} = 70°. The position of the M coordinate frame is therefore located at

$$ {}^{W}\mathbf{p}^2_{knee} = \begin{pmatrix} l_{thigh} \cdot sin(\varphi^2_{thigh} - 90°) + l_{shank} \cdot cos(70°) \\ \\ l_{shank} \cdot sin(70°) \end{pmatrix} \tag{5.20} $$

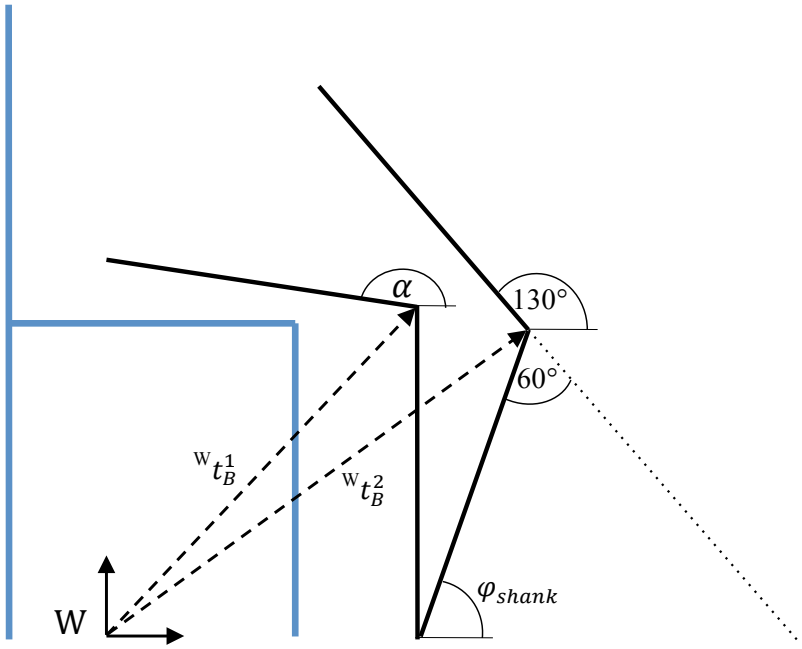

Figure 25 Schematic view of the first and second task position (Drawing by Corinna Eder)

Task Position: Stand

The final task position is defined at a knee flexion of 20° as seen in Fig. 26. While standing would imply no knee flexion - as the thigh is approximately aligned with the shank - this angle was chosen, again arbitrarily to illustrate the concept behind this computational bio-kinematic approach to individualize this particular lift-assist mechanism. The *stand* task position is therefore positioned at

$$ {}^{W}\mathbf{p}^{3}_{knee} = \begin{pmatrix} l_{thigh} \cdot sin(\varphi^{3}_{thigh} - 90°) + s \cdot cos(80°) \\ \\ l_{shank} \cdot sin(80°) \end{pmatrix} \tag{5.21} $$

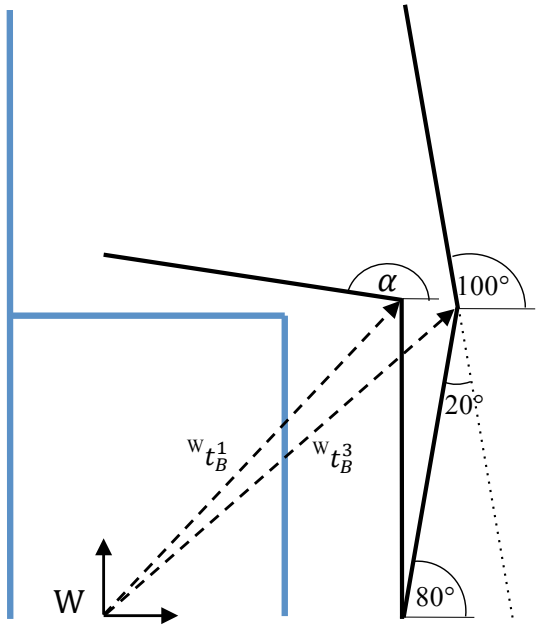

Figure 26 Schematic view of the first and third task position (Drawing by Corinna Eder)

Table 2 Definition of task positions

Task Position	Orientation φ^i	Position ${}^W\mathbf{t}_B^i$
Sit ($i = 1$)	φ^1_{thigh}	$\begin{pmatrix} l_{thigh} \cdot sin(\varphi^1_{thigh} - 90°) \\ l_{shank} \end{pmatrix}$
Transition ($i = 2$)	130°	$\begin{pmatrix} l_{thigh} \cdot sin(\varphi^2_{thigh} - 90°) + l_{shank} \cdot cos(70°) \\ l_{shank} \cdot sin(70°) \end{pmatrix}$
Stand ($i = 3$)	100°	$\begin{pmatrix} l_{thigh} \cdot sin(\varphi^3_{thigh} - 90°) + s \cdot cos(80°) \\ l_{shank} \cdot sin(80°) \end{pmatrix}$

The task positions are summarized in Tab. 2. To calculate each task position we require data on the length of the thigh l_{thigh}, the shank l_{shank}. Further to determine $\varphi^1_t high$ we must determine the width of the thigh a and the width of the body h as summarized here:

- Femoral length l_{thigh}
- Tibial length l_{shank}
- Width of the thigh w_{thigh}
- Body depth w_{body}

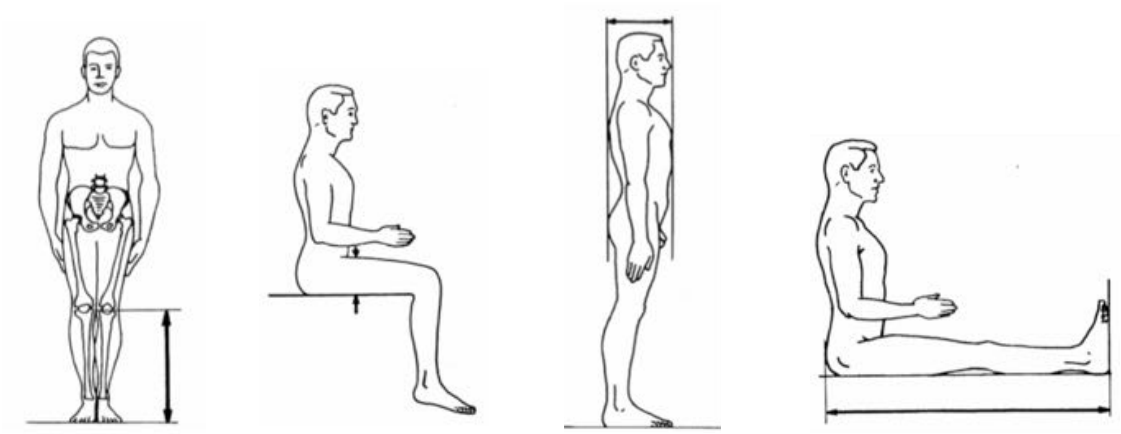

Figure 27 Tibial length, width of thigh, body width and total length of lower limb taken from DIN 33402-2:2005-12

As seen in Fig. 27, DIN 33402 provides statistical body measurements on the tibial length l_{shank}, width of the thigh w_{thigh}, width of the body w_{thigh} and total lower limb length l_{leg}. Since the femoral length it is calculated by subtracting half of the body length and the tibial length as seen here

$$l_{thigh} = l_{leg} - l_{shank} - \frac{1}{2} \cdot w_{body} \tag{5.22}$$

Table 3 lists the body measurements for the 5th, 50th and 95th percentile for female and males for 18 - 65 year olds.

Table 3 Anthropometric Data based on DIN 33402-2:2005-12

Segment	Gender	5th Percentile	50th Percentile	95th Percentile
Tibial length l_{shank}	male	430 mm	460 mm	480 mm
	female	400 mm	425 mm	450 mm
Width of thigh w_{thigh}	male	130 mm	150 mm	180 mm
	female	125 mm	145 mm	175 mm
Width of body w_{body}	male	260 mm	285 mm	380 mm
	female	245 mm	290 mm	345 mm
Total length of lower limb w_{leg}	male	965 mm	1045 mm	1140 mm
	female	925 mm	990 mm	1055 mm
Calculated femoral length l_{thigh}	male	405 mm	442.5 mm	470 mm
	female	402.5 mm	420 mm	432.5 mm

5.4. Exhaustive Search for suitable Dyads

The four-bar linkage is to be synthesized such that its dimensions fit into the chair illustrated in Fig. 28. The workspace has a rectangular area which is 437 mm in height and 396 mm in width as seen in Fig. 28.

The values of $\mathbf{p}^1$ are varied inside the workspace along the x-axis in 200 mm steps and in 200 mm steps in the negative direction of the y axis. For each position of $\mathbf{p}^1$ q values are calculated according to Eq. 5.17. When a $\mathbf{q}$ value exists its corresponding $\mathbf{p}^1$ and the $\mathbf{q}$ value are saved in a matrix. Table 4 shows the result of an exhaustive search of the 50th percentile group of men.

Table 4 $\mathbf{q}$ und $\mathbf{p}^1$ of 2R chains of the 50th male percentile

x_q	y_q	x_p	y_p
-122.1381	411.2290	217.5000	217.4000
-2.3186	417.0006	237.5000	237.4000
-61.5232	389.5234	237.5000	217.4000
-133.7908	357.0829	237.5000	197.4000

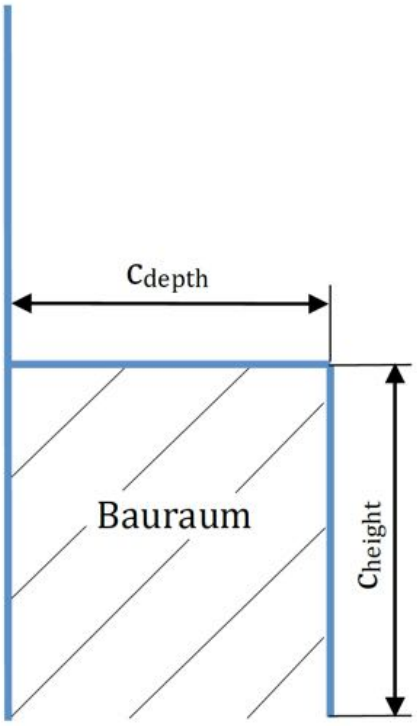

Figure 28 Available workspace for the four-bar linkage (Drawing by Corinna Eder)

From Table 4 we receive four possible 2R dyads, however combining the values gives us a total of six different four-bar constellations. The number of constellations based on different 2R dyads can be determined given the binomial coefficient equation

$$\frac{n!}{(n-k)! \cdot k!} = \binom{n}{k} \tag{5.23}$$

Given the mentioned range of values for $\mathbf{t}_M^i$, $\mathbf{p}_A^1$, $\mathbf{p}_B^1$ and $\mathbf{R}_M^i(\varphi_{thigh}^i)$, where $i = 2, 3$, an exhaustive search can be conducted to find real solutions for $\mathbf{q}_A$ and $\mathbf{q}_B$ that are within the boundaries of the chair frame. This yields eight variables for each 2R diad configuration.

An exhaustive search, also known as a *brute-force method* is a well known problem-solving technique of systematically enumerating all possible parameter configurations and may find a solution. With respect to the amount of open parameters it is important to reduce the range of values for each parameter as much as possible to avoid a *combinatorial explosion*.

Should a solution be found it is worth increasing the depth of search within a smaller radius of the open parameters to find a set of solutions for the four-bar linkage configuration.

5.5. Kinematic Analysis

Once a set of linkage configurations is found a kinematic analysis of the earlier mentioned *Stephenson III* linkage is applied to validate Eq. (5.1). The solution that satisfies Eq. (5.1) best is chosen. Retrace from Fig. 20 that φ_{hip} may be calculated easily from a given φ_{thigh} and φ_{seat}

A linkage analysis determines each of the joints angles for a given input angle. For the linkage φ_{thigh} is the input rotation and φ_A, φ_B, φ_{seat} and φ_{shank} are the unknown output rotations. In order to solve the relationship between input and output angles we introduce a fixed world frame W and split the six-bar linkage into two seperate vector loops. The first loop consists of the 4R chain, $\mathbf{q}_A$, $\mathbf{p}_A$, $\mathbf{p}_B$ and $\mathbf{q}_B$, while the second loop is expressed by the 5R chain, $\mathbf{q}_B$, $\mathbf{p}_B$, $\mathbf{p}_{hip}$, $\mathbf{p}_{knee}$ and $\mathbf{q}_{ankle}$ as seen in Fig. 20. From each loop two *constraint* equations can be obtained that are

$$\mathbf{f}(\overrightarrow{\phi}) = \begin{bmatrix} f_1(\overrightarrow{\phi}) \\ f_2(\overrightarrow{\phi}) \\ f_3(\overrightarrow{\phi}) \\ f_4(\overrightarrow{\phi}) \end{bmatrix} = \begin{bmatrix} \mathbf{k}+\mathbf{l}-\mathbf{m}-\mathbf{n} \\ \mathbf{n}+\mathbf{w}-\mathbf{v}-\mathbf{u}-\mathbf{r} \end{bmatrix} = \overrightarrow{0} \tag{5.24}$$

where $\mathbf{f}$ contains the functions $f_i(\overrightarrow{\phi})$ and $\overrightarrow{\phi}$ contains the independent variables φ_A, φ_B, φ_{seat} and φ_{shank}. Expending Eq. (5.24) produces four non-linear equations which can be solved numerically by applying the *Newton-Raphson* method. This requires the evaluation of a matrix, known as the *Jacobian* of the system, which is defined as

$$\mathbf{J} = \begin{bmatrix} \frac{\partial f_1}{\partial \varphi_A} & \frac{\partial f_1}{\partial \varphi_B} & \frac{\partial f_1}{\partial \varphi_{seat}} & \frac{\partial f_1}{\partial \varphi_{shank}} \\ \frac{\partial f_2}{\partial \varphi_A} & \frac{\partial f_2}{\partial \varphi_B} & \frac{\partial f_2}{\partial \varphi_{seat}} & \frac{\partial f_2}{\partial \varphi_{shank}} \\ \frac{\partial f_3}{\partial \varphi_A} & \frac{\partial f_3}{\partial \varphi_B} & \frac{\partial f_3}{\partial \varphi_{seat}} & \frac{\partial f_3}{\partial \varphi_{shank}} \\ \frac{\partial f_4}{\partial \varphi_A} & \frac{\partial f_4}{\partial \varphi_B} & \frac{\partial f_4}{\partial \varphi_{seat}} & \frac{\partial f_4}{\partial \varphi_{shank}} \end{bmatrix}. \tag{5.25}$$

If $\overrightarrow{\phi} = \overrightarrow{\phi}^1$ represents the first guess for the solution successive approximations to the solution are obtained from

$$\overrightarrow{\phi}^{m+1} = \overrightarrow{\phi}^m - \mathbf{J}^{-1} \cdot \mathbf{f}(\overrightarrow{\phi}^m). \tag{5.26}$$

Retrace, that $\overrightarrow{\phi}^1$ is easily calculated from the synthesis results.

5.6. Example

Here, an exemplary investigation of the aforementioned computational bio-kinematic design procedure is presented. For this experiment a digital single-lens reflex camera (*Nikon D800E*) was used to capture motion data rather than installing a sophisticated motion tracking system. White markers were positioned onto the hip, knee and ankle joints according to *Helen Hayes* marker placement as seen in Fig. 29.

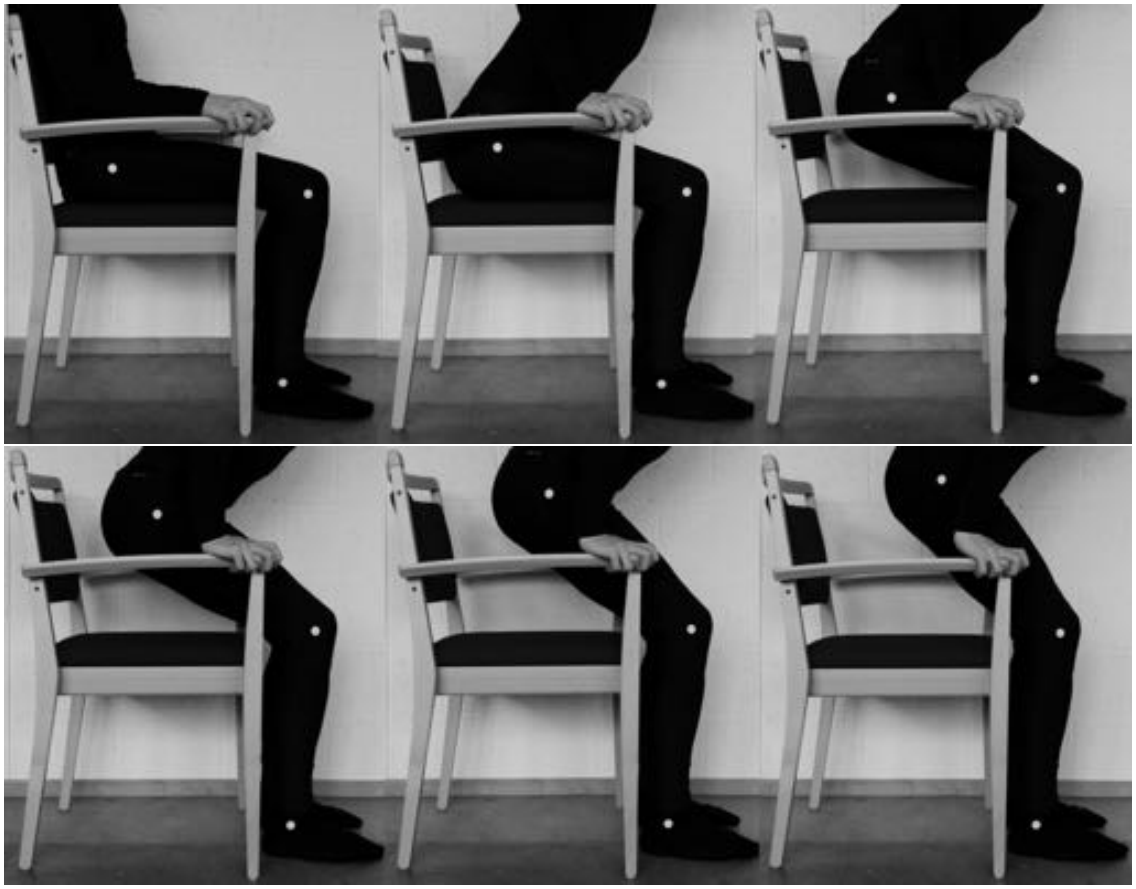

Figure 29 Sit-to-stand movement of a test person

To avoid excessive movement of the fabric relative to the lower limb the volunteer was asked to wear close-fitting trunks. While sitting the volunteer had his back rest against the backrest of the chair and the arms hold on to the armrests. During STS movement the volunteer was asked to lift himself from the chair using his legs and arms.

Table 5 Mean lower limb coordinates of task positions defined in Fig. 29

Task Position, i	x_{hip}	y_{hip}	x_{knee}	y_{knee}	x_{ankle}	y_{ankle}
1	1055	716	1467	663	1371	295
2	1086	758	1475	660	1373	298
3	1105	794	1482	659	1371	299
4	1127	838	1487	657	1369	301
5	1147	882	1484	658	1372	298
6	1166	915	1481	660	1370	299

The camera was fixed onto a tripod with its imaging plane parallel to the sagittal plane of the volunteer's STS movement and six images were captured representing different task positions of the lower leg during STS movement. Since each captured image has the same format we were able to extract a range of hip, knee and ankle joint positions across multiple STS movements. Joint positions are captured as *pixel* coordinates in reference to a picture coordinate system fixed to the lower left edge of the image. Similarly we defined corner points of the workspace below the chair from the images. The mean values of joint positions are displayed in Table 5.

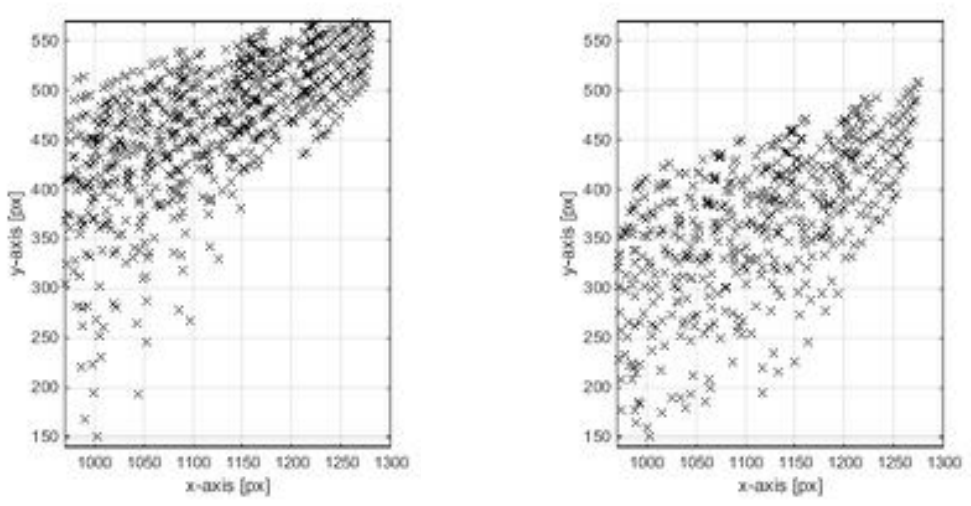

(a) (b)

Figure 30 Results of an exhaustive search for positions of $\mathbf{q}_A$ (a) and $\mathbf{q}_B$ (b) within the rectangular workspace of the chair

Table 6 Joint positions in *pixel* of the *Stephenson III* linkage

Coordinates	$\mathbf{q}_A$	$\mathbf{p}_A^1$	$\mathbf{q}_B$	$\mathbf{p}_B^1$	$\mathbf{p}_{hip}^1$	$\mathbf{p}_{knee}^1$	$\mathbf{q}_{ankle}$
x	1016	1168	1068	1201	1055	1467	1371
y	422	589	357	549	816	663	298

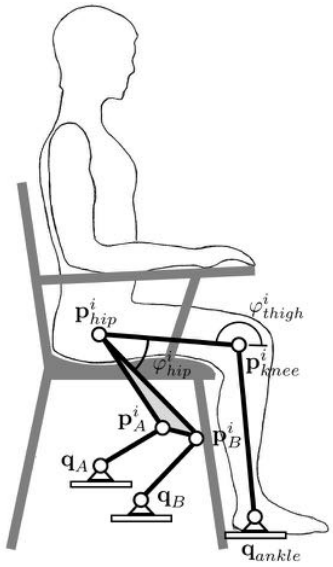

Figure 31 Individualized four-bar linkage attached to the lower limb model based on the results shown in Table 6

From Table 5 $\mathbf{t}_M^i$ and $\mathbf{R}_M^i(\varphi_{thigh}^i)$ are easily established. Using a dimensional finite position synthesis with $n = 3$ task positions we selected task position 1, 3 and 5 from Table 5. These values were inserted into an exhaustive search algorithm implemented in *MATLAB R2014b* to find a set of values for $\mathbf{q}_A$ and $\mathbf{q}_B$. Fig. 30a and 30b display the exhaustive search results for $\mathbf{q}_A$ and $\mathbf{q}_B$ respectively. Each task position is varied within a range of values deduced from the images. In addition, values for $\mathbf{p}_A^1$ and $\mathbf{p}_B^1$ are varied within a range close to the seat. The range in the x and y-axis represents the available space within the chair.

From the exhaustive search two random points were chosen for $\mathbf{q}_A$ and $\mathbf{q}_B$. Combined with the joint positions of the hip, knee and ankle joint we receive the following *Stephenson III* configuration shown in Table 6. Finally we were able to analyze the 7R linkage structure using the mentioned *Newton-Raphson* method. The results are seen in Table 6 and Fig. 31. Using φ_{thigh} as the input angle produced a $\Delta\varphi_{hip}$ range of 3.2 degrees between 172 to 155 degrees of φ_{thigh}, which corresponds to the first 15% of STS movement.

6. Mechanical Design of a Functional Prototype

In this section first the functional requirements that act upon the design of the mechanical lift-assist device are analyzed, i.e. dimensions and characteristics according to DIN standards. This is followed by a description of the nomenclature used for the subsequent sections: kinematic and kinetostatic analysis of the structure as well as the actuation of the mechanism. Finally, the customization process of the LAD is described.

6.1. Functional Prerequisites

The German Institute of Standardization (Deutsches Institut für Normung e.V.) requires chairs for domestic use to be built according to DIN 68878:

- Seat height (a) must lie within 380 mm to 490 mm
- Seat depth (b) must exceed 360 mm
- Seat width (c) must exceed 300 mm
- Backrest (d) must be at least 300 mm high
- Inside seat width must exceed 460 mm

This means that the seat height must lie within 380 mm to 490 mm, seat width must exceed at least 300 mm and the seat depth must at least be 360 mm as seen in Fig. 32.

The developed lift-assist mechanism is integrated into the chair *Luca 1507/4* by *Kusch+Co GmbH & Co. KG*. Four prototypes of the lift-assist mechanism have been designed to fit into this particular chair. This chair was chosen as it is used in the nursing home *Kuratorium Wohnen im Alter, Luise-Kiesselbach Haus* which is cooperating with the *Institute of Micro and Medical Device Technology* at the *Technical University of Munich*. It is important to emphasize that other similar chair types could have been equally suitable for this type of device.

The chair as seen in 33 consists of a wooden frame with back- and armrests made from natural beech. The dimensions of the chair according to Fig. 32 are

- Seat height, a = 450 mm
- Seat depth, b = 465 mm
- Seat width (inside), c = 600 mm
- Backrest height, d = 436 mm
- Seat width (outside), e = 495 mm

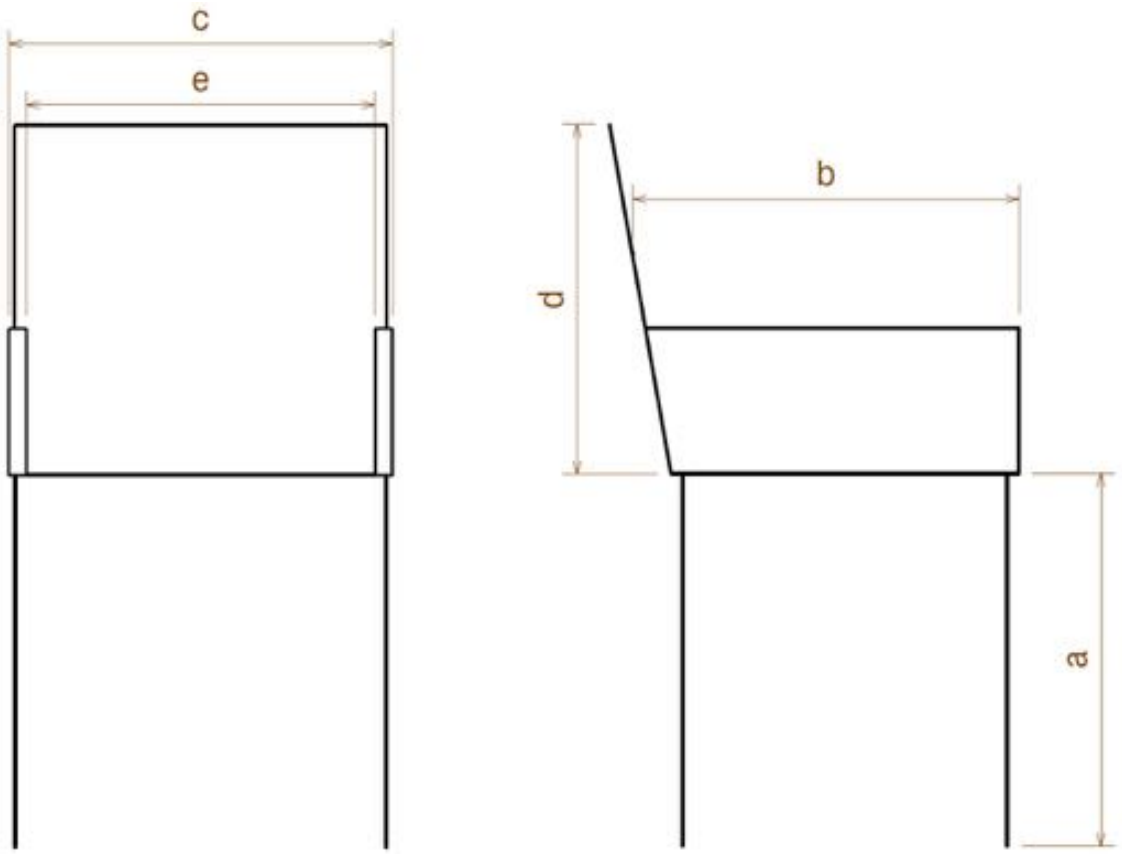

Figure 32 Sketch of specified dimensions of a chair according to DIN 68878 standards, Deutsches Institut für Normung e.V. 2011

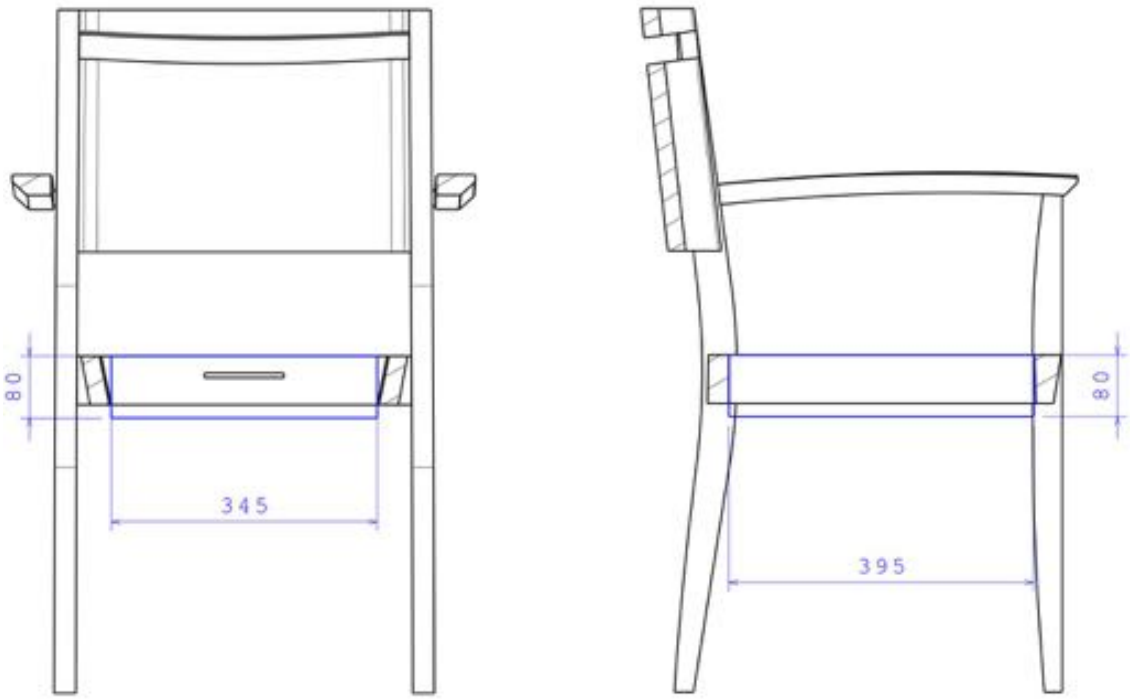

Figure 33 Sectional view of the prototype chair and its work space for the lift-assist mechanism measured in mm

The dimensions of the chair are therefore compliant with DIN 68878. The seat cushion is protected by a waterproof cover. The chair *Luca 1507/4* is designed so that the seat pan can be easily separated from the chair frame by turning a z-profile locking mechanism by 90° to the side underneath the seat pan. The seat sits on an approximate rectangular frame that connects the four legs, the backrest and the armrests of the chair as seen in Fig. 33. This provides an ideal working space for the lift-assist mechanism which can be placed in the middle of the frame without removing parts or altering the design of the chair. The workspace is limited only by the chair frame which is 345 mm wide, 395 mm deep and 80 mm high. While technically the lift-assist mechanism could use the entire height of the chair, it was thought to be optically more pleasing, if the mechanism were integrated into the chair in such a way that it is barely visible when the chair is configured in its seated position. As the seat pan is easily removable the lift-mechanism would lie just underneath the seat.

6.2. Kinematic Structure

The kinematic structure of the lift-assist mechanism is based on a four-bar linkage. In kinematics a kinematic chain is a system of rigid links connected via joints forming different kinds of kinematic structures such as open, semi-open or closed planar, spherical or 3-dimensional chains depending on the topology of the structure (Husty et al., 1997). Here the attention to joints is limited to rotary hinges, called revolute joint (denoted by R), and the linear slider, or prismatic joint (denoted by P). These joints allow one DOF movement between the two links that they connect (McCarthy and Soh, 2011). The number of rigid links n usually identifies the linkage.

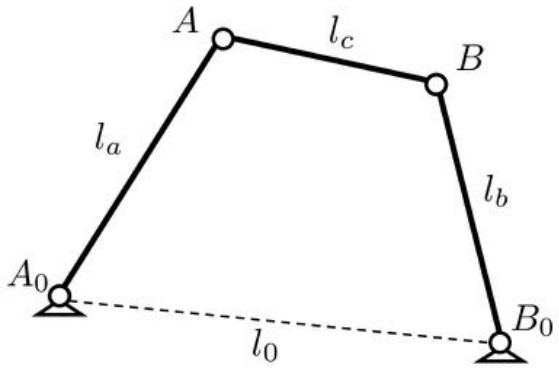

Figure 34 Schematic structure and nomenclature of a four-bar linkage with four revolute (4R) joints

In case of the lift-assist mechanism there are four rigid links connected via single revolute joints with one degree of freedom. The rotation axes of all joints are in parallel to each other thereby creating a closed planar four-bar linkage or 4R closed loop. According to the *Chebychev-Grüblers-Kreutzbach* criterion this structure yields a degree of freedom of:

$$F = 3 \cdot (n - 1 - g) + \sum_{i=1}^{g} b_i = 3 \cdot (4 - 1 - 4) + 4 = 1 \tag{6.1}$$

where g and n are the number of revolute joints and links respectively. b_i represents the number of DOF for the ith joint. When one of the links is fixed to ground the mechanism can be described as a coupler linkage as seen in Fig. 34, where link 0 composed of the imaginary line that connects A_0 and B_0 is fixed to ground. Link a and b consist of the beam that connects the two revolute joints $\overline{AA_0}$ and $\overline{BB_0}$ respectively and are defined as 2R chains. Link c, commonly described as the coupler link connects link a and b at joint A and B respectively. The two revolute joints A_0 and B_0 that are connected to link 0 are called fixed pivots as they cannot move. Similarly revolute joints A and B are defined as moving pivots (Husty et al., 1997). In case of the lift-assist mechanism the fixed link is attached to the chair frame thereby acting as a fixed link. The coupler is attached to the seat, while link a and b take the form of rigid beams.

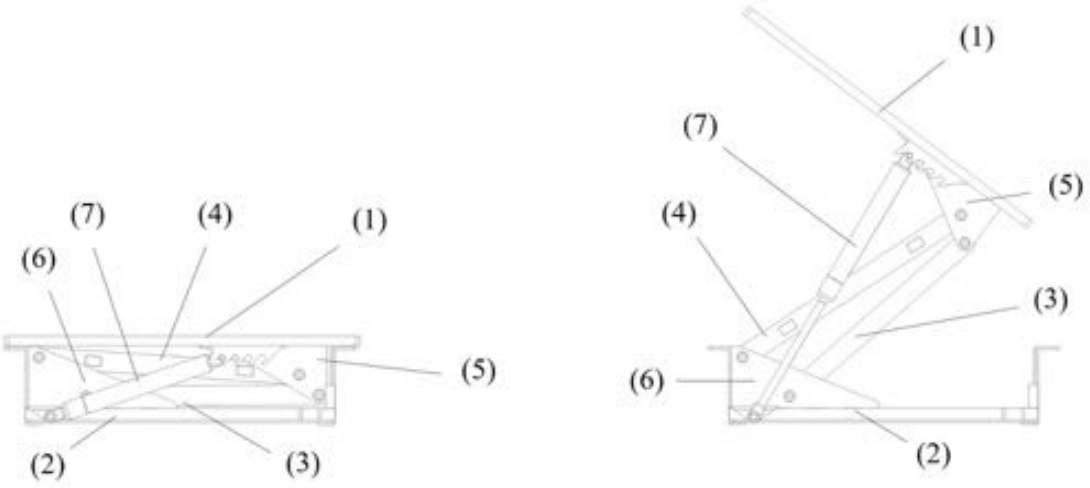

Figure 35 Structure of the lift-assist mechanism with (1) seat plate, (2) base plate, (3) beam b, (4) beam a, (5) seat mounting bracket, (6) base mounting bracket, (7) gas spring strut

The mechanical design of the LAD can be seen in Fig. 35 in two different task positions. The initial position of the device is the ‘stand’ task position and it can only reach the ‘seated’ task position when a user sits down on the chair. This movement sequence between ‘stand’ an ‘seated’ task position is enabled by a four-bar linkage that connects the chair frame with the seat pan. The seat pan (1) is connected to a base plate via two pairs of rigid beams ((4) and (5)) and a seat and base mounting bracket ((5) and (6) respectively). To increase the stability of lateral movement both beam (4) are connected to each other to reinforce the structure. The lifting force that helps a user to stand up is delivered by a gas spring strut (7). This piston is connected to the seat and base plate via revolute joints. When no force other than gravity acts on the seat pan the gas spring strut moves the seat pan in its ‘stand’ configuration. This is the reason why this is considered the initial position of the LAD.

Thee seat movement consists of a rotational as well as translational part which means that the instant center of rotation of the four-bar linkage shifts between ‘sit’ and ‘stand’ task position. The distance between the instant center of rotation and the rotational hinge creates a lever arm about which the gas spring strut applies a force creating a moment about the instant

center of rotation. To adjust the moment for different users the moving pivot point of the gas spring strut can be changed on a perforated rail.

6.3. Kinematic Analysis

The LAD is a mechanism in which the position of the seat pan is always predetermined. The actuation of the seat pan is a combination of the gas spring strut as well as the weight of the user. During stand-to-sit movement the weight of the user that acts on the seat pan increases when the user leans backwards. When the weight overcomes the force that the gas spring strut applies to the seat the gas spring strut starts to compress. While standing up the upper body of the user must lean forward, thereby decreasing the weight acting on the seat pan. When the force in the gas spring strut overcomes the weight of the user the seat starts to rise until it reaches its final 'stand' configuration.

Movement of the seat occurs solely within the xy-plane. It can be easily expressed with the general movement equations. The movement of a body within the xy-plane is expressed as a translational and/or rotational movement of a virtual coordinate frame attached to the body W_{body} with respect to a fixed coordinate frame W_{world}:

$$x_0 = a + \cos\varphi - y \cdot \sin\varphi \tag{6.2}$$

$$y_0 = b + \sin\varphi - y \cdot \cos\varphi \tag{6.3}$$

where x_0 and x_0 are Cartesian coordinates of the fixed reference frame and x and y are Cartesian coordinates of the moving coordinate frame. φ denotes the anti-clockwise rotation of W_{body} with respect to the x-axis of the fixed coordinates frame W_{world} whereas a and b determine the time depending original coordinates of W_{body}. From Eq. 6.2 and Eq. 6.3 it is obvious that the movement of the seat pan depends on a, b and φ. If $a = b = 0$ and φ is set free then there is only rotation of W_{body}. Similarly, if $\varphi = 0$ and a and b are free to move then W_{body} will only be able to move along the x- and y-axis.

Generally, a and b can be expressed as a function of φ or vice-versa. Therefore the movement of the seat-pan (link $\overline{AB}$) can be expressed as an equation with respect to the angle φ_s the angle of the seat with respect the x-axis of the fixed coordinates frame. Due to the fact that the four-bar linkage has only one DOF, the movement of link $\overline{AA_0}$ and link $\overline{BB_0}$ depend on the movement of link $\overline{AB}$. This is of great advantage as the forces of each link depend solely on the angle φ_s.

Before the forces on each link can be calculated, the angle dependencies of link $\overline{AA_0}$ and $\overline{BB_0}$ with respect to link $\overline{AB}$ must be determined. That is, $\varphi_A(\varphi_s)$ and $\varphi_B(\varphi_s)$ as seen in Fig. 36.

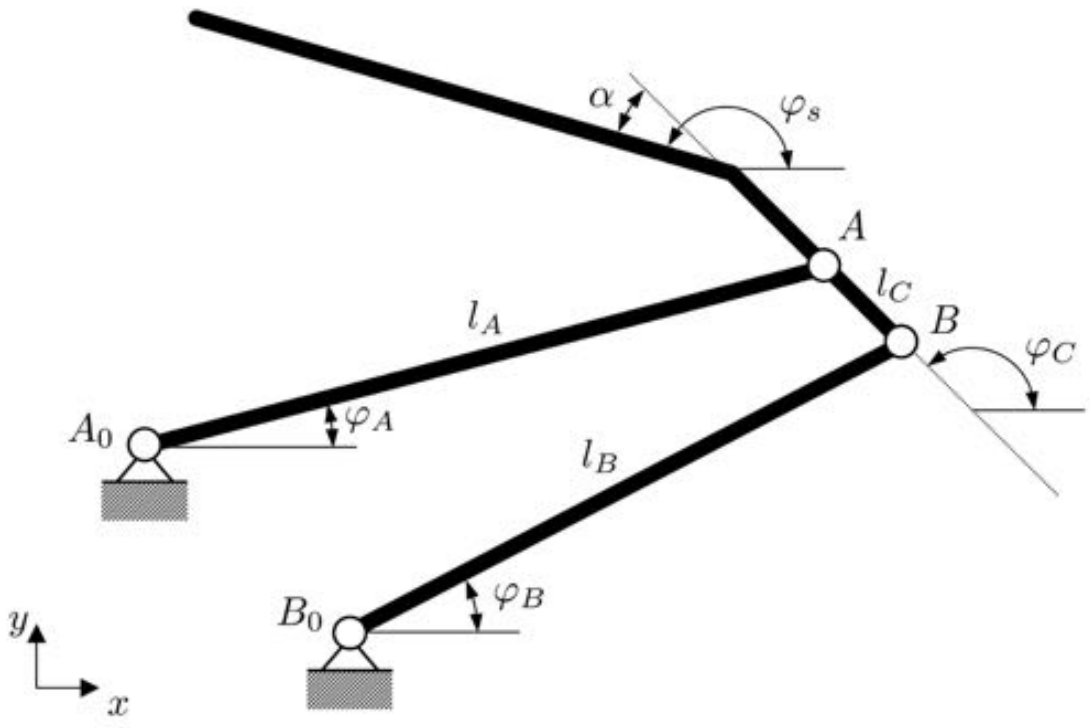

Figure 36 Structure and nomenclature of the four-bar linkage

Given the nomenclature from Fig. 36, a loop equation for the four-bar linkage can be defined. Let the vectors from the world coordinate frame W_{world} to the fixed pivot points of A_0 and B_0 be defined as $\mathbf{q}_A$ and $\mathbf{q}_B$ respectively. The moving pivots of link a and b shall be defined by $\mathbf{p}_A$ and $\mathbf{p}_B$. This yields:

$$0 = (\mathbf{q}_A - \mathbf{q}_B) + (\mathbf{p}_A - \mathbf{q}_A) - (\mathbf{p}_B - \mathbf{q}_B) - (\mathbf{p}_A - \mathbf{p}_B) \tag{6.4}$$

Since the distance between $\mathbf{q}_A$ and $\mathbf{q}_B$ is fixed at all times $(\mathbf{q}_A - \mathbf{q}_B) = [\Delta x, \Delta y]^T$. Eq. 6.4 can therefore be expressed as:

$$0 = \begin{bmatrix} \Delta x \\ \Delta y \end{bmatrix} + \begin{bmatrix} l_A \cos\varphi_A \\ l_A \sin\varphi_A \end{bmatrix} - \begin{bmatrix} l_B \cos\varphi_B \\ l_B \sin\varphi_B \end{bmatrix} - \begin{bmatrix} l_C \cos\varphi_C \\ l_C \sin\varphi_C \end{bmatrix} \tag{6.5}$$

In order for φ_A and φ_B to be solely dependent of φ_C one must eliminate φ_B and φ_A respectively. This is achieved by formulating constraint equations. A contraint equation can be formulated by the fact that the distance between $\overline{AA_0}$ and $\overline{BB_0}$ must stay constant. Applying the dot product by multiplying $(\mathbf{q}_A - \mathbf{q}_A)$ by itself yields:

$${l_A}^2 = (l_B \cos\varphi_B + l_C \cos\varphi_C - \Delta x)^2 + (l_B \sin\varphi_B + l_C \sin\varphi_C - \Delta y)^2 \tag{6.6}$$

Eq. 6.6 can be simplified by reducing the known parameters to $\xi(\varphi_C) = l_C \cos\varphi_C - \Delta x$ and

$\chi(\varphi_C) = l_C \sin\varphi_C - \Delta y$:

$$l_A{}^2 = (l_B \cos\varphi_B + \xi(\varphi_C))^2 + (l_B \sin\varphi_B + \chi(\varphi_C))^2 \tag{6.7}$$

$$l_A{}^2 - l_B{}^2 - \xi(\varphi_C)^2 - \chi(\varphi_C)^2 = 2 \cdot l_B \xi(\varphi_C) \cos\varphi_B + 2 \cdot l_B \chi(\varphi_C) \sin\varphi_B \tag{6.8}$$

Eq. 6.8 can be further simplified by reducing the known parameters to $a(\varphi_C) = 2 \cdot l_B \xi(\varphi_C)$, $b(\varphi_C) = 2 \cdot l_B \chi(\varphi_C)$ and $c(\varphi_C) = l_A{}^2 - l_B{}^2 - \xi(\varphi_C)^2 - \chi(\varphi_C)^2$ which reduces the equation to the standard form of the loop equation:

$$c(\varphi_C) = a(\varphi_C) \cdot \cos\varphi_B + b(\varphi_C) \cdot \sin\varphi_B \tag{6.9}$$

Eq. 6.9 expresses the dependency of φ_B with respect to φ_C. φ_A has been eliminated due to the constraint equation 6.6. Expressing $\tau = \tan\frac{\varphi_B}{2}$ we can solve Eq. 6.9 for $\varphi_B(\varphi_C)$ by applying the known tangent half-angle formulas $\cos\varphi_B = \frac{1-\tau^2}{1+\tau^2}$ and $\sin\varphi_B = \frac{2\tau}{1+\tau^2}$:

$$\varphi_B(\varphi_C) = 2 \cdot \arctan \frac{b(\varphi_C) \pm \sqrt{a(\varphi_C)^2 + b(\varphi_C)^2 - c(\varphi_C)^2}}{a(\varphi_C) + c(\varphi_C)} \tag{6.10}$$

The desired dependency of $\varphi_B(\varphi_s)$ can now easily be derived from Eq. 6.10 since $\varphi_C = \varphi_s - |\alpha|$:

$$\varphi_B(\varphi_s) = 2 \cdot \arctan \frac{b(\varphi_s - |\alpha|) \pm \sqrt{a(\varphi_s - |\alpha|)^2 + b(\varphi_s - |\alpha|)^2 - c(\varphi_s - |\alpha|)^2}}{a(\varphi_s - |\alpha|) + c(\varphi_s - |\alpha|)} \tag{6.11}$$

Similarly Eq. 6.6-6.11 can be applied for solving $\varphi_A(\varphi_s)$.

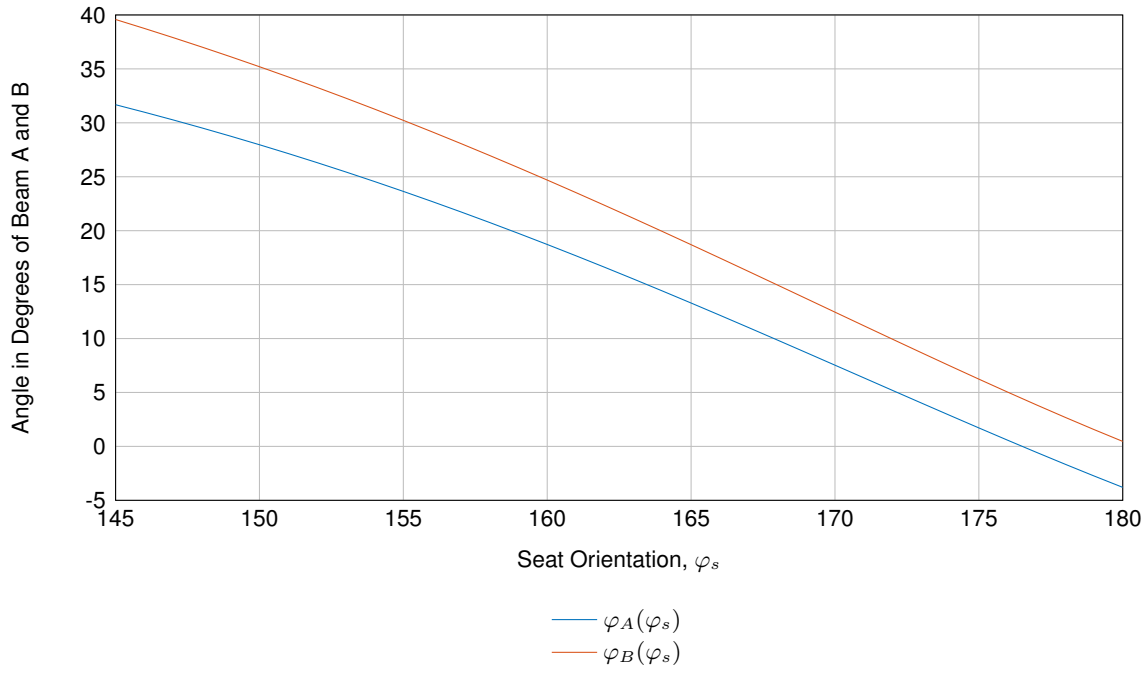

Figure 37 Kinematics of the four-bar linkage of Beam $\overline{AA_0}$ and $\overline{BB_0}$ with respect to φ_s

6.4. Kinetostatic Analysis

In this section we carry out a kinetostatic analysis of the lift-assist mechanism in form of free body diagrams. This section as well as the following 'Example' section are taken from (Reimer et al., 2017). There are a number of simplifications that are considered:

- The forces acting on the joints, the rigid bodies as well as the gas spring strut are considered as point forces - an idealized concentrated force assumed to act on a point of a body.
- The movement of the system is considered as a sequence of static equilibrium states as only very small velocities occur during STS movement.
- The CoM (center of mass) position of the user does not move with respect to the coordinate frame of the seat.
- Friction forces within the joints are neglected.

As was described in the aforementioned section the four-bar linkage consists of four parts - beam A, beam B, the seat plate and the ground plate. To calculate the bearing reaction forces and moments we can split the system into three separate free body diagrams while the reaction forces acting on the ground plate can be integrated into the forces acting on beam $\overline{AA_0}$ and $\overline{BB_0}$. Since movement only takes place in the sagittal plane, i.e. the xy-plane forces can be split into forces acting in the x and y direction. Finally, the forces acting in x and y direction are combined for the design of the slide bearings that are integrated into the lift-assist mechanism.

The forces acting on the system are the reaction forces $\mathbf{F}_{A0_x}$, $\mathbf{F}_{A0_y}$, $\mathbf{F}_{A_x}$, $\mathbf{F}_{A_y}$ and $\mathbf{F}_{B0_x}$, $\mathbf{F}_{B0_y}$, $\mathbf{F}_{B_x}$, $\mathbf{F}_{B_y}$ acting on body $\overline{AA_0}$ and $\overline{BB_0}$ respectively. The weight of each body is defined by $\mathbf{W}_A$, $\mathbf{W}_B$ and $\mathbf{W}_C$ and the force of the gas spring strut and the weight of the user are defined by $\mathbf{F}_G$ and $\mathbf{W}_U$ respectively.

Fig. 38 illustrates the system with the forces acting upon the system. During STS movement the system is considered to stay in equilibrium at every point in time. We solve the equilibrium equations to understand what weight of the user is required to lift and lower the device. The system is divided into three separate free body diagrams. Each free body diagram is freed from the other parts at the bearings. For each free body diagram forces in the x and y direction are summed up and the moment is taken at an arbitrary point. The first free body diagram is illustrated in Fig. 39 and represents beam a:

$$\sum \mathbf{F}_x = 0 : \mathbf{F}_{A0_x} + \mathbf{F}_{A_x} = 0 \tag{6.12}$$

$$\sum \mathbf{F}_y = 0 : \mathbf{F}_{A0_y} + \mathbf{F}_{A_y} - \mathbf{W}_A = 0 \tag{6.13}$$

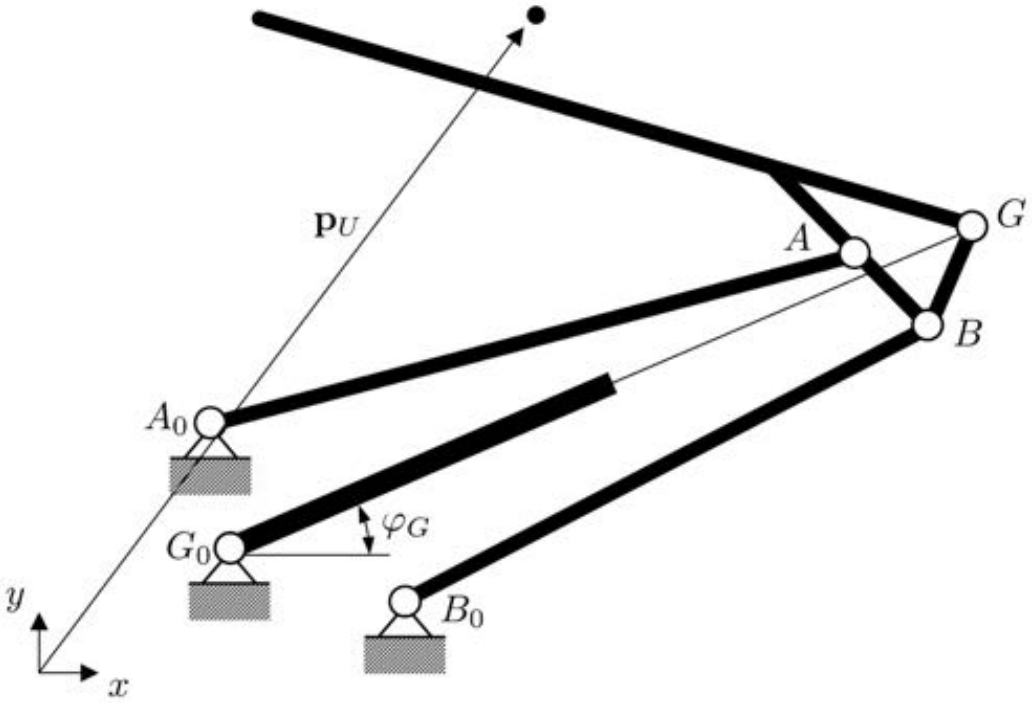

Figure 38 Schematic representation of the four-bar linkage with gas spring strut and center of mass of user

$$\sum \mathbf{M}_{A0} = 0 : \mathbf{F}_{A_y} \cdot l_A \cos\varphi_A - \mathbf{W}_A \cdot \frac{l_A}{2} \cos\varphi_A - \mathbf{F}_{A_x} \cdot l_A \sin\varphi_A = 0 \tag{6.14}$$

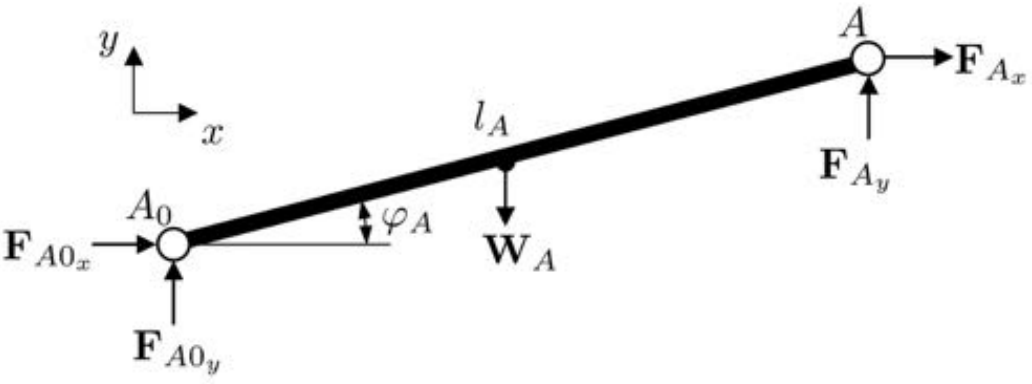

Figure 39 Free body diagram of beam a

Beam $\overline{AA_0}$ is geometrically symmetrical about the xy-, xz- and yz-plane. Thus the CoM lies exactly halfway between the two bearings. This is also true for beam b as seen in Fig. 40. The sum of forces and moments is similar to Eq. 6.12 - 6.14:

$$\sum \mathbf{F}_x = 0 : \mathbf{F}_{B0_x} + \mathbf{F}_{B_x} = 0 \tag{6.15}$$

$$\sum \mathbf{F}_y = 0 : \mathbf{F}_{B0_y} + \mathbf{F}_{B_y} - \mathbf{W}_B = 0 \tag{6.16}$$

$$\sum \mathbf{M}_{B0} = 0 : \mathbf{F}_{B_y} \cdot l_B \cos\varphi_B - \mathbf{W}_B \cdot \frac{l_B}{2} \cos\varphi_B - \mathbf{F}_{B_x} \cdot l_B \sin\varphi_B = 0 \tag{6.17}$$

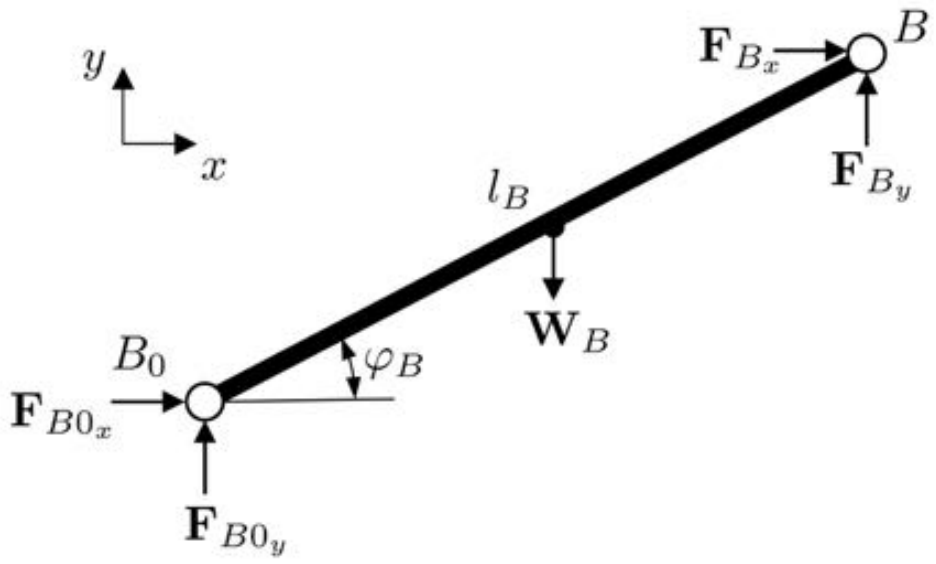

Figure 40 Free body diagram of beam b

For the free body diagram of the seat as seen in Fig. 41 we receive the following constellations:

$$\sum \mathbf{F}_x = 0 : -\mathbf{F}_{A_x} - \mathbf{F}_{B_x} + \mathbf{F}_G \cos\varphi_G = 0 \tag{6.18}$$

$$\sum \mathbf{F}_y = 0 : -\mathbf{F}_{A_y} - \mathbf{F}_{B_y} + \mathbf{F}_G \sin\varphi_G - \mathbf{W}_U - \mathbf{W}_C = 0 \tag{6.19}$$

$$\begin{aligned} \sum \mathbf{M}_0 = \; & \mathbf{F}_G \cdot l_{S_2} \sin\varphi_G \cos\varphi_S - \mathbf{F}_G \cdot l_{S_2} \cos\varphi_G \sin\varphi_S - \mathbf{W}_U \cdot l_U \cos\varphi_U - \\ & \mathbf{W}_C \cdot l_{S_1} \cos\varphi_S + \mathbf{F}_{A_x} \cdot l_{C_1} \sin\varphi_C + \mathbf{F}_{B_x} \cdot l_{C_2} \sin\varphi_C - \\ & \mathbf{F}_{A_y} \cdot l_{C_1} \cos\varphi_C - \mathbf{F}_{B_y} \cdot l_{C_2} \cos\varphi_C \end{aligned} = 0 \tag{6.20}$$

The weight of the user $\mathbf{W}_U$ acts on point $\mathbf{p}_U$ which correlates to the calculated CoM of the user. The CoM of the seat pan including the seat mounting brackets was calculated and acts at point c. The force of the gas spring strut $\mathbf{F}_G$ acts on bearing point $\mathbf{p}_G$. As the seat moves up, the direction of the force vector changes which is indicated by φ_G.

From the free body diagrams we receive nine linear equations (Eq. 6.12 - 6.20) in nine unknowns. The unknown variables are the x and y parts of the four bearing reaction forces $\mathbf{F}_{A0}$, $\mathbf{F}_{B0}$, $\mathbf{F}_A$ and $\mathbf{F}_B$ as well as the weight of the user $\mathbf{W}_U$.

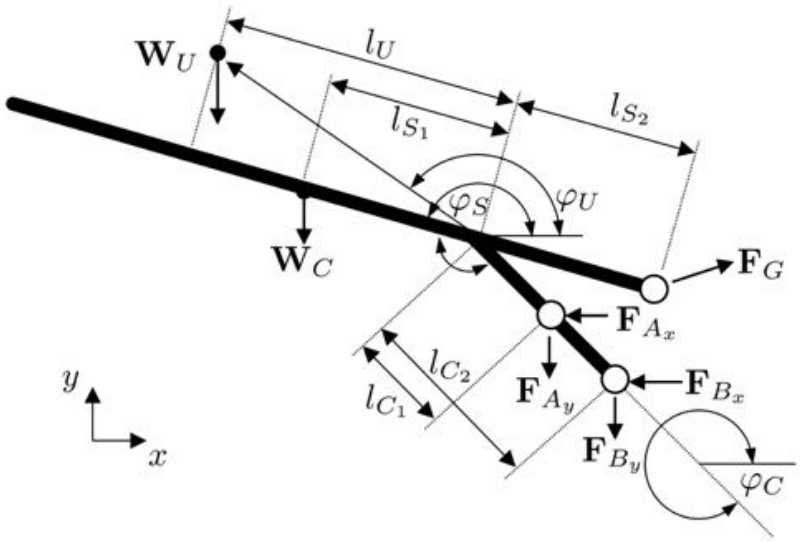

Figure 41 Free body diagram of the seat pan

From this we can constitute a linear system of equations:

$$[A] \cdot [x] = [b] \tag{6.21}$$

where $[A]$ is a matrix $\in \mathbb{R}^{9\times9}$, $[b]$ a vector $\in \mathbb{R}^9$ of all known weight variables as well as the force of the gas spring strut. $[x]$ is a vector $\in \mathbb{R}^9$ which contains all the unknown variables. Since matrix $[A]$ is of quadratic shape and of rank($[A]$) = 9 it is possible to invert Eq. 6.21 to solve the equation for the unknown variables $[x]$ simultaneously:

$$[x] = [A]^{-1} \cdot [b] \tag{6.22}$$

The forces are calculated for each configuration of the chair from the 'sit' to 'stand' configuration. The configuration is defined by the seat angle φ_s which starts at the horizontal 'sit' configuration of 180° and moves to the final 'stand' configuration (e.g. at 146°). The force calculations are conducted at every angle step of 1°.

The following dimensions were used for the kinetostatic analysis of the prototype:

- Length of beam A, $l_A = 332$ mm
- Length of beam B, $l_B = 297$ mm
- Distance between bearing A and 0, $l_{C_1} = 52$ mm
- Distance between bearing B and 0, $l_{C_2} = 88$ mm
- Distance between $\mathbf{p}_S$ and $\mathbf{p}_U$ and 0, $l_U = 99$ mm
- Length of $l_U = 151$ mm

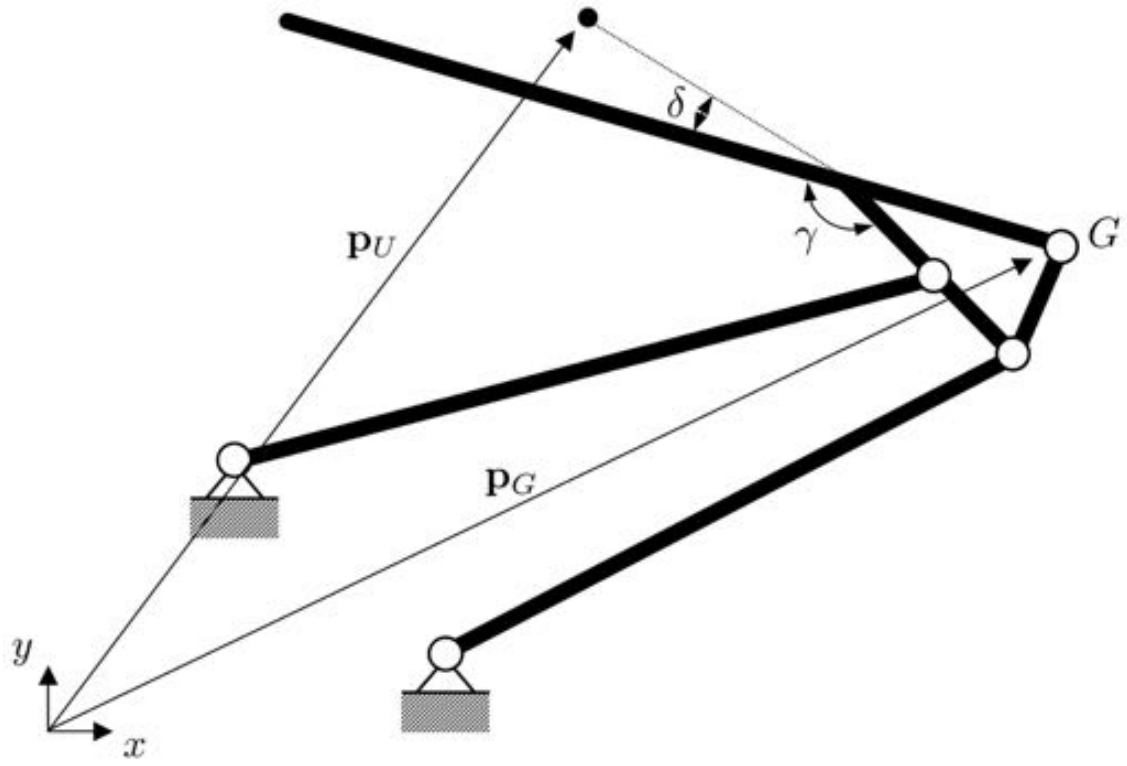

Figure 42 Schematic representation of four-bar linkage with gas spring strut

The weight of each rigid body is derived from the material property and the dimensions. *Multiplex-Beech* is a plywood material made out of beech. Its density is $\rho = 800\ kg/m^3$. Thus the weight of each body yields:

- Weight of beam A, $\mathbf{W}_A = 2.99$ N
- Weight of beam B, $\mathbf{W}_B = 1.86$ N
- Weight of the seat C, $\mathbf{W}_C = 22.66$ N

The gas spring strut has an almost linear force dependency of the length of the stroke length. The force decreases slightly as the gas spring strut extends and vice versa. The length of the gas spring can be determined from the absolute value $l_G = |\mathbf{p}_G - \mathbf{q}_G|$. The length l_G can be determined from the known vectors of $\mathbf{q}_A$, $\mathbf{p}_A$, $\mathbf{q}_G$ and $\mathbf{p}_G$ as seen in Fig. 42:

$$l_G(\varphi_S) = |(\mathbf{q}_A - \mathbf{p}_G) + (\mathbf{p}_A - \mathbf{q}_A) + (\mathbf{p}_G - \mathbf{p}_A)| \tag{6.23}$$

The distance from bearing point $\mathbf{p}_A$ and moving pivot point of the gas spring strut $\mathbf{p}_G$ is constant and can be best determined when the lift-assist mechanism is in 'sit' configuration, i.e. φ_S = 180°. This allows us to calculate $|\mathbf{p}_{G_{180}} - \mathbf{p}_{A_{180}}|$. This yields:

$$l_G(\varphi_S) = |\mathbf{q}_A - \mathbf{q}_{GF} + \begin{bmatrix} l_A \cos(\varphi_S) \\ l_A \sin(\varphi_S) \end{bmatrix} + \begin{bmatrix} |\mathbf{p}_{G_{180}} - \mathbf{p}_{A_{180}}| \cos(\varphi_S - \beta) \\ |\mathbf{p}_{G_{180}} - \mathbf{p}_{A_{180}}| \sin(\varphi_S - \beta) \end{bmatrix}| \tag{6.24}$$

For the prototype a gas spring strut by *Sodemann Industrifjedre* was chosen that has a force of 400 N and which strength reduces by 0.1 N per mm. This results in the following equation of the gas spring strut force:

$$F_G = 400 - 0.1(N/mm) \cdot l_G(\varphi_S) \tag{6.25}$$

Since the length $l_G(\varphi_S)$ has already been determined from Eq. 6.24 one can determine the angle φ_G which also depends on φ_S:

$$\varphi_G(\varphi_S) = \arctan \frac{\varphi_G(\varphi_S)_y}{\varphi_G(\varphi_S)_x} \tag{6.26}$$

For Eq. 6.20 two new angles were specified φ_C and φ_U. Both again depend on φ_S:

$$\varphi_C(\varphi_S) = \varphi_S + \gamma \tag{6.27}$$

$$\varphi_U(\varphi_S) = \varphi_S - |\delta| \tag{6.28}$$

where γ is the constant angle between seat and the seat mounting brackets and $|\delta|$ = 29° is the constant angle between the seat and the vector to the CoM of the user as seen in Fig. 42.

All of the known parameters are now defined which allows us to compute $[A]$ and $[b]$ to solve for the nine unknown forces in $[x]$. The calculations were completed in *MATLAB R2015b* which can be found in the Appendix F.

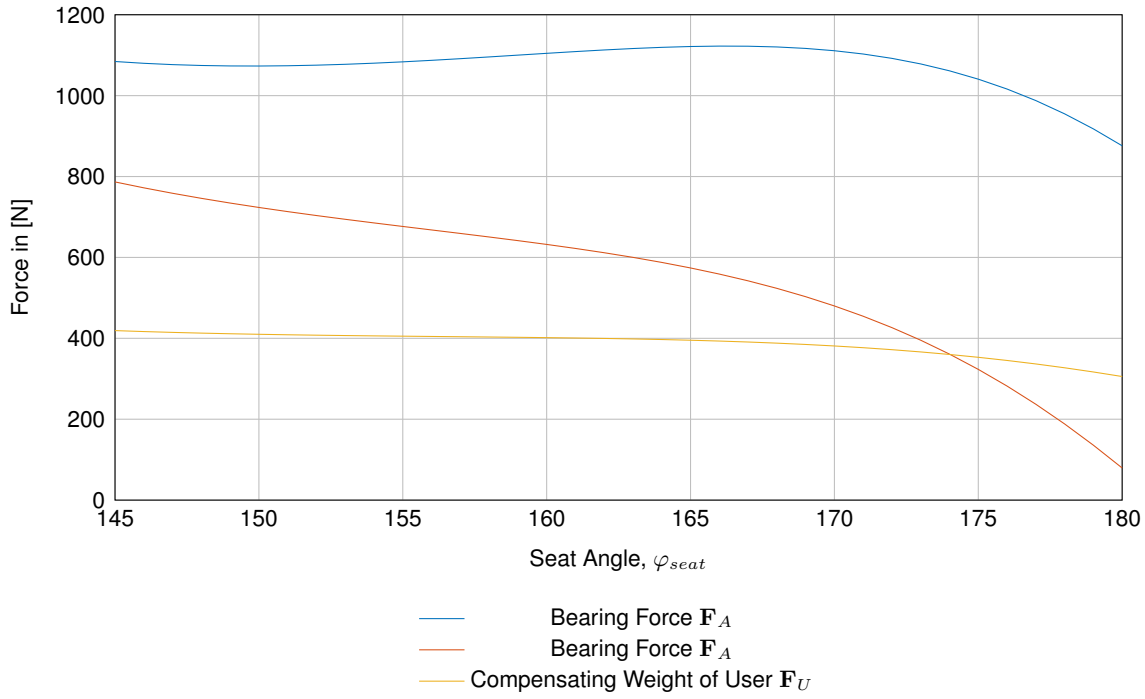

Figure 43 Forces acting on the lift-assist device

Fig. 43 represents the resulting equilibrium forces that act on the system during stand-to-sit motion and sit-to-stand motion. The 'stand' configuration starts at a 145° tilt of the seat with respect the the horizontal axis. The 'sit' configuration is reached when the seat angle reaches a horizontal position, i.e. 180°. Equilibrium forces were calculated for every angle step between 145° and 180°.

The unknown force were plotted in *MATLAB R2015b* as seen in Fig. 43 from 'stand' to 'sit' configuration. The forces in $\mathbf{F}_A$ and $\mathbf{F}_B$ are the sum of the vectors $\mathbf{F}_{A_x}$, $\mathbf{F}_{A_y}$ and $\mathbf{F}_{B_x}$, $\mathbf{F}_{B_y}$ respectively. $\mathbf{F}_{A0}$ and $\mathbf{F}_{B0}$ are almost identical to $\mathbf{F}_A$ and $\mathbf{F}_B$ which is why only $\mathbf{F}_A$ and $\mathbf{F}_B$ were plotted in Fig. 43.

From Fig. 43 one can deduce that the compensated weight of the user is almost constant throughout the movement, decreasing only slightly towards the 'sit' configuration. As was mentioned earlier, the gas spring strut ought to be installed into the LAD such that its direction of force is perpendicular to the seat pan. Due to its limited space constraint, however, the gas spring is tilted slightly to fit into the work space of the LAD during 'sit' configuration as seen in as seen in Fig. 35. Fig. 43 shows that the compensating force of the gas spring strut slightly decreases towards the seated configuration of the chair.

6.5. Configuration of the Lift-Assist Device

The LAD can be customized to the needs of the user by changing the moving gas spring strut bearing along a rail underneath the seat. Secondly the gas spring strut can be interchanged with other gas spring struts that differ in stroke length and pressure. While the latter depends on the chosen product the former is designed to allow as many different configurations as possible. The further away the moving bearing point is moved towards the back of the chair, the steeper the angle φ_G and therefore the greater the moment. This is useful as the LAD can be set to different users of different weights.

In addition, vector $\mathbf{p}_G$ is also dependent on the distance l_{S_1} (see Fig. 41), since the moving pivot point of the gas spring strut can be moved discretely along a configuration rail. There are four possible configurations which are 17 mm apart. This yields:

$$\mathbf{p}_G(\varphi_S) = \begin{bmatrix} 248 + j \cdot 17 \\ \\ 64 \end{bmatrix}; j \in \{0, 1, 2, 3\} \tag{6.29}$$

Changing the position of the moving pivot of the gas spring strut also alters the lever that acts on the seat. This means that the seat can be configured for four different classes of user weight. Fig. 44. represents the force of the user's weight W_U that must act on the seat such that it stays in equilibrium. Changing the gas spring strut's position towards the back of the chair therefore increases the required weight of the user.

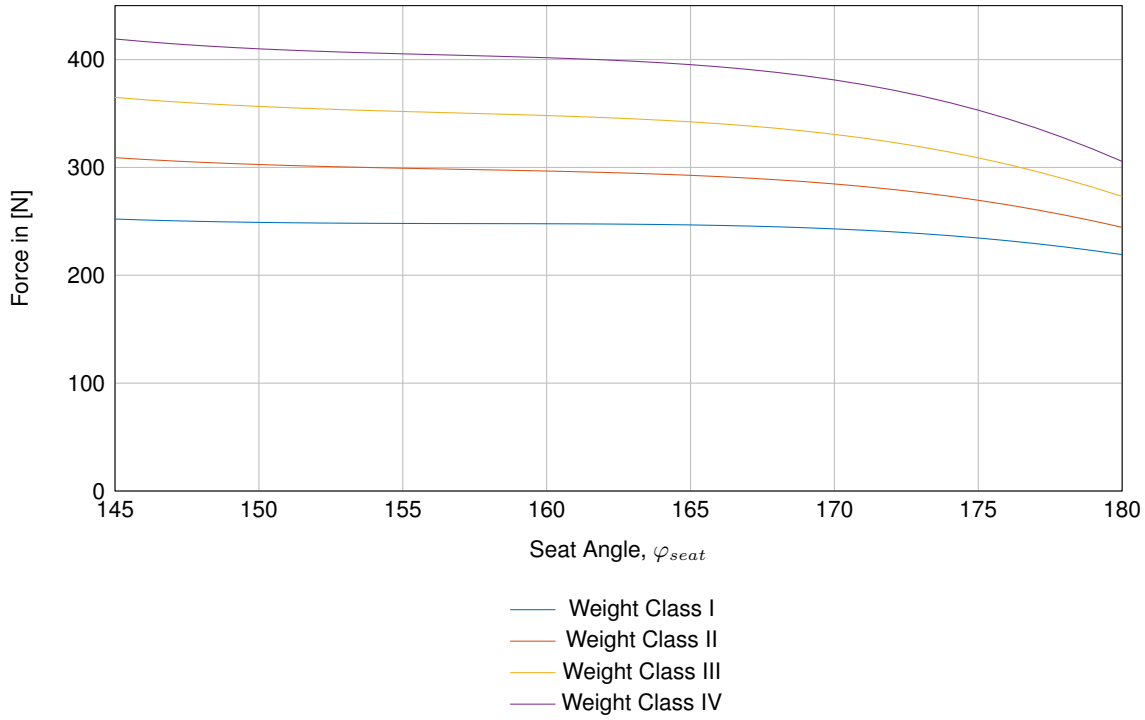

Figure 44 User weight required for the mechanism to stay in equilibrium for each configurable weight class

The four positions available can be interpreted as available weight classes for the chair. These are as follows:

- Weight Class I: 219 N - 252 N
- Weight Class II: 244 N - 309 N
- Weight Class III: 273 N - 365 N
- Weight Class IV: 306 N - 419 N

The first value of each weight class is the required force at 'sit' configuration while the latter is at 'stand' configuration of the chair. (Bashford et al., 1998, P. 102) stated that users were worried about the continued degeneration of muscle tissue when using the ejector chair over a continuous period of time. The ejector chair was said to compensate 70-80%. The gas spring however was so strong that some users were not able to sit down unless the gas spring was decreased accordingly. These weight class configurations of the LAD are laid out to neither under- nor over strain the user while sitting or standing up from the chair. For this reason the ideal weight of the user for each class (I-IV) are 51 kg, 64 kg, 76 kg and 87 kg respectively.

Since the force towards the seat changes with the seat angle the weight of the user is either sufficiently large or too low in order to move the seat pan. Ideally the weights for Class I - IV are as follows:

- Weight Class I: 45 kg < $\mathbf{W}_U$ < 57 kg
- Weight Class II: 58 kg < $\mathbf{W}_U$ < 70 kg
- Weight Class III: 71 kg < $\mathbf{W}_U$ < 81 kg
- Weight Class IV: 82 kg < $\mathbf{W}_U$ < 92 kg

Therefore, users with the recommended weight must compensate their weight by pushing their upper body upwards using the armrests. Similarly, users might have to pull themselves into a seated position using the arm rests to decline the seat pan, if the force in the gas spring strut is too strong.

6.6. Bearing Forces

Based on the results of the forces acting on the bearings A, A_0, B and B_0 one can determine the properties of bearings required for the LAD according to the permissible surface pressure $\tau_{permissible}$. Tensile forces, P are transmitted across the joint being carried by shearing action on the cross section of the joints (Niemann et al., 2005). Assuming that there is a uniform shear stress τ over the cross-sectional area A_P of the pin, then the permissible shear stress of the pin is

$$\tau = \frac{P}{A_P} < \tau_{permissible} \tag{6.30}$$

The permissible shear stress is a property that is dependent on the material used. In this case the bearings are made from sintered bronze which has a perimissible shear stress of $\tau_{permissible} = 35$ N/mm^2.

The following applies to the cross-sectional area

$$A_P = b \cdot d \tag{6.31}$$

For joints A, A_0, B and B_0 the bearings are all the same, which has dimensions $b = 8$ mm and $d = 8$ mm. The aforementioned calculations on the forces that act on the bearings are conducted on a single beam A and beam B. However, the structure consists of two parallel beams A and beam B. The forces are therefore distributed equally on the left and right side of the four-bar linkage. This is included in the following calculations. Since the maximum force acting on each joint A is $\mathbf{F}_{A_{max}} = 561.3$ N the shear stress is

$$\tau_A = \frac{\mathbf{F}_{A_{max}}}{b \cdot d} = 8.77 \frac{N}{mm^2} < 35 \frac{N}{mm^2} \tag{6.32}$$

The maximum forces in joint A_0, B and B_0 are $\mathbf{F}_{A0_{max}} = 561.4$ N, $\mathbf{F}_{B_{max}} = 393.3$ N and $\mathbf{F}_{B0_{max}} = 393.9$ N respectively. This yields

$$\tau_{A0} = \frac{\mathbf{F}_{A0_{max}}}{b \cdot d} = 8.77 \frac{N}{mm^2} < 35 \frac{N}{mm^2} \tag{6.33}$$

$$\tau_B = \frac{\mathbf{F}_{B_{max}}}{b \cdot d} = 6.15 \frac{N}{mm^2} < 35 \frac{N}{mm^2} \tag{6.34}$$

$$\tau_{B0} = \frac{\mathbf{F}_{B0_{max}}}{b \cdot d} = 6.15 \frac{N}{mm^2} < 35 \frac{N}{mm^2} \tag{6.35}$$

6.7. Construction of the Lift-Assist Chair Prototype

The modular designed LAD is mostly made out of beech multiplex wood of 12 mm thickness. This material is applied for the linkages, the base as well as the seat. Custom designed aluminum parts were manufactured for the shafts and the mounting assembly. Other parts such as the bearings were purchased. In what follows is a rough overview of the main manufacturing steps that lead to the realization of the current prototype:

Step 1: Manufacturing of the Wood Parts

The LAD was designed in *CATIA V5-6R2014* a computer-aided design software which enables a virtual assembly of the device. The parts were converted into *.svg* files and imported into the laser cutting machine which cuts materials to the specified dimensions of the file. For this design a beech multiplex wood board of 600 $\times$ 1000 mm dimension was used as seen in Fig. 45.

Figure 45 Manufactured wooden components of the modular lift-assist chair

After the laser cutting process each individual component, especially around the cutting edges was ground with a rough grinding paper and glazed. After a 24 hour waiting period the process was repeated with a finer grinding paper and glazed once more. The laser cutter also marked the exact drilling locations, which were subsequently drilled and grounded at the edges.

Step 2: Manufacturing and Assembly of Subassembly Parts

The base plate, seat plate and linkages as seen in Fig. 46a-46c respectively are assembled together by a wood glue. Afterwards the subassembly parts where left to dry for 24 hours.

(a) (b) (c)

Figure 46 Construction of subassembly parts consisting of base plate (a), seat plate (b) and the linkages (c)

The subassembly parts are merged together with mechanical shafts and bearings as seen in Fig. 47. At first the linkages are connected to the base plate as seen in Fig. 47a followed by the assembly of the seat plate to the linkages.

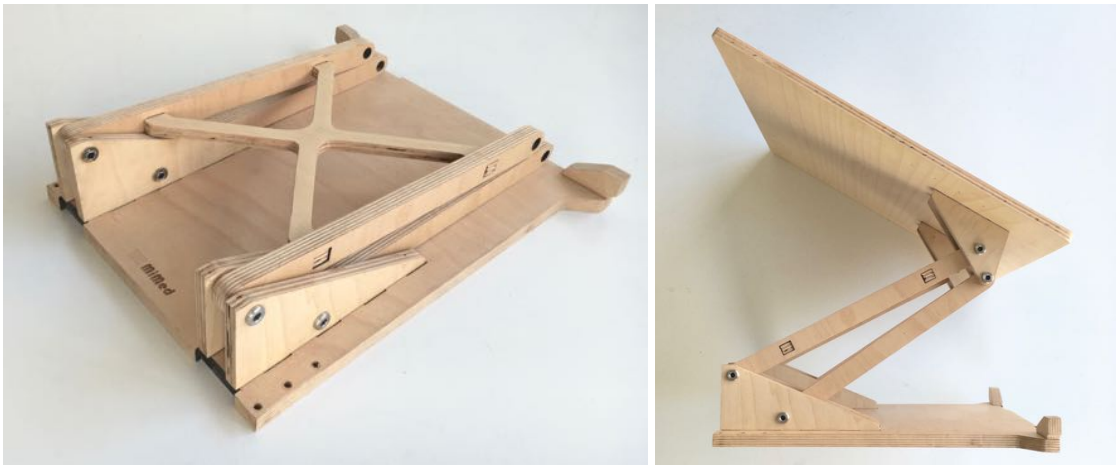

(a) (b)

Figure 47 Assembly of subassembly parts with shafts and bearings of base plate and linkages (a), and subsequently seat plate with the linkages (b)

Step 3: Installation of the Gas Spring Strut, Seat Cushion and Hanger Assembly

The gas spring strut connects the seat plate with the base plate. When a user applies downward pressure on the seat plate, the gas spring is subsequently compressed and stores energy that is released when the pressure on the seat is reduced. The gas spring strut is connected to the front part of the seat with a stainless steal bracket. The gas spring is similarly connected to the seat plate. Here, however, a perforated rail was installed which allows the user to customize the lever of the gas spring, therefore changing the power required to compress the gas spring. The installation of the gas spring can be seen in Fig. 48.

(a) (b) (c)

Figure 48 Construction of subassembly parts consisting of base plate (a), seat plate (b) and the linkages (c)

The final step of the construction consists of screwing on the aluminum hanger plates and installing the seat cushion and cover as seen in Fig. 49.

(a) (b) (c)

Figure 49 Construction of subassembly parts consisting of base plate (a), seat plate (b) and the linkages (c)

Step 4: Placing the Lift-Assist Device into the Chairframe

In the final step, the seat cushion from the original chair can be taken off and the LAD can be placed inside the rectangular chair frame as seen in Fig. 50.

Figure 50 Fully assembled chair with integrated lift-assist mechanism

7. Experiments

7.1. Verification of Individualized Lift-Assist Devices

This experiment is based on the computational design and analysis of individualized LADs.To verify the individualization process, first a synthesis based on biomechanical parameters is conducted which results, if solutions exist, in a number of 2R chains as is explained in detail in Section 5. Once a set of solutions is computed a bio-kinematic analysis is carried out that evaluates the compatibility of the linkage to the dimensions of the user. In this experiment, the angle between modeled user and lift-assist mechanism is analyzed during STS movement. The device with an angle range that stays almost constant throughout this process is chosen.

Experimental Set-Up and Hypothesis

One or more four-bar linkages were found for each percentile group based on the DIN 33402-2:2005-12 standard table of biomechanical measurements of males and females in Germany. The hypothesis therefore assumes that a four-bar linkage can be found within each percentile group and that the angle between seat and thigh of the user stays approximately constant, i.e. $\Delta\varphi_{hip} < 15°$.

The experimental parameters consist of the biomechanical measurements of the thigh, shank, depth of the body and total leg length. These parameters change based on percentile groups for female and male populations. The synthesis is conducted on the basis that the moving pivot point of a $2R$ chain $\mathbf{p}^1$ stays constant while the fixed pivot point $\mathbf{q}$ is varied in the x and y direction in discrete steps creating a grid of possible configurations in the workspace of the chair. By means of a bio-kinematic analysis φ_{hip} can be calculated.

Experimental Procedure

The verification process was carried out in *MATLAB 2015b* on a MacBook Pro (Dual-Core Intel Core i5 - 4278U 2.60 GHz, 8 GB 1600 MHz DDR3L on-board RAM). Exemplary *MATLAB* scripts can be found in Appendices B-E. Different percentile groups for females and males carry different biomechanical measurements which are analyzed in different *MATLAB* scripts as seen in Table 7 and 8.

Table 7 *MATLAB* scripts for the synthesis of 2R chains based on male or female percentile groups

Percentile Groups	5th Percentile	50th Percentile	95th Percentile
Male	FBL_p5m.m	FBL_p50m.m	FBL_p95m.m
Female	FBL_p5w.m	FBL_p50w.m	FBL_p95w.m

Table 8 *MATLAB* scripts for the analysis of the six-bar bio-kinematic linkage

Percentile Groups	5th Percentile	50th Percentile	95th Percentile
Male	NRM_p5m.m	NRM_p50m.m	NRM_p95m.m
Female	NRM_p5w.m	NRM_p50w.m	NRM_p95w.m

Experimental Results

The execution times of the scripts vary dramatically. Since the running time of solving systems of linear equations for the analysis of the six-bar linkage is substantial, some of the execution times taking several ours. In one case even 43 hours as seen in Table 9. This was the case for 5th percentile group of females which received a very large number of possible 2R chain configurations in the synthesis part of the computational procedure. On the other hand results of the 95th male percentile group did not yield any 2R chain configuration results at all.

Table 9 Execution times of the different *MATLAB* scripts

MATLAB Script	Percentile Group	Filename	Execution Time
2R chain Synthesis	5th Male Percentile	FBL_p5m.m	10 s
2R chain Synthesis	50th Male Percentile	FBL_p50m.m	6 s
2R chain Synthesis	95th Male Percentile	FBL_p95m.m	0 s
2R chain Synthesis	5th Female Percentile	FBL_p5w.m	14 s
2R chain Synthesis	50th Female Percentile	FBL_p50w.m	9 s
2R chain Synthesis	95th Female Percentile	FBL_p95w.m	6 s
Six-Bar Linkage Analysis	5th Male Percentile	NRM_p5m.m	42184 s
Six-Bar Linkage Analysis	50th Male Percentile	NRM_p50m.m	558 s
Six-Bar Linkage Analysis	95th Male Percentile	NRM_p95m.m	-
Six-Bar Linkage Analysis	5th Female Percentile	NRM_p5w.m	157357 s
Six-Bar Linkage Analysis	50th Female Percentile	NRM_p50w.m	26038 s
Six-Bar Linkage Analysis	95th Female Percentile	NRM_p95w.m	862 s

5th Male Percentile

The exhaustive search as seen in Fig. 51 found 29 fixed pivot points $\mathbf{q}$ for 440 moving pivot points $\mathbf{p}^1$. Fig. 51 illustrates the fixed pivot points as blue dots and the moving pivot points as $\times$. The corresponding pairs are illustrated in Fig. 52. These 29 2R dyads as seen in Fig. 52 can be combined to assemble 406 different four-bar linkages according to Eq. 5.23.

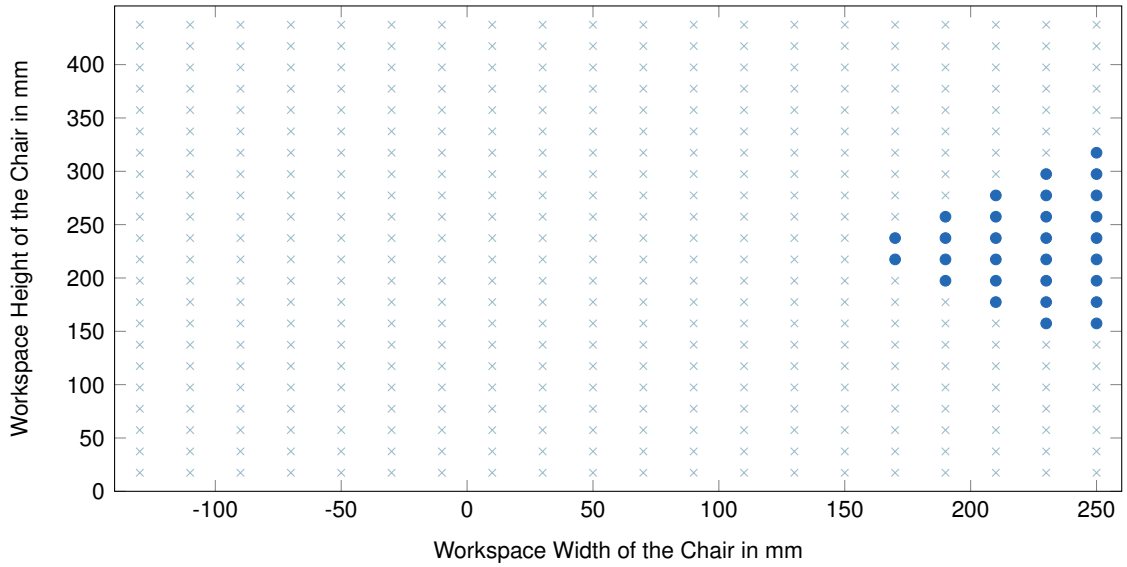

Figure 51 5th male percentile results of an exhaustive search for positions of moving pivot points within the rectangular workspace of the chair

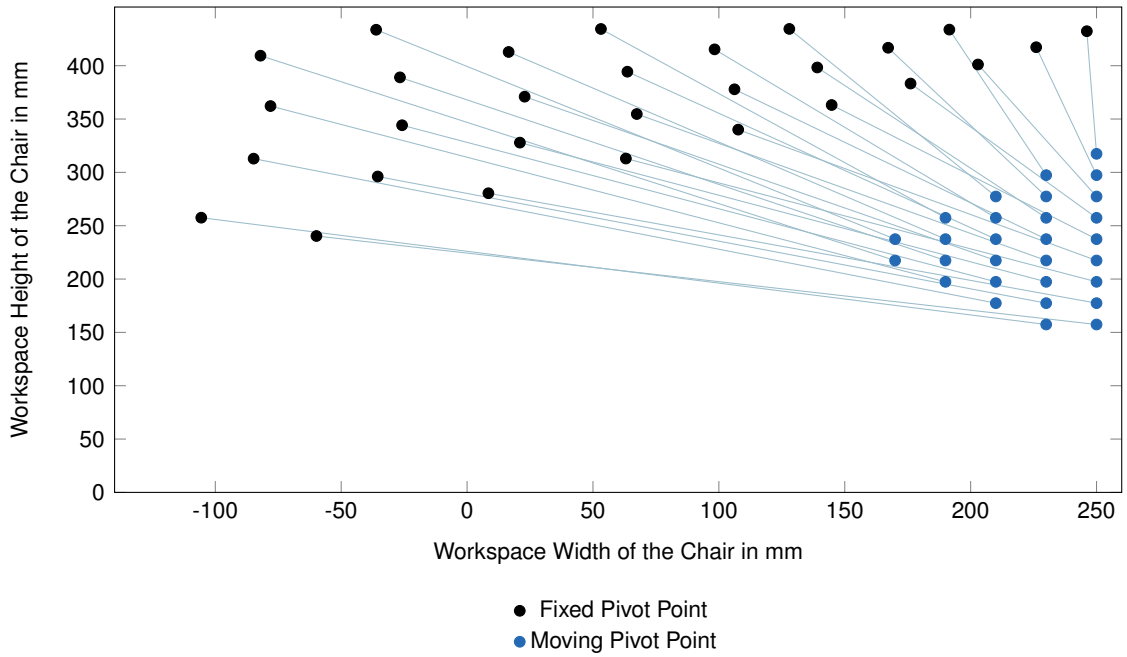

Figure 52 5th male percentile results of suitable 2R dyads configurations within the workspace of the chair

Once the dyads are found a bio-kinematic analysis is carried out which computes $\Delta\varphi_{hip}$ during a full STS movement for each six-bar linkage that consists of the four-bar linkage and the modeled 3R chain of the user. The four-bar linkage that creates the smallest $\Delta\varphi_{hip}$ value between the coupler and the thigh is shown in Table 10 and illustrated in Fig. 53:

Table 10 Four-bar linkage in 'sit' configuration for the 5th male percentile with the smallest $\Delta\varphi_{hip}$

${}^W\mathbf{q}_A$	${}^W\mathbf{q}_B$	${}^W\mathbf{p}_A^1$	${}^W\mathbf{p}_B^1$
$\begin{pmatrix} 21.0 \\ 327.9 \end{pmatrix}$	$\begin{pmatrix} -59.8 \\ 240.4 \end{pmatrix}$	$\begin{pmatrix} 230 \\ 197.4 \end{pmatrix}$	$\begin{pmatrix} 250 \\ 157.4 \end{pmatrix}$

As seen in Fig. 53 the movement between hip and seat stays approximately constant during a STS movement. The angle between thigh and seat starts at roughly 44° then starts to increase slightly followed by a small decrease thereby making a sinusoidal-like shape until the person stands. The maximum $\Delta\varphi_{hip}$ = 5.16°.

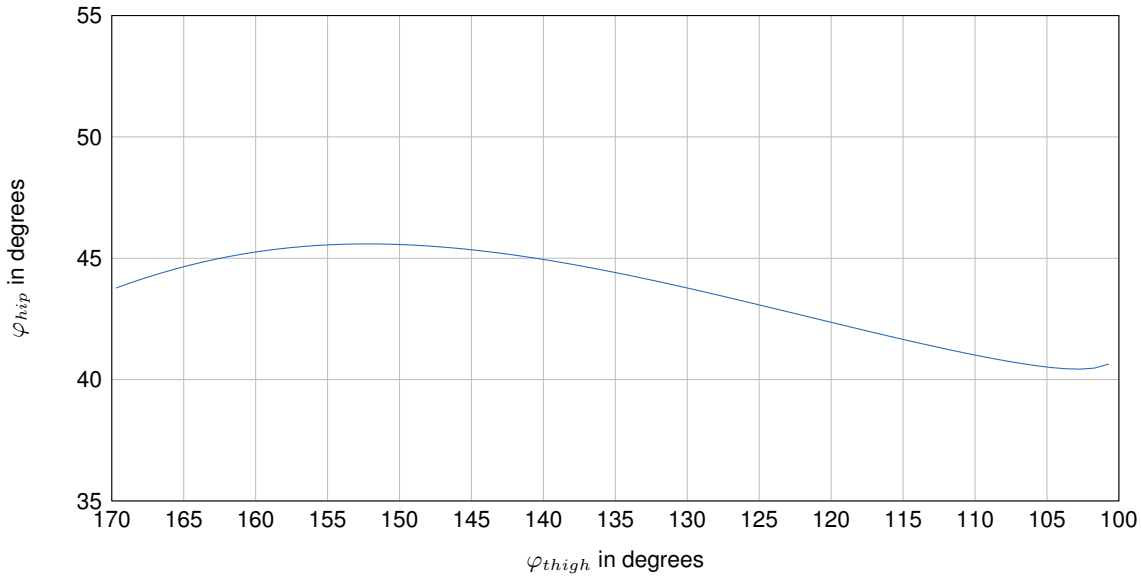

Figure 53 $\Delta\varphi_{hip}$ during sit-to-stand movement of a four-bar linkage individualized for the 5th male percentile

50th Male Percentile

The exhaustive search as seen in Fig. 54 found 4 fixed pivot points $\mathbf{q}$ for 440 moving pivot points $\mathbf{p}^1$. Fig. 54 illustrates the fixed pivot points as blue dots and the moving pivot points as $\times$. The corresponding pairs are illustrated in Fig. 55. These 4 2R dyads as seen in Fig. 55 can be combined to assemble 6 different four-bar linkages according to Eq. 5.23.

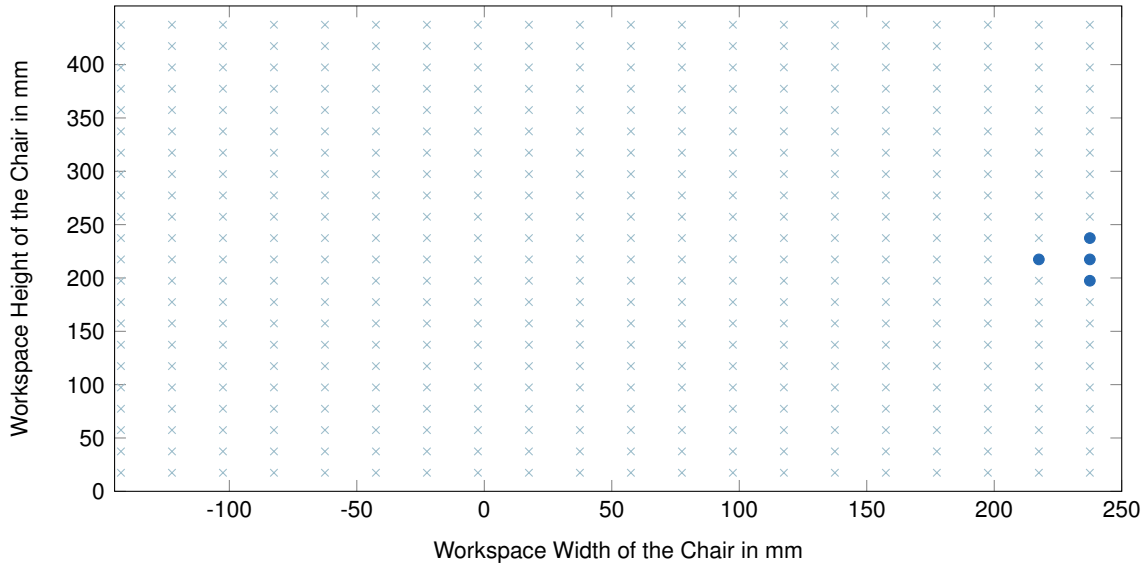

Figure 54 50th male percentile results of an exhaustive search for positions of moving pivot points within the rectangular workspace of the chair

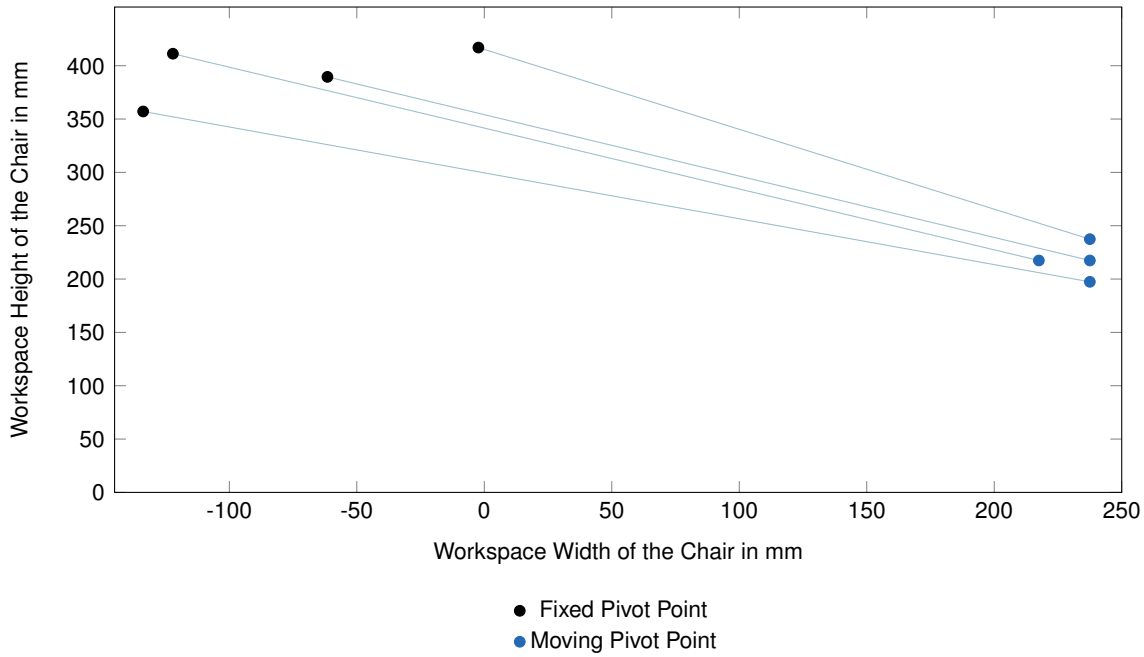

Figure 55 50th male percentile results of suitable 2R dyads configurations within the workspace of the chair

Once the dyads are found a bio-kinematic analysis is carried out which computes $\Delta\varphi_{hip}$ during a full STS movement for each six-bar linkage that consists of the four-bar linkage and the modeled 3R chain of the user. The six-bar linkage that creates the smallest $\Delta\varphi_{hip}$ value between the coupler and the thigh is shown in Table 11 and illustrated in Fig. 56:

Table 11 Four-bar linkage in 'sit' configuration for the 50th male percentile with the smallest $\Delta\varphi_{hip}$

${}^W\mathbf{q}_A$	${}^W\mathbf{q}_B$	${}^W\mathbf{p}_A^1$	${}^W\mathbf{p}_B^1$
$\begin{pmatrix} -122.2 \\ 411.2 \end{pmatrix}$	$\begin{pmatrix} -133.8 \\ 357.1 \end{pmatrix}$	$\begin{pmatrix} 217.5 \\ 217.4 \end{pmatrix}$	$\begin{pmatrix} 237.5 \\ 197.4 \end{pmatrix}$

As seen in Fig. 56 the movement between hip and seat stays approximately constant during a STS movement. The angle between thigh and seat starts at roughly 47° then starts to increase slightly followed by a small decrease thereby making a sinusoidal-like shape until the person stands. The maximum $\Delta\varphi_{hip}$ = 8.35°.

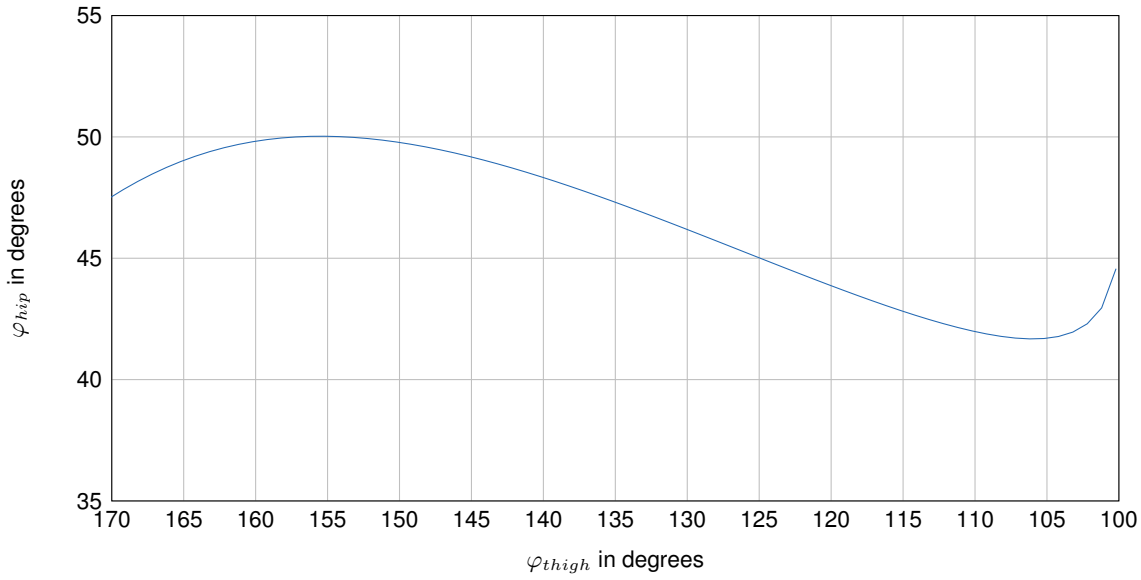

Figure 56 $\Delta\varphi_{hip}$ during sit-to-stand movement of a four-bar linkage individualized for the 50th male percentile

5th Female Percentile

The exhaustive search as seen in Fig. 57 found 51 fixed pivot points $\mathbf{q}$ for 440 moving pivot points $\mathbf{p}^1$. Fig. 57 illustrates the fixed pivot points as blue dots and the moving pivot points as $\times$. The corresponding pairs are illustrated in Fig. 58. These 51 2R dyads as seen in Fig. 58 can be combined to assemble 1275 different four-bar linkages according to Eq. 5.23. This percentile group achieved the most results compared to the other percentile groups.

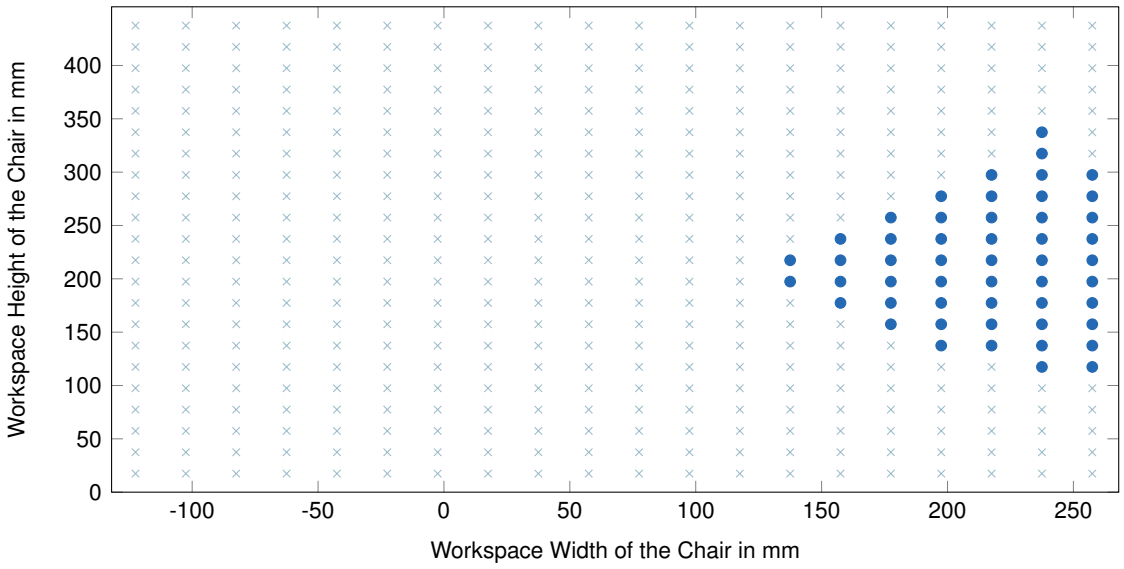

Figure 57 5th female percentile results of an exhaustive search for positions of moving pivot points within the rectangular workspace of the chair

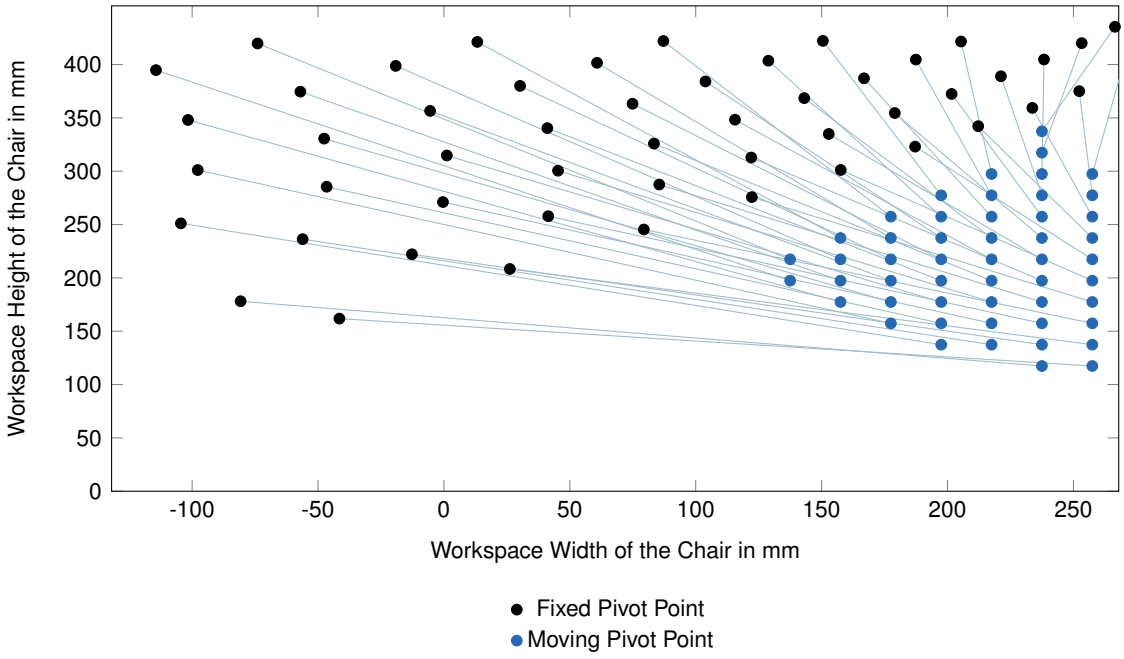

Figure 58 5th female percentile results of suitable 2R dyads configurations within the workspace of the chair

Once the dyads are found a bio-kinematic analysis is carried out which computes $\Delta\varphi_{hip}$ during a full STS movement for each six-bar linkage that consists of the four-bar linkage and the modeled 3R chain of the user. The six-bar linkage that creates the smallest $\Delta\varphi_{hip}$ value between the coupler and the thigh is shown in Table 12 and illustrated in Fig. 59:

Table 12 Four-bar linkage in 'sit' configuration for the 5th female percentile with the smallest $\Delta\varphi_{hip}$

${}^W\mathbf{q}_A$	${}^W\mathbf{q}_B$	${}^W\mathbf{p}_A^1$	${}^W\mathbf{p}_B^1$
$\begin{pmatrix} -0.4 \\ 271.1 \end{pmatrix}$	$\begin{pmatrix} -80.8 \\ 178.1 \end{pmatrix}$	$\begin{pmatrix} 217.5 \\ 157.4 \end{pmatrix}$	$\begin{pmatrix} 237.5 \\ 117.4 \end{pmatrix}$

As seen in Fig. 59 the movement between hip and seat stays nearly constant during a STS movement. The angle between thigh and seat starts at roughly 44° then starts to increase slightly followed by a small decrease thereby making a sinusoidal-like shape until the person stands. The maximum $\Delta\varphi_{hip}$ = 3.09°.

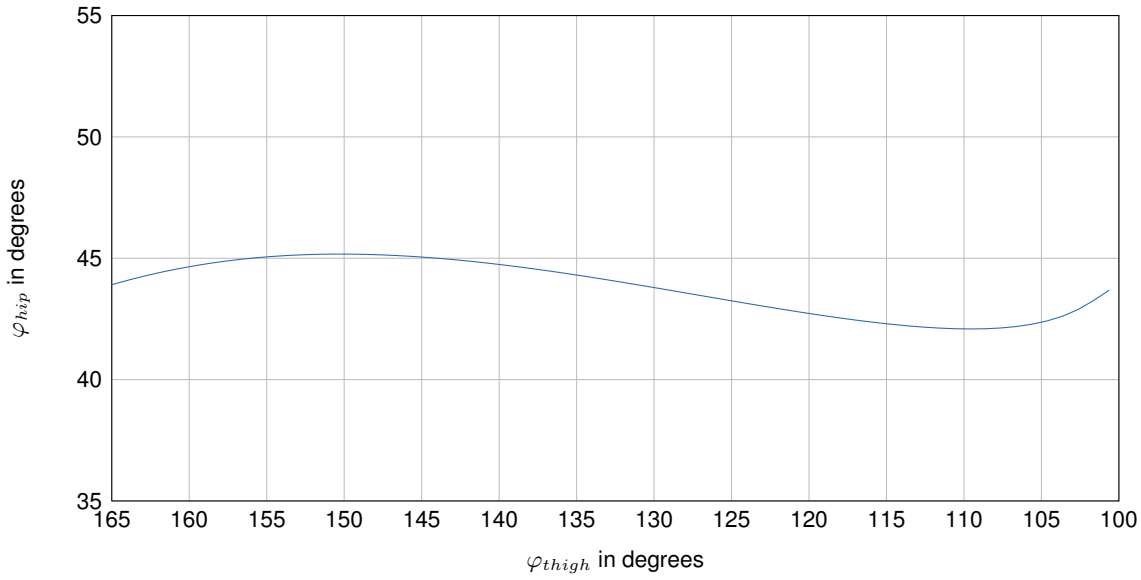

Figure 59 $\Delta\varphi_{hip}$ during sit-to-stand movement of a four-bar linkage individualized for the 5th female percentile

50th Female Percentile

The exhaustive search as seen in Fig. 60 found 24 fixed pivot points $\mathbf{q}$ for 440 moving pivot points $\mathbf{p}^1$. Fig. 60 illustrates the fixed pivot points as blue dots and the moving pivot points as $\times$. The corresponding pairs are illustrated in Fig. 61. These 24 2R dyads as seen in Fig. 61 can be combined to assemble 276 different four-bar linkages according to Eq. 5.23.

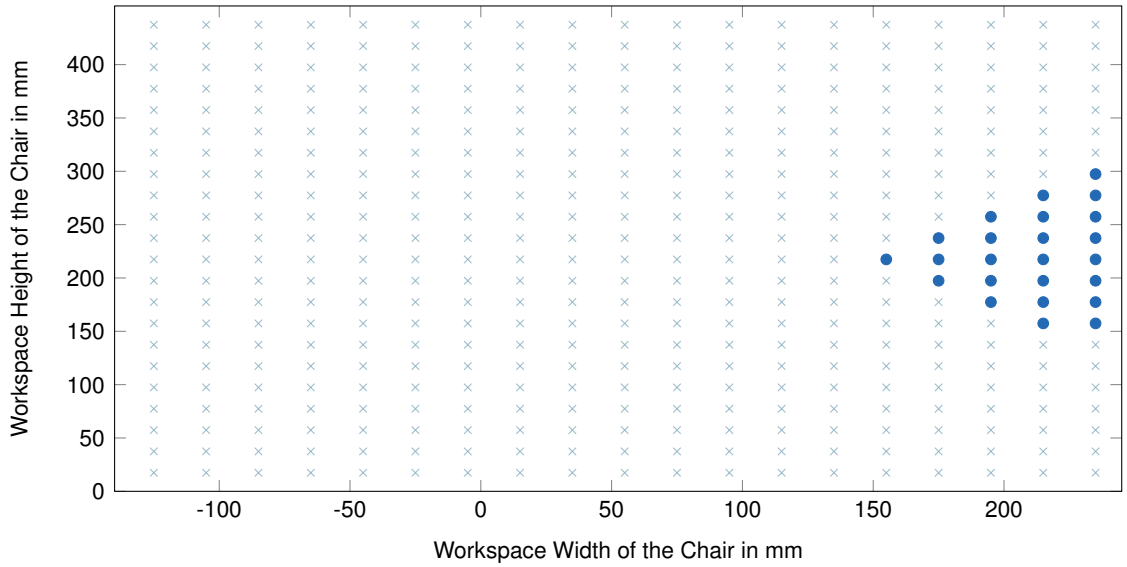

Figure 60 50th female percentile results of an exhaustive search for positions of moving pivot points within the rectangular workspace of the chair

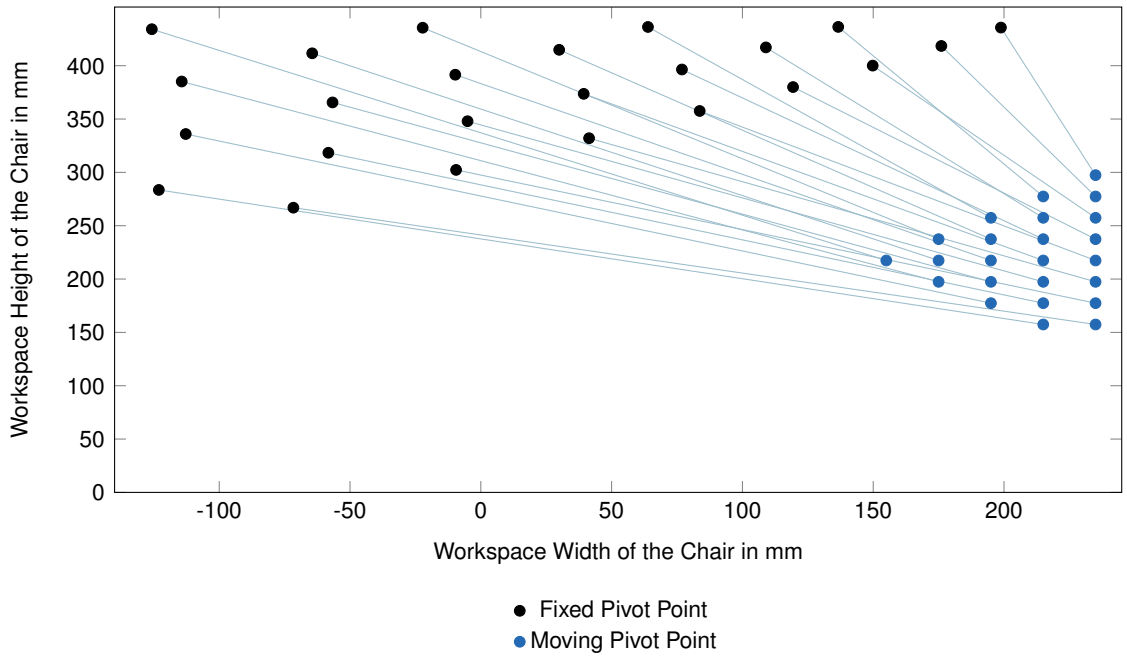

Figure 61 50th female percentile results of suitable 2R dyads configurations within the workspace of the chair

Once the dyads are found a bio-kinematic analysis is carried out which computes $\Delta\varphi_{hip}$ during a full STS movement for each six-bar linkage that consists of the four-bar linkage and the modeled 3R chain of the user. The six-bar linkage that creates the smallest $\Delta\varphi_{hip}$ value between the coupler and the thigh is shown in Table 13 and illustrated in Fig. 62:

Table 13 Four-bar linkage in 'sit' configuration for the 50th female percentile with the smallest $\Delta\varphi_{hip}$

${}^W\mathbf{q}_A$	${}^W\mathbf{q}_B$	${}^W\mathbf{p}_A^1$	${}^W\mathbf{p}_B^1$
$\begin{pmatrix} -56.7 \\ 365.6 \end{pmatrix}$	$\begin{pmatrix} -123.1 \\ 283.5 \end{pmatrix}$	$\begin{pmatrix} 195.0 \\ 197.4 \end{pmatrix}$	$\begin{pmatrix} 215.0 \\ 157.4 \end{pmatrix}$

As seen in Fig. 62 the movement between hip and seat stays nearly constant during a STS movement. The angle between thigh and seat starts at roughly 48° then starts to increase slightly followed by a small decrease thereby making a sinusoidal-like shape until the person stands. The maximum $\Delta\varphi_{hip}$ = 8.06°.

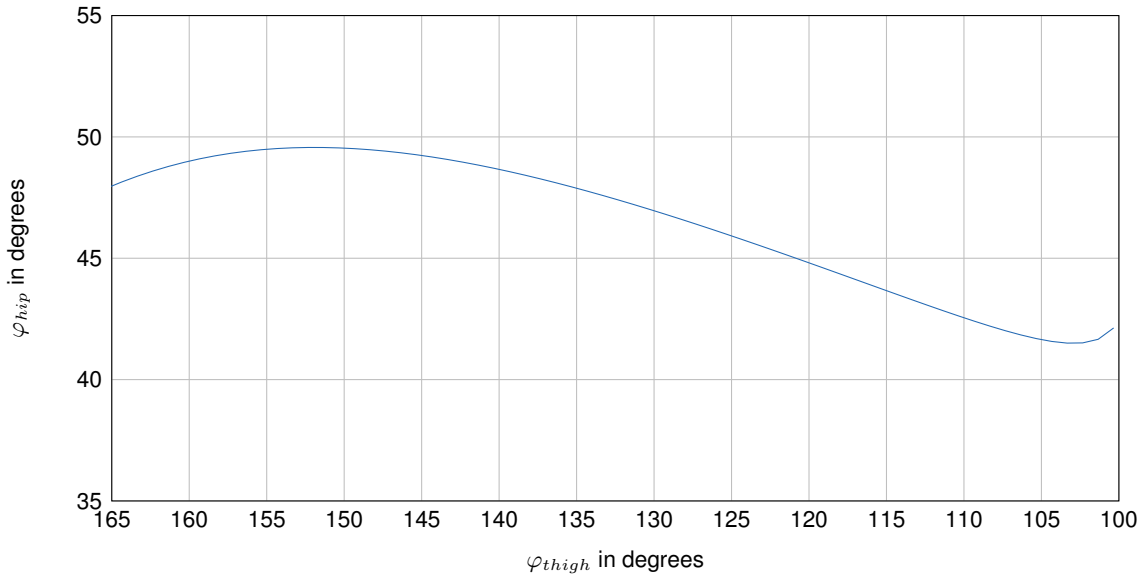

Figure 62 $\Delta\varphi_{hip}$ during sit-to-stand movement of a four-bar linkage individualized for the 50th female percentile

95th Female Percentile

The exhaustive search as seen in Fig. 63 found only 5 fixed pivot points $\mathbf{q}$ for 440 moving pivot points $\mathbf{p}^1$. Fig. 63 illustrates the fixed pivot points as blue dots and the moving pivot points as $\times$. The corresponding pairs are illustrated in Fig. 61. These 5 2R dyads as seen in Fig. 64 can be combined to assemble 10 different four-bar linkages according to Eq. 5.23.

Figure 63 95th female percentile results of an exhaustive search for positions of moving pivot points within the rectangular workspace of the chair

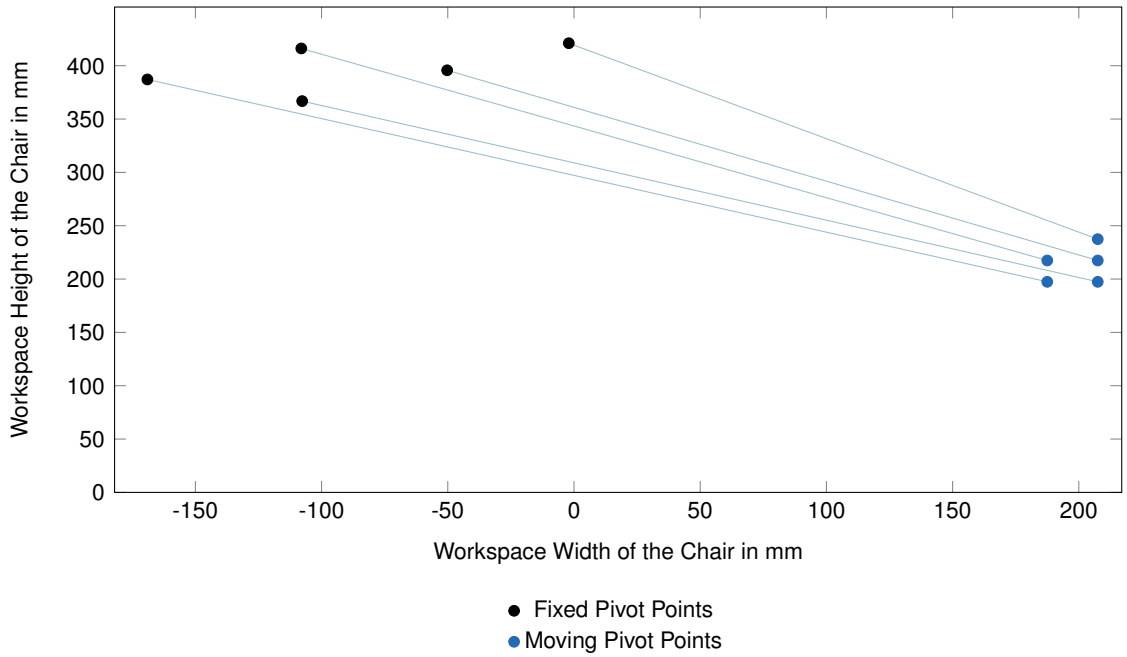

Figure 64 95th female percentile results of suitable 2R dyads configurations within the workspace of the chair

Once the dyads are found a bio-kinematic analysis is carried out which computes $\Delta\varphi_{hip}$ during a full STS movement for each six-bar linkage that consists of the four-bar linkage and the modeled 3R chain of the user. The six-bar linkage that creates the smallest $\Delta\varphi_{hip}$ value between the coupler and the thigh is shown in Table 14 and illustrated in Fig. 65:

Table 14 Four-bar linkage in 'sit' configuration for the 95th female percentile with the smallest $\Delta\varphi_{hip}$

${}^W\mathbf{q}_A$	${}^W\mathbf{q}_B$	${}^W\mathbf{p}_A^1$	${}^W\mathbf{p}_B^1$
$\begin{pmatrix} -108.0 \\ 416.2 \end{pmatrix}$	$\begin{pmatrix} -107.7 \\ 366.8 \end{pmatrix}$	$\begin{pmatrix} 187.5 \\ 217.4 \end{pmatrix}$	$\begin{pmatrix} 207.5 \\ 197.4 \end{pmatrix}$

As seen in Fig. 65 the movement between hip and seat stays nearly constant during a STS movement. The angle between thigh and seat starts at roughly 48° then starts to increase slightly followed by a small decrease thereby making a sinusoidal-like shape until the person stands. The maximum $\Delta\varphi_{hip}$ = 10.31°.

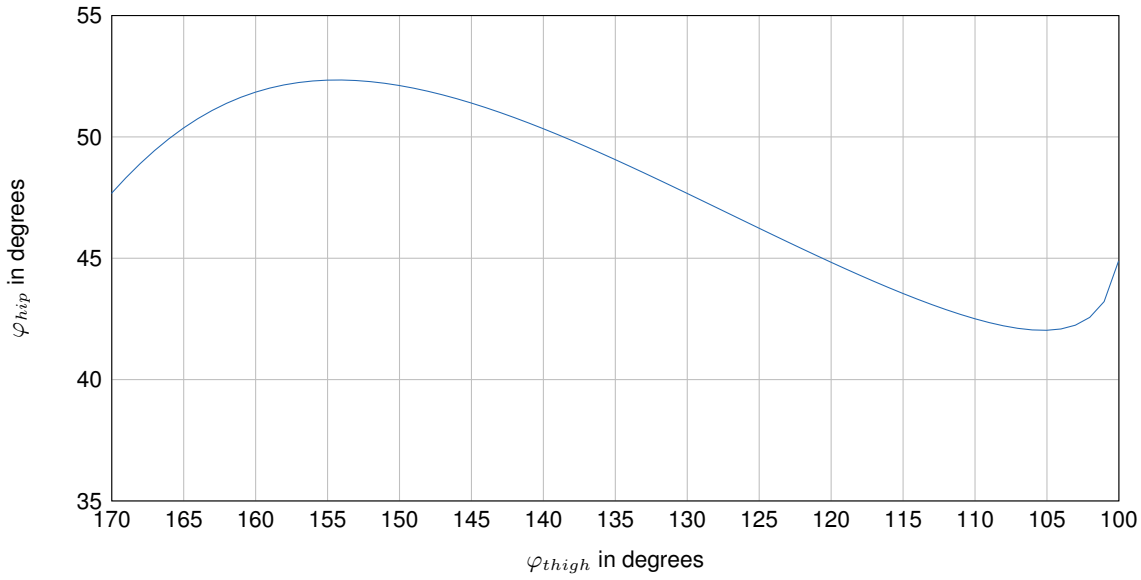

Figure 65 $\Delta\varphi_{hip}$ during sit-to-stand movement of a four-bar linkage individualized for the 95th female percentile

7.2. Verification of the Mechanical Design

Four prototypes based on the bio-kinematic design procedure have been realized as was explained in detail in section 6. Through a number of questioners the prototypes were evaluated and their purpose to assist elderly during STS movement verified. The purpose of the modular LAD is to assist people during the sit-down and stand-up process without the need of any other technological or professional help. The device partially fulfills the requirements for verification if the user is able to perform STS movement with additional help of a nurse or caregiver.

The target group of this experiments are people who have difficulties with STS movement. People who require technological assistance or even help from a nursing professional. To establish the correct target audience, residents of a long-term nursing home were asked on a discrete scale from left 'no difficulties' to right 'STS movement impossible'. Those that answered this question with 'with difficulties' and 'STS movement with external assistance' were selected for this study. Residents who were able to carry out STS movement were invited to try out the LAD. However, they were not asked to fill-out the questionnaire as it would falsify the results. Those, that are not able to stand up or sit down independently are usually helped out and into the chair using external lifting devices controlled by a nursing professional. The long-term nursing home *Luise-Kiesselbach-Haus* in Munich, Germany, was willing to participate in this experiment and written consent from the participants was obtained.

The first part of the experiment consists of a short questionnaire about the participants. The second part is a questionnaire about the LAD to be filled out by the participant testing the device for the following characteristics:

- Safety
- Adaptability
- Usability
- Promote Independence

With the first aspect the stability and safe handling of the LAD is verified and whether the participant feels stable throughout the stand-up and sit-down movement. The questionnaire assesses lateral stability as well as the damping of the device during STS movement.

The second aspect tests the device for its configuration options. Discrete position changes can be established for the gas spring strut which allows the user to configure the power of the device to the user's need. This is assessed by observation as wellas the user's subjective feeling whenever the participants sits down and stands up on the LAD. If configured incorrectly the device can be too weak to lift the user appropriately and if configured too powerfully

the device becomes too difficult to fold to its seated configuration.

During the ‘usability’ assessment the user is asked to answer questions about how easy the device is to use and to configure and whether the participant is able to use the device without any sophisticated instructions manual. In the fourth part of the questionnaire the user verifies if the device promotes the user’s independence, i.e. if the user is able to stand up and sit down without any help from another person.

Combining all of the aforementioned aspects of the questionnaire results in the user’s acceptance of the device which consists of those four aspects as has been mentioned by (Lektorad Pflege and Menche, 2014, p. 475). Last but not least the corresponding nursing professional is asked about their acceptance of this device and if they voice any concerns about this device.

Hypotheses

The downward spiral of mobility as was discussed in detail in section 2 and illustrated in Fig. 4 can only be decelerated if the use of this LAD promotes independence and achieves high user acceptance among participants. Subsequently, the following two hypotheses are proposed:

1. The modular LAD supports a person of the targeted audience such that the user is able to perform a STS movement independently without the assistance of another person or another device.
2. The acceptance of the modular LAD is achieved, once the entirety of the questionnaire achieves a positive result on average.

The following testimonies are allocated to the second hypothesis, which test the hypothesis on the aforementioned aspects:

- **Safety:** Sufficient precautions have been made to guarantee that the user is adequately secured.

  Secured against lateral falling

  A stable standing position is achieved

  Adequate damping of the device when sitting down

- **Adaptability:** The device is designed in such way that is customizable to the needs of the user and an effective help during STS movement

  Support during sit-down movement

  Support during stand-up movement

- **Usability:** The device is easy to use such that it can be seamlessly integrated into ADL.
- **Promote Independence:** The device relieves STS movement such that the user is able to perform the movement independently.

    Promote more frequent STS movements

    Promote independent STS movement

Testing the first hypothesis will achieve no significant results since it cannot be tested through variable metric sizes. It is merely based on categories such as 'no help', 'with help' or 'impossible'. Subsequently the LAD is fully functional, if 100% of the target group $p_{withoutHelp}$ are able to complete STS movement without any other assistance. However, the functionality of the device is partially fulfilled, if 100% of the target audience $p_{withoutorwithHelp}$ is able to complete STS movement. The functionality of the LAD is not achieved, if at least one participant of the target audience is not able to stand up or sit down. This yields the following expressions:

$$H_{Full\ Functionality} : p_{Without\ Help} = 100 \tag{7.1}$$

$$H_{Partial\ Functionality} : p_{With\ or\ Without\ Help} = 100 \tag{7.2}$$

The second hypothesis is related to the four aspects 'safety', 'adaptability', 'usability' and 'promote independence' which in turn are evaluated based on answers of one or more questions in the questionnaire as was explained earlier. Each question is given a discrete scale from '1 - Strongly Disagree' to '5 - Strongly Agree' which allows the subject to answer neutrally with '3 - Neither Agree, Nor Disagree'. To calculate an average value on these so-called *Likertscales* the values between the intervals must be equidistant. Such a quasi-metric scale presented in this questionnaire allows the use of statistical test evaluation methods.

The statements that are to be evaluated by the participant are phrased in such a way that '5 - Strongly Agree' reflects the full benefit of this LAD while '1 - Strongly Disagree' rejects the use of this device. The second hypothesis is satisfied if all answers of a single participant are greater than a predicted average value μ, where $\mu > 3$.

This results in a one-tailed t-test through which with help of the null hypothesis H_0 and the alternative hypothesis H_1 a decision can be made for or against the null-hypothesis with respect to the average value μ. Such specific test cases are verified either by acknowledging the alternative hypothesis or repudiating the null-hypothesis by a significant value.

The following null and alternative hypotheses are formed based on the judgment of the statements:

$$H_0 : \mu \leq \mu_0 = 3 \tag{7.3}$$

$$H_1 : \mu > \mu_0 = 3 \tag{7.4}$$

Materials & Experimental Set-Up

Center of the study are the LADs specifically designed for the chairs that are used within the nursing home *KWA Luise-Kiesselbach-Haus*. This facility makes use of a great number of 'Luca 1508/4*' chairs by *Kusch+Co GmbH & Co. KG* which was the primary reason that the modular LAD was tailored towards this chair. The seat has a seat hight of 450 mm and seat depth of 465 mm. Seat width measures 600 mm and the back rest is 436 mm high. For this study three of those chairs were required:

- The original unaltered chair
- A chair with integrated modular LAD with a gas spring strut of 100 mm
- A chair with integrated modular LAD with a gas spring strut of 150 mm

To clarify to correct use of chair for each participants weight and height of the participant are measured first. This is achieved through a weight scale and measuring tape. The digital scale 'Linea' by *Soehnle* gives accurate measurements to 100 g according to the manufacturer.

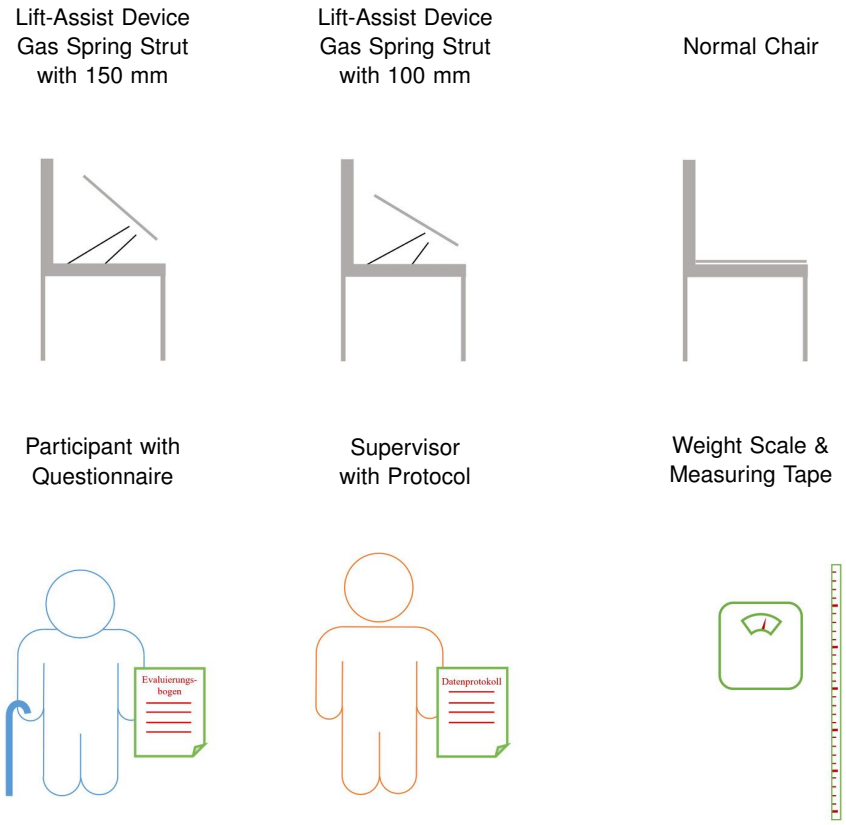

Figure 66 Schematic representation of the experimental materials and set-up

The experiment, i.e. the first and second phase of the experiment was conducted at the residential nursing home *KWA Luise-Kiesselbach-Haus* in Munich, Germany. The concept of the experimental set-up can be seen in Fig. 66. It consists of the three aforementioned chairs, a participant, supervisor in form of a nurse or caregiver, a weight scale and a measuring

tape.

The first part of the experiment will assess personal data of each participant. This will allow for the correct adjustment of the gas spring strut to the needs of the user. The second part of the experiment consists of nine single-choice questions about different aspects of the glsLAD. The questionnaire is illustrated in Appendix H.

Experimental Parameters

Two parameters can be changed at the modular LAD:

1. Stroke length of the gas spring strut depending on the hight of the user
   - for people up to 180 cm tall the 100 mm gas spring strut should be installed
   - for people over 180 cm tall the 150 mm gas spring strut should be installed
2. Gas spring position changes results in different weight classes depending on the weight of the user
   - Weight class I: 45 kg $\leq$ G $\leq$ 57 kg
   - Weight class II: 58 kg $\leq$ G $\leq$ 70 kg
   - Weight class III: 71 kg $\leq$ G $\leq$ 81 kg
   - Weight class IV: 82 kg $\leq$ G $\leq$ 92 kg

The parameters must be adjusted before the user sits on the device. This is to ensure that the appropriate calculations of the configurations fit to the user's needs. During the experiment the LAD is tested by the user and no other person or machine. Consequently, the user presents another variable in this experiment. This variable stands for the physical condition of that person, which is assumed to stay constant throughout this experiment.

Methods

The classification into the appropriate weight class of the LAD is accomplished by taking the weight of the participant. Smaller adjustments to the weight class can be made depending on the physical condition of the user which is assessed either by the participant himself or the corresponding nurse professional. The second hypothesis is confirmed or declined based on the null and alternative hypothesis. It is a question, as was mentioned earlier, about a one-tailed t-test. Based on a sample mean the null hypothesis must be tested. The null hypothesis H_0 can be proved as follows for a sufficiently approximated normal distribution of sample size n and an unknown variance of the population σ^2 (G. Kauermann et al. 2014, p. 27ff.):

$$T = \frac{\bar{X} - \mu_0}{S}\sqrt{n} \tag{7.5}$$

The sample mean $\bar{X}$ is calculated as follows:

$$\bar{X} = \frac{1}{n}\sum_{i=1}^{n} X_i \tag{7.6}$$

The standard deviation S is calculated as follows:

$$S = \sqrt{\frac{1}{n-1}\sum_{i=1}^{n}(X_i - \bar{X})^2} \tag{7.7}$$

In the approach of Fisher, 1970, the null hypothesis H_0 will be rejected, when the p-value of the test statistic is sufficiently extreme (vis-a-vis the test statistic's sampling distribution) and thus judged unlikely to be the result of chance. In a one-tailed test, "extreme" is decided beforehand as either meaning “sufficiently small” or meaning “sufficiently large”. The definition of μ_0 for the alternative hypothesis is therefore either confirmed when the significance level of $p = 0.05$ or declined with the null hypothesis with significance level $p = 0.05$.

Sit-to-Stand Experiment

Before the experiments were carried out, written consent was acquired from the nursing home director as well as the participants. The experiments were conducted on multiple days from Tuesday, July 26th 2016 through Friday, July 29th 2016 in the administration office on the first floor. The following describes the experimental procedure:

- **Phase I of the Experiment**

  Step 1: At first the LAD is demonstrated and explained in detail by the experimental supervisor during the presence of the participant. The participants then receive the following instructions verbally about the experiment:

  The participant stands in front of the chair in a stable standing position.

  The participant must carry out STS movement while making use of the armrests on both sides.

  The participant ought to sit as far back on the chair as comfortably possible

  The experiment can be aborted at any time, should the participant feel uncomfortable or unsafe with the study.

  Step 2: The participant was asked to stand on the weight scale or if not physically possible role onto a larger weight scale designed for wheelchairs. The weight of the wheelchair is known such that the weight of ther user can be calculated. The height of the participant is either measured or taken from records if available.

  Step 3: Depending on the measured height and weight of the participant the appropriate LAD and weight class are selected respectively.

Step 4: The participant is asked to sit down and stand up as part of a trial run. In case this action requires additional help by another person, the help is documented in the protocol. Last changes to the power of the LAD can be made, if asked for by the user.

- **Phase II of the Experiment**

  Step 1: The participant is asked to sit down and stand up from the normal chair without LAD. A nurse or caregiver helps the user to carry out these movements if help is necessary.

  Step 2: During the next step the participant is asked to carry out the same movement on the chair with LAD. Step 1 and 2 are repeated three times.

  Step 3: The participant can now rest on a chair and is asked to fill out the questionnaire about the four aspects discussed above about the LAD.

Results

None of the 50 participants, who successfully took part in this experiment had a history of immobilization. Participants were primarily selected by the nursing staff. However, voluntary participants were permitted to take part in this study, if they were subject to age-related physical disabilities. Some patients were suffering from a starting or even chronic dementia. On the other hand, participants were only allowed to participate in this study, if they were able to fill out the questionnaire by themselves.

The presence of a nurse or caregiver played a fundamental role in this experiment, especially for patients suffering from dementia. The participation of the nurse gave many participants a feeling of safety and comfort. As a result no experiment had to be aborted prematurely.

The following shows the age histogram of the participants:

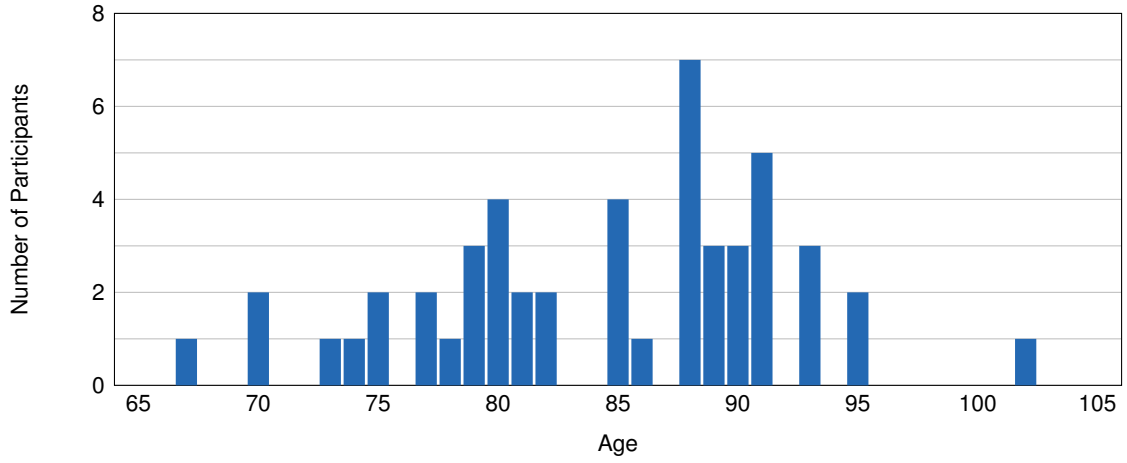

Figure 67 Histogram of the weight distribution of 50 participants in absolute numbers

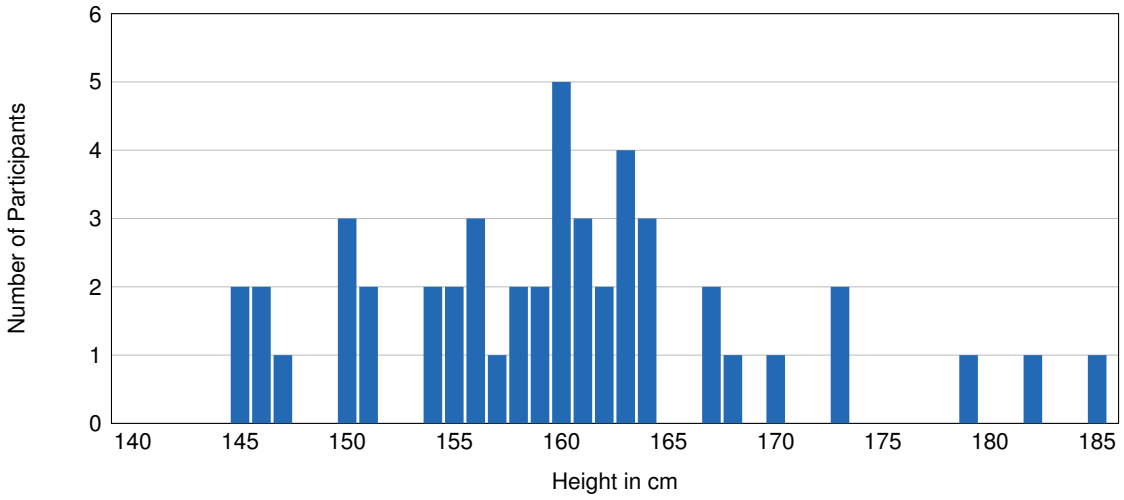

Figure 68 Histogram of the height distribution of 50 participants in absolute numbers

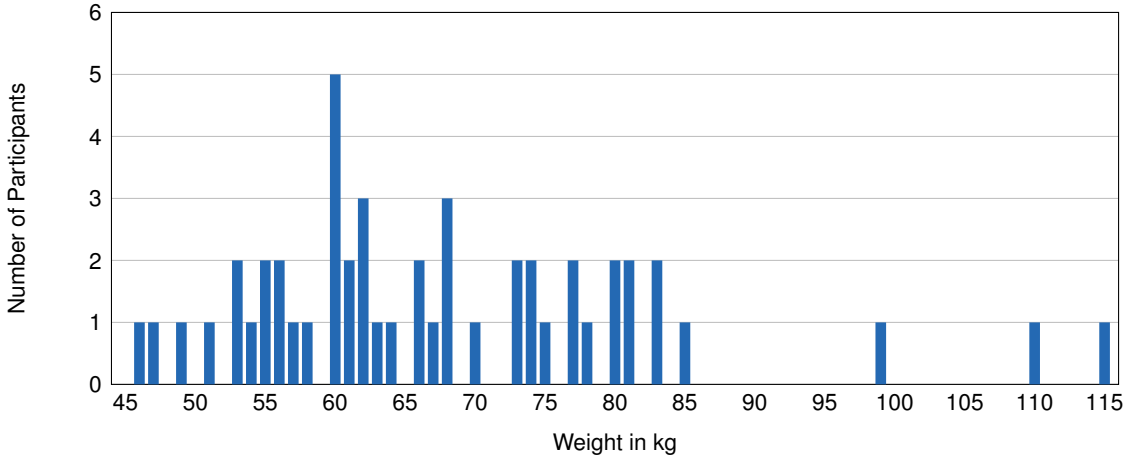

Figure 69 Histogram of the weight distribution of 50 participants in absolute numbers

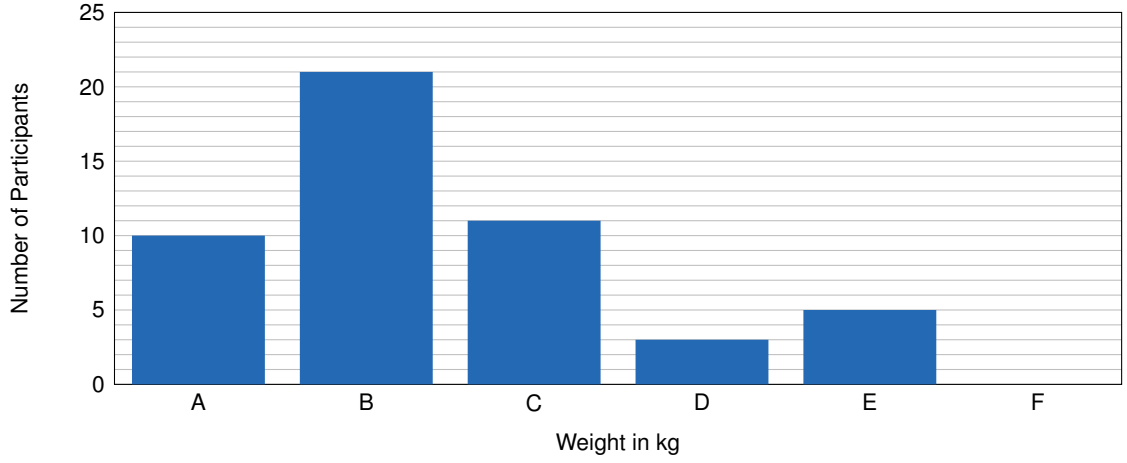

Figure 70 Histogram of the physically disabled scale distribution of 50 participants in absolute numbers

84% of the participants were female, while 16% were male. The average age was 84.5 years and the average height and weight was 160.1 cm and 67.9 kg respectively. For 20% of the participants a weaker gas springs strut position to a lower weight class was applied by request of the participant. However, no one asked for a stronger gas spring strut. 34%, 36%, 22% and 8% of the participants were assigned to weight class I, II, III and IV respectively.

86% of the participants were able to sit down and stand up successfully without help, 14% with assistance by a nurse and 0% were not able to complete a STS movement. Subsequently the first hypothesis is not met which required 100% of all participant to stand up independently with the LAD. However, the first hypothesis is partially confirmed since all participants were either able to sit down and stand up independently or with assistance of another person.

The evaluation questionnaire was filled out by every one of the 50 participants resulting in mostly '4 - Agree' or '5 - Strongly Agree' results on average as seen in Fig. 71-78.

The second hypothesis is acknowledged or declined based on the null and alternative hypothesis based on the cumulative results of the evaluation questionnaire. This means that it is only confirmed when the average rating of the LAD is significantly larger (α = 0.05) than a threshold value $\mu > 3$. Results are displayed in Fig. 79.

Under the assumption that the group of participants $n = 50$ is approximately normally distributed with an unknown variance of the population σ^2, a sample mean $\bar{X} = 3.8$ and variance $\sigma^2 = 0.7$ was established. Applying the aforementioned t-test results in $t = 7.7$ which is significantly larger than $t_{1-\alpha,n-1} = t_{0.95,49} = 1.68$. The t-test value lies within the region of rejection. Subsequently, H_0 is rejected and H_1 is significantly acknowledged. The second hypothesis is therefore confirmed.

Question 1: “You feel secured against lateral falling while using the lift-assist chair”

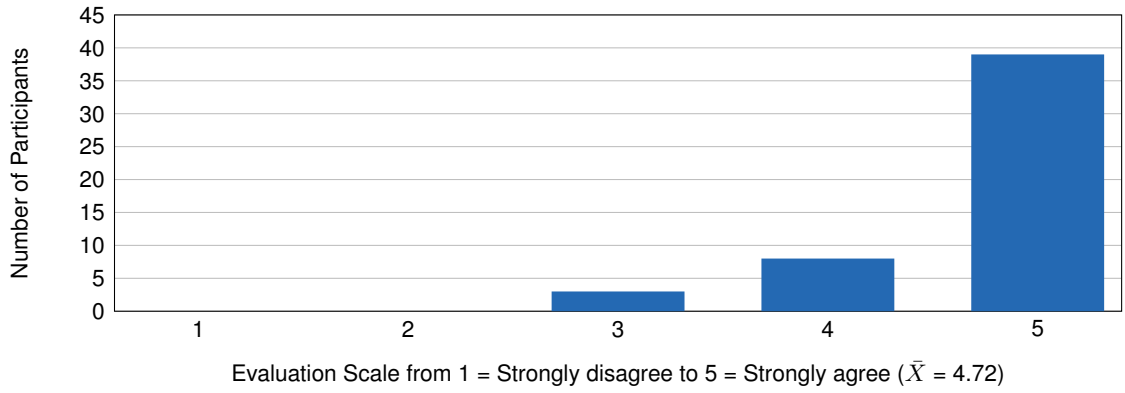

Figure 71 Histogram of the results of the first question answered by 50 participants

Question 2: “You are being lifted to a stable standing position while using the lift-assist chair”

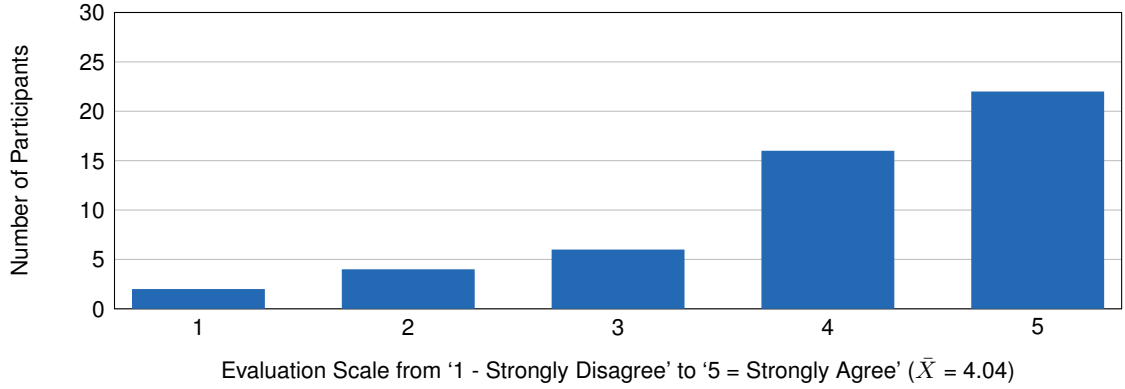

Figure 72 Histogram of the results of the second question answered by 50 participants

Question 3: “You feel sufficiently cushioned while sitting down on the lift-assist chair”

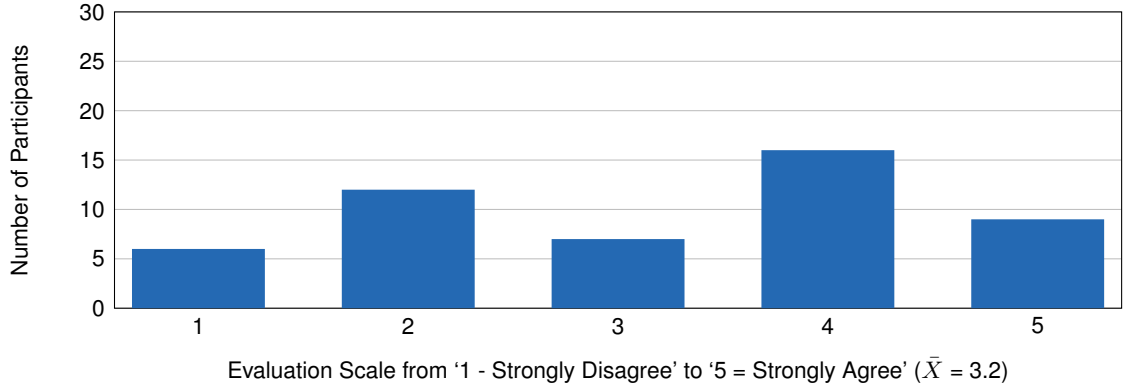

Figure 73 Histogram of the results of the third question answered by 50 participants

Question 4: “The lift-assist chair is easy to use”

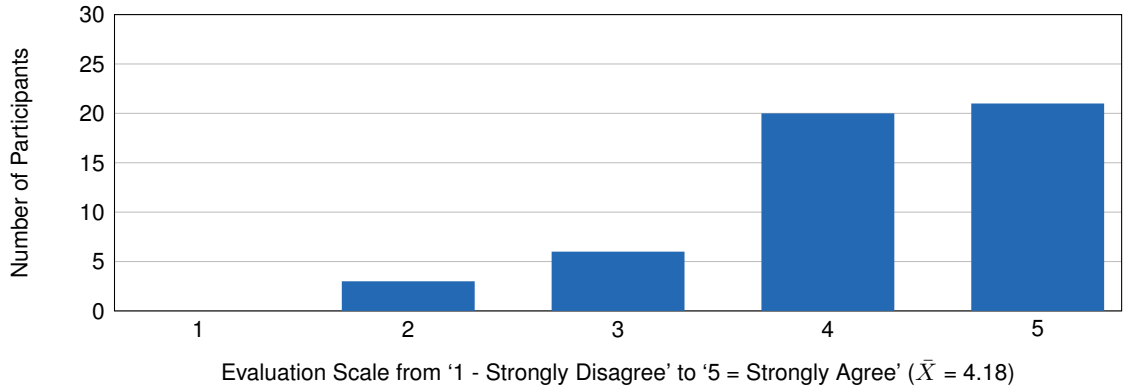

Figure 74 Histogram of the results of the fourth question answered by 50 participants

Question 5: “The lift-assist chair motivated me to stand up more frequently”

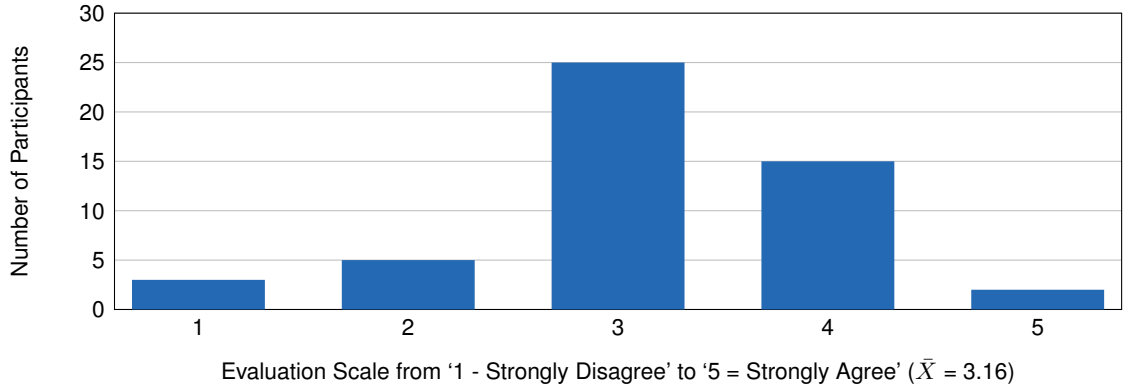

Figure 75 Histogram of the results of the fifth question answered by 50 participants

Question 6: “The lift-assist chair allows me to stand up independently without the help of another person or device”

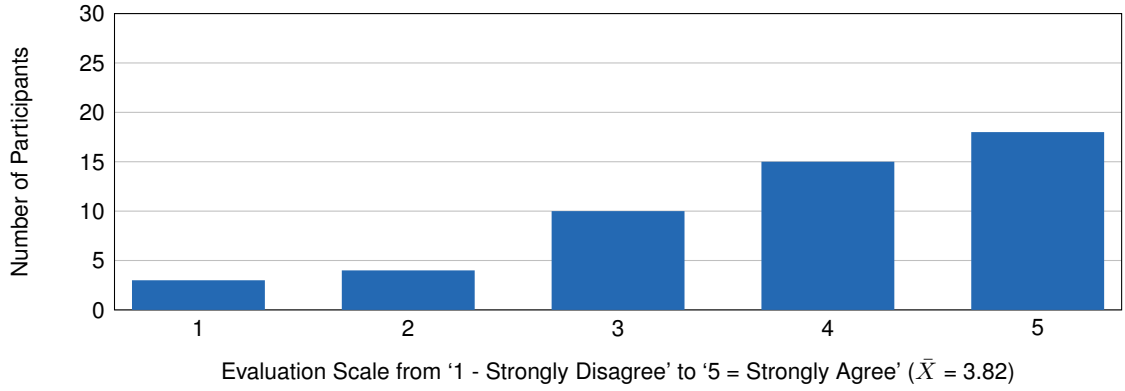

Figure 76 Histogram of the results of the sixth question answered by 50 participants

Question 7: “You feel supported when sitting down with the lift-assist chair compared to a normal chair”

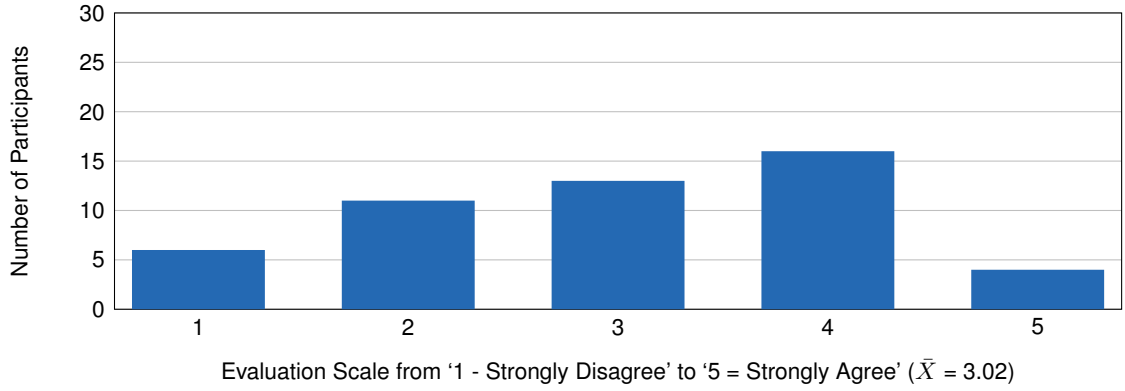

Figure 77 Histogram of the results of the seventh question answered by 50 participants

Question 8: “You feel supported when standing up from the lift-assist chair compared to a normal chair”

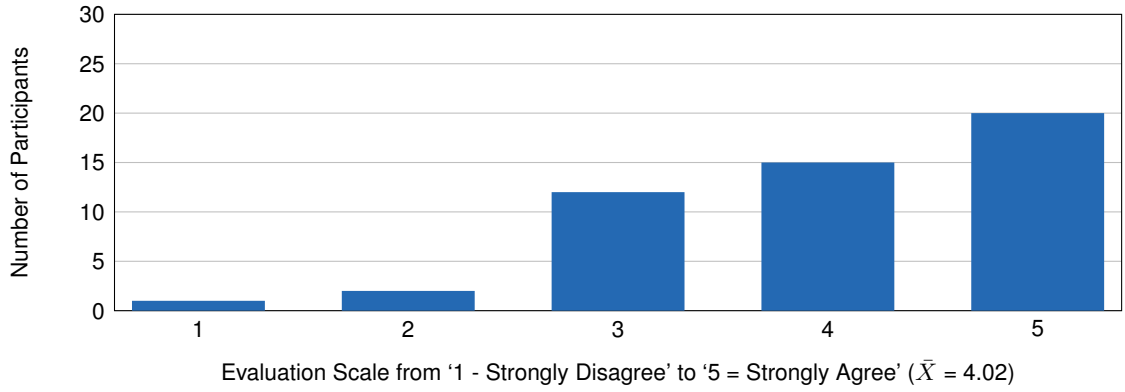

Figure 78 Histogram of the results of the eighth question answered by 50 participants

Cumulative results of all questions:

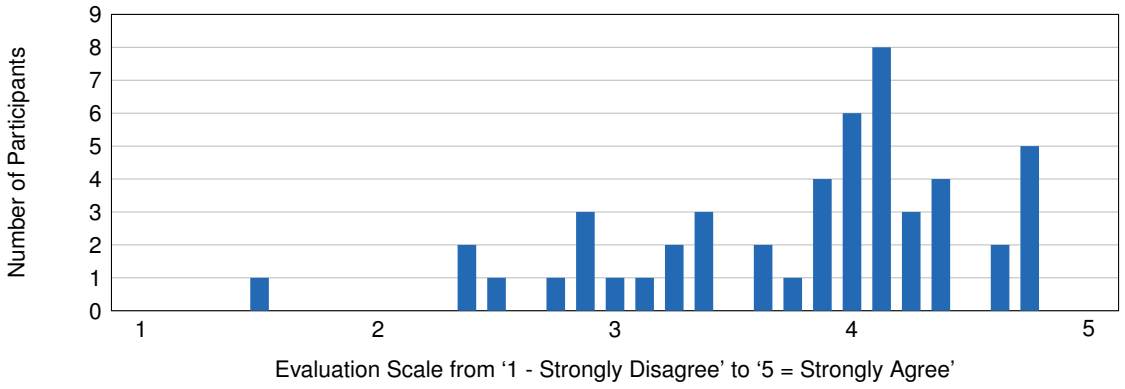

Figure 79 Histogram of the frequency of average results for each of the 50 participants

7.3. Discussion

The results of the experiment showed that the device can support people with problems during STS movement. 86% of all participants were able to stand up with the device while 14% still required additional help from another person. Given the fact, that the device only helps passively, i.e. the participant must initiate the movement, these results are especially significant given the fact that only 62% of the participants said that they were able to stand up independently as seen in Fig. 70. Based on these results one could argue that the device closes the gap between functional independence by 24% with respect to this experimental set-up.

The results of the evaluation questionnaire showed that the device was received mostly positively with a percentage of $p \leq 50\%$ of the participants with a rating of 4 or 5. This was especially the case for the questions relating to sit down, stand up, comfort and whether the device would promote personal independence.

Some participants complained that the device was still too tall making it sometimes more difficult to sit down on the LAD. In turn, however, it provided a better stand up support. The chairs that were used in this experiment have a seat hight that is already higher than the average chair measuring 45 cm in height. This is because higher chairs make is easier to stand up from as was discussed in detail in Section 4.3. While available lift-assist cushions would only increase the natural seat hight even more, this LAD has the benefit of being seamlessly integrated into the chair thereby not rising the seat height.

Last but not least, 50% of the participants had neither agreed nor disagreed with the statement that they would feel the benefit of standing up more frequently during the day with the LAD. Partially, this is because many of the participants are still very active throughout the day.

8. Conclusion

Loss of mobility is a serious disability that impacts all major physiological systems in the human body and is the most common diagnosis for long-term care dependency. To live a long and healthy life, i.e. to keep the respiratory and blood circulation active as well as preventing muscle tissue from degenerating, regular exercise is necessary. Physical exercise starts with STS movement. A physical motion that is carried out countless times during the day and a prerequisite to all other activities. As we age, this motion becomes increasingly difficult thereby accelerating towards care dependency. The lack of both professional nursing staff and long-term nursing facilities in Germany compels elderly people to stay independent and to live at home for a longer period of time.

A broad range of technological devices exist to help the elderly to stand up from a chair. Lifting cushions that can be placed on to a chair and unfold to lift the user up, lifting mechanisms integrated into armchairs or wheelchairs and exoskeleton robots that are being developed at many institutes around the world. However, intense time constraints inhibit nursing staff from using these devices. One solution to this problem is presented in this thesis by integrating a lift-assist mechanism into furniture such as a chair. The lift-assist mechanism raises the seat pan with a gas spring strut to help the user to stand up independently thereby potentially eliminating the need for physical assistance of a nursing staff for this activity. Furthermore, this mechanism is designed to fit to the biomechanical parameters of the user, such as leg length and weight, as well as to the limited dimensions of the workspace of the chair, i.e., the mechanism ought to fit underneath the seat pan and between the chair legs.

In this thesis, the outline of necessary design steps to synthesize a bio-kinematic LAD is explained. Herein, a kinematic six-bar linkage is analyzed that combines mechanical elements with biological elements of the user to improve support of the STS. A four-bar linkage is individualized to the biomechanical parameters of the user and the amount of support the user needs. These could be determined either by a medical doctor or physiotherapist or by the user independently. The swiftly growing rapid prototyping industry combined with rapid manufacturing techniques supports the argument of more customization and individualization to a smaller group of people or even a single user. These types of manufacturing techniques permit for the swift manufacturing of crucial assembly parts, which by traditional manufacturing means would have been very expensive to be produced.

This thesis also highlights an in-depth kinetostatic analysis of the forces acting on the system, the chair as well as the user. The prototype is actuated by a gas spring strut. The decision to place such type of actuation into the chair rests on the fact that an electrically driven unit would have required batteries, or even a power socket which places severe limitations to the operation of the device. In addition, a gas spring strut is a passive device. Energy is stored within the gas spring strut when the user sits down. When the user stands up the user

must provide some initial energy in order to feel the energy supplied by the gas spring strut. This is expected to help decelerate the degeneration process of muscle tissue as the user must provide their own muscle force. Furthermore, the device can be used without the need of a locking mechanism to prevent the mechanism of lifting a person against their will.This improves accessibility and usability as was found in the evaluation of the device.

The experiments for the computational design procedure showed a high density of possible four-bar linkages for different percentile groups of males and females in Germany. In most cases, a kinematic analysis showed that the individualization process was partially successful showing minimal deviation only in form of movement of the thigh of the user on the seat pan. However, cases exist where no four-bar linkage could be found within the restricted workspace of the chair. To find a solution to this problem, perhaps deviations of the task positions must be taken into consideration in order for the four-bar linkage to be placed within the dimensions of the chair.

8.1. Future Work

The concept of individualizing mechanical structures to biological structures such as human limbs is an area that becomes increasingly important as areas of wearable robotics for rehabilitation purposes advance. In particular, many wearable devices are being used by paraplegics. While they cannot physically feel if the device inflicts any discomfort or even pain, it is uncertain if the mechanical structures mapped onto the user cause damages to the ligaments of the joints in the long term. Future work could therefore combine a more in depth biomechanical analysis of the joint forces in conjunction with mechanical structures such as ortheses or even actuated ortheses, i.e. wearable robots.

The mechanical design could be improved by integrating a damping mechanism during sit down. This would increase the comfort of the user as mentioned many times during the evaluation of the device. Furthermore, the use of this device should be placed within a nursing home over several weeks or months to see if there is some form of rehabilitation. It would be interesting to find out if the device rehabilitates independent STS movement in people with a form of musculoskeletal disorder. Last but not least, it would be interesting to find out how much the device can actually help the user during the stand up process with quantitative data. In particular comparing data taken from other assist devices - devices that have not been individualized to the measurements of the user.

Finally, this thesis has focused primarily on the stand up process. The sit-to-stand motion is far more challenging than stand-to-sit motion, which is primarily the reason why only sit-to-stand motion has been taken into consideration. However, a deeper analysis of stand-to-sit motion, i.e. sitting down could improve the ergonomics of the four-bar linkage.

Bibliography

Akram, Sakineh B. and McIlroy, William E. (2011): Challenging Horizontal Movement of the Body During Sit-to-Stand: Impact on Stability in the Young and Elderly, Journal of Motor Behavior **43**(2): 147–153.
URL: *http://www.tandfonline.com/doi/full/10.1080/00222895.2011.552077*

Alley, Dawn, Liebig, Phoebe, Pynoos, Jon, Banerjee, Tridib and Choi, In Hee (2007): Creating Elder-Friendly Communities, Journal of Gerontological Social Work **49**(1-2): 1–18.
URL: *http://www.tandfonline.com/doi/abs/10.1300/J083v49n01_01*

Bashford, Guy M., Steele, Julie R., Munro, Bridget J., Westcott, Grant and Jones, Maren E. (1998): Ejector chairs: do they work and are they safe?, Australian Occupational Therapy Journal **45**(3): 99–106.
URL: *http://onlinelibrary.wiley.com/doi/10.1111/j.1440-1630.1998.tb00790.x/abstract*

Behrens, Johann, Horbach, Annegret and Müller, Rolf (2008): Forschungsstudie zur Verweildauer in Pflegeberufen in Rheinland-Pfalz (ViPb): Abschlussbericht, Hallesche Beiträge zu den Gesundheits- und Pflegewissenschaften (12): 1–74.

Burdett, Ray G., Habasevich, Robert, Pisciotta, Jeffrey and Simon, Sheldon R. (1985): Biomechanical comparison of rising from two types of chairs, Physical therapy **65**(8): 1177–1183.
URL: *http://ptjournal.apta.org/content/65/8/1177*

Cohen-Mansfield, J., Culpepper, W. J. 2nd and Carter, P. (1996): Nursing staff back injuries: prevalence and cost in long term care facilities, AAOHN Journal **44**(1): 9–17.

Curdija, Mladen, Dusak, Slavko, Golubic, Ivan, Marko, Ines, Svetec, Drago, Storga, Ivan, Hajdu, Alexander, Sauter, Karl-Juergen and Weinzierl, Richard (2010): Seating furniture with lifting mechanism to assist getting up. EP 1891921 B1.

Dall, Philippa M. and Kerr, Andrew (2010): Frequency of the sit to stand task: An observational study of free-living adults, Applied Ergonomics **41**(1): 58–61.
URL: *http://www.sciencedirect.com/science/article/pii/S000368700900057X*

D'Angelo, Lorenzo T., Abdul-Sater, Kassim, Pfluegl, Florian and Lueth, Tim C. (2015): Wheelchair models with integrated transfer support mechanisms and passive actuation, Journal of Medical Devices **9**(1): 011012.
URL: *http://medicaldevices.asmedigitalcollection.asme.org/article.aspx?articleid=2089565*

Dmitry Chervyakov, DIW Berlin (2015): Population Ageing and Its Effects on the German Economy.
URL: *https://www.diw.de/en/diw_01.c.514092.en/press/diw_roundup/population_ageing_and_its_effects_on_the_german_economy.html*

Fisher, Ronald Aylmer (1970): Statistical methods for research workers, 14 Aufl., Oliver & Boyd, Edinburgh.

Fuchs, J., Busch, M. A., Gosswald, A., Holling, H., Kuhnert, R. and Scheidt-Nave, C. (2013): Korperliche und geistige Funktionsfahigkeit bei Personen im Alter von 65 bis 79 Jahren in Deutschland: Ergebnisse der Studie zur Gesundheit Erwachsener in Deutschland, Bundesgesundheitsblatt, Gesundheitsforschung, Gesundheitsschutz **56**(5-6): 723–732.
URL: *http://rd.springer.com/article/10.1007/s00103-013-1684-7*

Hackmann, Tobias (2010): Arbeitsmarkt Pflege: Bestimmung der künftigen Altenpflegekräfte unter Berücksichtigung der Berufsverweildauer, Sozialer Fortschritt **59**(9): 235–244.
URL: *http://ejournals.duncker-humblot.de/doi/abs/10.3790/sfo.59.9.235*

Hakamiun, Reza, Genereux, Douglas P., Falin, Michael D., Mutka, Michael J. and Brooke, Jason Conrad (2001): Stand assist lift. US6175973 B1.

Hamm, Ingrid, Seitz, Helmut and Werding, Martin (eds) (2008): Demographic Change in Germany, Springer Berlin Heidelberg, Berlin, Heidelberg.

Heidenblut, S. and Zank, S. (2015): Selbstständigkeitsinterventionen, in A. Maercker (ed.), Alterspsychotherapie und klinische Gerontopsychologie, Springer, Berlin, S. 315–336.
URL: *http://rd.springer.com/chapter/10.1007/978-3-642-54723-2_14*

Hirsch, Kathleen and Lindenberg, Sebastian (2013): Beschwerden im Bereich des Bewegungsapparats bei Pflegekräften in einem Krankenhaus der Schwerpunktversorgung in Sachsen-Anhalt, HeilberufeScience **4**(4): 136–141.
URL: *http://link.springer.com/content/pdf/10.1007*

Hughes, M. A., Myers, B. S. and Schenkman, M. L. (1996): The role of strength in rising from a chair in the functionally impaired elderly, Journal of Biomechanics **29**(12): 1509–1513.
URL: *http://www.ncbi.nlm.nih.gov/pubmed/8945648*

Husty, Manfred, Karger, Adolf, Sachs, Hans and Steinhilper, Waldemar (1997): Kinematik und Robotik, Springer-Verlag, Berlin, Heidelberg.

Ikeda, Elizabeth R., Schenkman, Margaret L., Riley, Patrick O. and Hodge, W. Andrew (1991): Influence of Age on Dynamics of Rising from a Chair, Physical therapy **71**(6): 473–481.
URL: *http://ptjournal.apta.org/content/71/6/473*

Janssen, W. G., Bussmann, H. B. and Stam, H. J. (2002): Determinants of the sit-to-stand movement: a review, Physical therapy Journal of the American Physical Therapy Association **82**(9): 866–879.
URL: *http://ptjournal.apta.org/content/82/9/866*

Kazerooni, Homayoon, Harding, Nathan H. and Angold, Russdon (2011): Lower extremity exoskeleton. US 7947004 B2.

Kerr, Kathleen M., White, John A., Mollan, Raymond A. B. and Baird, Helen E. (1991): Rising from a Chair: A Review of the Literature, Physiotherapy **77**(1): 15–19.
URL: *http://www.physiotherapyjournal.com/article/S0031-9406(10)61663-X/abstract*

Kong, Kyoungchul and Jeon, Doyoung (2006): Design and control of an exoskeleton for the elderly and patients, IEEE/ASME Transactions on Mechatronics **11**(4): 428–432.
URL: *http://ieeexplore.ieee.org/document/1677574/*

Leiter, M. P. and Harvie, P. L. (1996): Burnout Among Mental Health Workers: A Review and a Research Agenda, International Journal of Social Psychiatry **42**(2): 90–101.
URL: *http://isp.sagepub.com/content/42/2/90*

Lektorad Pflege and Menche, Nicole (2014): Pflege Heute, 6 Aufl., Urban & Fischer Verlag, München.

Maier, Tobias and Afentakis, Anja (2013): Forecasting supply and demand in nursing professions: impacts of occupational flexibility and employment structure in Germany, Human resources for health **11**: 24.
URL: *http://rd.springer.com/article/10.1186/1478-4491-11-24*

Matjacic, Zlatko, Zadravec, Matjaz and Oblak, Jakob (2016): Sit-to-Stand Trainer: An Apparatus for Training "Normal-Like" Sit to Stand Movement, IEEE transactions on neural systems and rehabilitation engineering : a publication of the IEEE Engineering in Medicine and Biology Society **24**(6): 639–649.
URL: *http://ieeexplore.ieee.org/document/7119612/*

Matolycz, Esther (2016): Pflege von alten Menschen, Springer Berlin Heidelberg, Berlin, Heidelberg.

McCarthy, J. Michael and Soh, Gim Song (2011): Geometric Design of Linkages, Bd. 11, 2 Aufl., Springer-Verlag, New York, NY.

Mizner, Ryan L. and Snyder-Mackler, Lynn (2005): Altered loading during walking and sit–to–stand is affected by quadriceps weakness after total knee arthroplasty, Journal of Orthopaedic Research **23**(5): 1083–1090.
URL: *http://onlinelibrary.wiley.com/doi/10.1016/j.orthres.2005.01.021/*

Munro, Bridget J. and Steele, Julie R. (2000): Does using an ejector chair affect muscle activation patterns in rheumatoid arthritic patients? A preliminary investigation, Journal of Electromyography and Kinesiology **10**(1): 25–32.
URL: *http://www.jelectromyographykinesiology.com/article/S105064119900176/fulltext*

Munro, Bridget J., Steele, Julie R., Bashford, Guy M., Ryan, Melinda and Britten, Nicole (1998): A kinematic and kinetic analysis of the sit-to-stand transfer using an ejector chair: implications for elderly rheumatoid arthritic patients, Journal of Biomechanics **31**(3): 263–271.
URL: *http://www.sciencedirect.com/science/article/pii/S0021929097001309*

Munton, J. S., Ellie, M. I. and Anne Chamerlain, M. Wright, V. (1981): An Investigation into the Problems of Easy Chairs Used by the Arthritic and the Elderly, Rheumatology **20**(3): 164–173.
URL: *http://rheumatology.oxfordjournals.org/content/20/3/164*

Newman, Duncan and Knappers, Michael A. (2004): Electric lifting cushion. US 6702383 B2.

Niemann, Gustav, Winter, Hans and Höhn, Bernd-Robert (2005): Maschinenelemente: Band 1: Konstruktion und Berechnung von Verbindungen, Lagern, Wellen, Bd. 1, 4 Aufl., Springer-Verlag, Berlin, Heidelberg.

Pons, José L. (ed.) (2008): Wearable robots: Biomechatronic exoskeletons, Wiley, Chichester.

Rabe-Kleberg, Ursula, Krüger, Helga and Karsten, Maria-Eleonora (eds) (1991): Dienstleistungsberufe in Krankenpflege, Altenpflege und Kindererziehung: Pro Person: Ausbildung - Tätigkeitsfelder - Professionalisierung, Karin Böllert KT-Verlag, Bielefeld.

Razon, Eli (2004): Adjustable leg suppport and seated to stand up walker. US 6733018 B2.

Reimer, Samuel M. F., Abdul-Sater, Kassim and Lueth, Tim C. (eds) (2017): Bio-Kinematic Design of Individualized Lift-Assist Devices: (Manuscript submitted for publication), 1 Aufl.

Reimer, Samuel M. F., Lueth, Tim C. and D'Angelo, Lorenzo T. (2014): Individualized arm shells towards an ergonomic design of exoskeleton robots, IEEE International Conference on Systems, Man and Cybernetics (SMC), 2014, IEEE, Piscataway, NJ, S. 3958–3965.

Reimer, Samuel M. F., Pfeiffer, Wiebke L., Kreutzer, Joachim F., Lueth, Tim C. and D'Angelo, Lorenzo T. (2014): Evaluation of patient transfer assistance systems for nursing personnel at a residential home for the elderly, IEEE International Conference on Robotics and Biomimetics (ROBIO), 2014, IEEE, Piscataway, NJ, S. 2098–2103.

Roebroeck, M. E., Doorenbosch, C. A. M., Harlaar, J., Jacobs, R. and Lankhorst, G. J. (1994): Biomechanics and muscular activity during sit-to-stand transfer, Clinical Biomechanics **9**(4): 235–244.
URL: *http://www.clinbiomech.com/article/0268-0033(94)90004-3/fulltext*

Rutherford, D. J., Hurley, S. T. and Hubley-Kozey, C. (2014): Sit-to-stand transfer mechanics in healthy older adults: a comprehensive investigation of a portable lifting-seat device, Disability and rehabilitation - Assistive technology **11**(2): 158–165.
URL: *http://www.tandfonline.com/doi/abs/10.3109/17483107.2014.921843?journalCode=iidt20*

Sankai, Yoshiyuki (2006): Leading Edge of Cybernics: Robot Suit HAL, SICE-ICASE International Joint Conference S. P–1–P–2.
URL: *http://ieeexplore.ieee.org/document/4108030/*

Schenkman, M., Berger, R. A., Riley, P. O., Mann, R. W. and Hodge, W. A. (1990): Whole-body movements during rising to standing from sitting, Physical therapy **70**(10): 638–48; discussion 648–51.
URL: *http://ptjournal.apta.org/content/70/10/638*

Simon, Michael (2012): Beschäftigte und Beschäftigungsstrukturen in Pflegeberufen: Eine Analyse der Jahre 1999 bis 2009.
URL: *http://www.iab.de/764/section.aspx/Publikation/k120206r06*

Stagge, Maya (2014): Multikulturelle Teams in der Altenpflege, Dissertation, Universität Vechta, Vechta.
URL: *http://www.springer.com/de/book/9783658115098*

Statistisches Bundesamt (2015b): Pflegestatistik 2013: Pflege im Rahmen der Pflegeversicherung - Deutschlandergebnisse.
URL: *https://www.destatis.de/DE/Publikationen/Thematisch/Gesundheit/Pflege/PflegeDeutschlandergebnisse.html*

Statistisches Bundesamt (28.04.2015a): New projection of Germany's population by 2060.
URL: *https://www.destatis.de/EN/PressServices/Press/pr/2015/04/PE15_153_12421.html*

Steigele, Waltraud (2013): Transfermöglichkeiten: Sicher aufstehen, Das Pflegemagazin **65**(5): 26–28.

Tideiksaar, Rein (ed.) (2008): Stürze und Sturzprävention: Assessment - Prävention - Management, Pflegepraxis Altenpflege, 2 Aufl., Hans Huber, Bern.

TNS Infratest Sozialforschung (2011): Abschlussbericht zur Studie: Wirkungen des Pflege-Weiterentwicklungsgesetztes.

Vander Linden, D. (1994): Variant and Invariant Characteristics of the Sit-to-Stand Task in Healthy Elderly Adults, Archives of Physical Medicine and Rehabilitation **75**(6): 653–660.
URL: *http://www.archives-pmr.org/article/0003-9993(94)90188-0/abstract*

Weddendorf, Bruce (1994): Portable seat lift. US 5333931 A.

Werding, Martin (2008): Social Insurance: How to Pay for Pensions and Health Care?, in I. Hamm, H. Seitz and M. Werding (eds), Demographic Change in Germany, Springer Berlin Heidelberg, Berlin, Heidelberg, S. 89–128.
URL: *http://rd.springer.com/chapter/10.1007/978-3-540-68137-3_5*

Wheeler, Joyce, Woodward, Carol, Ucovich, Rae Lynn, Perry, Jacquelin and Walker, Joan M. (1985): Rising from a chair: influence of age and chair design, Physical therapy **65**(1): 22–26.
URL: *http://ptjournal.apta.org/content/65/1/22*

Wilms, H.-U., Riedel-Heller, S. G., Busse, A. and Angermeyer, M. C. (2001): Hilfe- und Pflegebedürftigkeit im Alter in den neuen Bundesländern: Ergebnisse aus der Leipziger Langzeitstudie in der Altenbevölkerung (LEILA75+), Zeitschrift für Gerontologie und Geriatrie **34**(5): 348–355.
URL: *http://rd.springer.com/article/10.1007/s003910170036*

Wretenberg, P., Arborelius, U. P., Weidenhielm, L. and Lindberg, F. (1993): Rising from a chair by a spring-loaded flap seat: a biomechanical analysis, Scandinavian journal of rehabilitation medicine **25**(4): 153–159.
URL: *https://www.ncbi.nlm.nih.gov/pubmed/8122081*

Zimber, A. (1998): Beanspruchung und Streß in der Altenpflege: Forschungsstand und Forschungsperspektiven, Zeitschrift für Gerontologie und Geriatrie **31**(6): 417–425.
URL: *http://rd.springer.com/article/10.1007/s003910050069*

A. Involved Students

Theses

Corinna Eder *Auslegung von patientenindividuellen Aufstehmechanismen mithilfe von Viergelenken*, Term Paper, June 2016 - November 2016
Included in Section 2.4, 3.1, 3.4, 4, 5, 7.1

Kyra Kleine *Entwicklung einer modularen Aufstehhilfe*, Bachelor Thesis at the Technical University of Munich, May 2016 - September 2016
Included in Section 2.1, 2.5, 3.2, 3.3, 3.4, 6, 7.2

Matthias Gehring *Optimierungsbasierte Auslegung von Rollstuhl-Transferkinematiken*, Bachelor Thesis at the Technical University of Munich, June 2014 - December 2014
Included in Section 5

Maximilian Binder *Konstruktion eines motorisierten Exoskeletts für den menschlichen Arm mit implementierter Nullkraftregelung*, Bachelor Thesis at the Technical University of Munich, June 2014 - November 2014
Included in Section 3.3, 3.4

Florian Pflügl *Entwicklung transferunterstützender Kinematiken für Rollstühle*, Bachelor Thesis at the Technical University of Munich, June 2013 - October 2013
Included in Section 3.3

Student Assistants

Thao Nguyen July 2016 - September 2016
Included in Section 6.7

Carolin Stöckl March 2016 - May 2016
Included in Section 6.7

Jonas Joachimmeyer May 2015 - March 2016
Included in Section 6, especially in Section 6.7

Karin Schmid March 2014 - October 2014
Included in Section 3.3

Wiebke Pfeiffer October 2013 - June 2014
Included in Section 3.4

B. MATLAB file: Distribution of Biomechanical Parameters

Distribution of Body Length

With this code the distribution of body lengths is obtained

Contents

Overview

```
% LITERATURE: http://de.statista.com/
%
% Useful Information:
% - North european people are one of the largest in the world
% - Body Length: normally distributed
% - Description in percentile groups
%
% Authors: Corinna Eder and Samuel Reimer
% Created: 18th of July 2016
```

Distribution of Body Length based of male (m) and female (w) (2006)

```
% Under 150 cm
p_m_1 = 0.001;
p_w_1 = 0.006;

% 150 - 154 cm
p_m_2 = 0.001;
p_w_2 = 0.04;

% 155 - 159 cm
p_m_3 = 0.003;
p_w_3 = 0.127;

% 160 - 164 cm
p_m_4 = 0.023;
p_w_4 = 0.27;

% 165 - 169 cm
p_m_5 = 0.09;
p_w_5 = 0.291;

% 170 - 174 cm
p_m_6 = 0.192;
p_w_6 = 0.176;

% 175 - 179 cm
p_m_7 = 0.261;
p_w_7 = 0.069;

% 180 - 184 cm
p_m_8 = 0.239;
p_w_8 = 0.018;
```

```
% 185 - 189 cm
p_m_9 = 0.128;
p_w_9 = 0.002;

% Over 190 cm
p_m_10 = 0.063;
p_w_10 = 0;

% Total
p_m = p_m_1+p_m_2+p_m_3+p_m_4+p_m_5+p_m_6+p_m_7+p_m_8+p_m_9+p_m_10;
p_w = p_w_1+p_w_2+p_w_3+p_w_4+p_w_5+p_w_6+p_w_7+p_w_8+p_w_9+p_w_10;

% Bar Chart of Distribution of Body Lengths in 2006
f1 = figure('NumberTitle', 'off', 'Name', ...
    'Verteilung der Körpergröße im Jahr 2006 nach Geschlecht');
bar([p_m_1 p_w_1; p_m_2 p_w_2; p_m_3 p_w_3; p_m_4 p_w_4; p_m_5 p_w_5; ...
    p_m_6 p_w_6; p_m_7 p_w_7; p_m_8 p_w_8; p_m_9 p_w_9; p_m_10 p_w_10]*100, ...
    'histc');
title('Verteilung der Körpergröße im Jahr 2006 nach Geschlecht');
ax=gca;
ax.XTickLabel = {'< 150', '150-154', '155-159', '160-164', '165-169', ...
    '170-174', '175-179', '180-184', '185-189', '> 190'};
ax.XTickLabelRotation = 45;
xlabel('Körpergrößen in cm');
ylabel('Anteile in %');
q = legend('männlich', 'weiblich');
set(q, 'FontSize',12);

% Save the Figure
newFolder = fullfile(pwd, 'Körpergröße-Verteilung');
if ~exist(newFolder, 'dir')
    mkdir(newFolder)
end
saveas(f1, fullfile(newFolder, ['2006', '.fig']));
set(f1, 'PaperPositionMode','auto');
print(f1, '-dpng', '-r100', fullfile(newFolder, ['2006', '.png']));
close(f1);
```

Distribution of Body Length (2014)

```
% Under 150 cm
p_1 = 0.003;

% 150 - 159 cm
p_2 = 0.071;

% 160 - 169 cm
p_3 = 0.318;

% 170 - 179 cm
p_4 = 0.361;

% 180 - 189 cm
p_5 = 0.209;

% 190 - 199 cm
p_6 = 0.036;

% Over 200 cm
```

```
p_7 = 0.002;

% Total
p = p_1+p_2+p_3+p_4+p_5+p_6+p_7;

% Bar Chart of Distribution of Body Lengths in 2014
f2 = figure('NumberTitle', 'off', 'Name', ...
    'Verteilung der Körpergröße im Jahr 2014');
bar([p_1; p_2; p_3; p_4; p_5; p_6; p_7]*100);
title('Verteilung der Körpergröße im Jahr 2014');
ax=gca;
ax.XTickLabel = {'< 150', '150-159', '160-169', '170-179', '180-189', ...
    '190-199', '> 200'};
ax.XTickLabelRotation = 45;
xlabel('Körpergrößen in cm');
ylabel('Anteile in %');

% Save the Figure
newFolder = fullfile(pwd, 'Körpergröße-Verteilung');
if ~exist(newFolder, 'dir')
    mkdir(newFolder)
end
saveas(f2, fullfile(newFolder, ['2014', '.fig']));
set(f2, 'PaperPositionMode','auto');
print(f2, '-dpng', '-r100', fullfile(newFolder, ['2014', '.png']));
close(f2);
```

Published with MATLAB® R2016b

C. MATLAB file: Input of Biomechanical Parameters

Classification of Body Length

With this code the necessary body measurements of different percentile groups (age band: 18-65) are obtained.

Contents

Overview

```
% Literature: DIN 33402-2:2005-12
% Authors: Corinna Eder and Samuel Reimer
% Created: 18th of July 2016
```

5th Male Percentile (only 5% are smaller)

Body Length in mm

```
l_m_1 = 1650;
```

Length of Shank in mm

```
s_m_1 = 430;
```

Total Leg Length in mm

```
b_m_1 = 965;
```

Width of Abdomen in mm

```
a_m_1 = 260;
```

Height of Thigh in mm

```
h_t_m_1 = 130;
```

Length of Thigh in mm

```
t_m_1 = b_m_1 - s_m_1 - 0.5*a_m_1;
```

50th Male Percentile (50% are smaller or larger)

Body Length in mm

```
l_m_2 = 1750;
```

Length of Shank in mm

```
s_m_2 = 460;
```

Totat Leg Length in mm

```
b_m_2 = 1045;
```

Width of Abdomen in mm

```
a_m_2 = 285;
```

Height of thigh in mm

```
h_t_m_2 = 150;
```

Length of Thigh in mm

```
t_m_2 = b_m_2 - s_m_2 - 0.5*a_m_2;
```

95th Male Percentile (only 5% are larger)

Body Length in mm

```
l_m_3 = 1855;
```

Length of Shank in mm

```
s_m_3 = 480;
```

Total Leg Length in mm

```
b_m_3 = 1140;
```

Width of Abdomen in mm

```
a_m_3 = 380;
```

Height of Thigh in mm

```
h_t_m_3 = 180;
```

length of Thigh in mm

```
t_m_3 = b_m_3 - s_m_3 - 0.5*a_m_3;
```

5th Female Percentile (only 5% are smaller)

Body Length in mm

```
l_w_1 = 1535;
```

Length of Shank in mm

```
s_w_1 = 400;
```

Total Leg Length in mm

```
b_w_1 = 925;
```

Width of Abdomen in mm

```
a_w_1 = 245;
```

Height of Thigh in mm

```
h_t_w_1 = 125;
```

Length of Thigh in mm

```
t_w_1 = b_w_1 - s_w_1 - 0.5*a_w_1;
```

50th Female Percentile (50% are smaller or larger)

body length in mm

```
l_w_2 = 1625;
```

Length of Shank in mm

```
s_w_2 = 425;
```

Total Leg Length in mm

```
b_w_2 = 990;
```

Width of Abdomen in mm

```
a_w_2 = 290;
```

Height of Thigh in mm

```
h_t_w_2 = 145;
```

Length of Thigh in mm

```
t_w_2 = b_w_2 - s_w_2 - 0.5*a_w_2;
```

95th Female Percentile (only 5% are larger)

Body Length in mm

```
l_w_3 = 1720;
```

Length of Shank in mm

```
s_w_3 = 450;
```

Total Leg Length in mm

```
b_w_3 = 1055;
```

Width of Abdomen in mm

```
a_w_3 = 345;
```

Height of Thigh in mm

```
h_t_w_3 = 175;
```

Length of Thigh in mm

```
t_w_3 = b_w_3 - s_w_3 - 0.5*a_w_3;
```

Published with MATLAB® R2016b

D. MATLAB file: Kinematic Synthesis of Three Task Positions

Design of Patient-Individual Lift-Assist Devices based on Four-Bar Linkages

FBL_p50m computes 2R chains based on 3 task positions for the 50th male percentile.

Contents

Overview

```
%   === INPUT PARAMETERS ===
%   T_1 = Homogeneous transformation matrix of task positon 1
%   T_2 = Homogeneous transformation matrix of task positon 2
%   T_3 = Homogeneous transformation matrix of task positon 3
%   p1 = x/y - coordinates of the moving pivot point at task position 1
%
%   === OUTPUT PARAMETERS ===
%   q = x/y - coordinates of the fixed pivot point of the 2R chain
%   p1 = x/y - coordinates of the moving pivot point at task position 1
%
%   ++ Example 1 ++
%   p1 =[100; 100];
%   T_1 = [cosd(alpha) -sind(alpha) t_m_2*sind(alpha-90); ...
%          sind(alpha) cosd(alpha) s_m_2; 0 0 1];
%   T_2 = [cosd(130) -sind(130) t_m_2*sind(alpha-90)+s_m_2*cosd(70); ...
%          sind(130) cosd(130) s_m_2*sind(70); 0 0 1];
%   T_3 = [cosd(100) -sind(100) t_m_2*sind(alpha-90)+s_m_2*cosd(80); ...
%          sind(100) cosd(100) s_m_2*sind(80); 0 0 1];
%
%   Authors: Corinna Eder and Samuel Reimer
%   Created: 22nd of August 2016
```

```
function [q,p1] = FBL_p50m(T_1,T_2,T_3,p1)
```

Load Necessary Lengths and Informations

Length of Shank, Length and Height of Thigh and Width of Abdomen

```
ClassificationOfBodyLength;
```

World Coordinate System

```
W = [0; 0];
```

Seat Depth

```
c_depth = 396;
```

Seat Height

```
c_height = 437.4;
```

α Reprents φ_{thigh}

```
alpha = round(180-asind((c_height+0.5*h_t_m_2-s_m_2)/t_m_2), 3);
```

Ankle Position (fixed point)

```
q_ankle = [t_m_2*sind(alpha-90); 0];
```

Knee Position

```
p_knee = [t_m_2*sind(alpha-90); s_m_2];
```

Hip Position

```
p_hip = [0; s_m_2 + t_m_2*cosd(alpha-90)];
```

Workspace of the Chair

```
c_1 = [- 0.5*a_m_2; 0];
c_2 = [- 0.5*a_m_2; c_height];
c_3 = [c_depth - 0.5*a_m_2; c_height];
c_4 = [c_depth - 0.5*a_m_2; 0];
```

Definition of Three Task Positions

```
if nargin == 0
    T_1 = [cosd(alpha) -sind(alpha) t_m_2*sind(alpha-90); ...
           sind(alpha) cosd(alpha) s_m_2; 0 0 1];
    T_2 = [cosd(130) -sind(130) t_m_2*sind(alpha-90)+s_m_2*cosd(70); ...
           sind(130) cosd(130) s_m_2*sind(70); 0 0 1];
    T_3 = [cosd(100) -sind(100) t_m_2*sind(alpha-90)+s_m_2*cosd(80); ...
           sind(100) cosd(100) s_m_2*sind(80); 0 0 1];
end
```

Synthesis

Translational part of the Three HTs: T_1, T_2 and T_3

```
t_WB_1 = T_1(1:2,3);
t_WB_2 = T_2(1:2,3);
t_WB_3 = T_3(1:2,3);
```

Rotational part of the Three HTs: T_1, T_2 and T_3

```
R_WB_1 = T_1(1:2,1:2);
R_WB_2 = T_2(1:2,1:2);
R_WB_3 = T_3(1:2,1:2);
```

Relative Angles

```
R_12 = R_WB_2*R_WB_1';
R_13 = R_WB_3*R_WB_1';
```

Relative Displacements

```
t_12 = t_WB_2 - R_12*t_WB_1;
t_13 = t_WB_3 - R_13*t_WB_1;
```

Unit Matrix

```
E = eye(2,2);
```

Simplify known Parameters

```
M_12 = (E - R_12)';
M_13 = (E - R_13)';

lambda_12_transp = (t_12)'*R_12;
lambda_13_transp = (t_13)'*R_13;

mue_12_transp = -(t_12)';
mue_13_transp = -(t_13)';

epsilon_12 = 0.5*(t_12)'*t_12;
epsilon_13 = 0.5*(t_13)'*t_13;
```

Definition of Two Matrices

In matrix_not the points p1 and q are saved, which are not in the workspace of the chair.

```
matrix_not = [];
```

In matrix the points p1 and q are saved, which are in the workspace of the chair.

```
matrix = [];
```

Definition of p1 and Solve the Design Equation

The x/y - coordinates of p1 are set in steps of 20 mm

```
for i = c_2(1,1):20:c_3(1,1)
    for j = c_2(2,1):-20:c_1(2,1)

        p1 = [i;j];

        liegen_12_p1 = p1'*M_12 + mue_12_transp;
        liegen_13_p1 = p1'*M_13 + mue_13_transp;

        a_12_p1 = liegen_12_p1(1,1);
        b_12_p1 = liegen_12_p1(1,2);
        a_13_p1 = liegen_13_p1(1,1);
        b_13_p1 = liegen_13_p1(1,2);

        r_12_p1 = lambda_12_transp*p1 + epsilon_12;
        r_13_p1 = lambda_13_transp*p1 + epsilon_13;

        K_p1 = [a_12_p1 b_12_p1; a_13_p1 b_13_p1];
        v_p1 = [-r_12_p1; -r_13_p1];

        q = K_p1\v_p1;

        if nargout == 0

            % if-loop (q is in the workspace of the chair)
            if (q(1,1) >= c_2(1,1) && q(1,1) <= c_3(1,1)) && ...
               (q(2,1) <= c_2(2,1) && q(2,1) >= c_1(2,1))
                q;
                p1;
                % in matrix the points q und p1 - which are in the
                % workspace of the chair - are saved
                matrix = [matrix; q(1,1) q(2,1) p1(1,1) p1(2,1)];

            else
            % Here all the q and p1 values which are not in the workspace
            % of the Chair can be saved if wanted
            q_not = q;
            p1_not = p1;
            matrix_not = [matrix_not; q_not(1,1) q_not(2,1) p1_not(1,1) p1_not(2,1)];
            end
        end
    end
end
```

Plots

Plot matrix (the fixed pivot points and the moving pivot points)

```
if ~isempty(matrix)

    f1=figure('NumberTitle', 'off', 'Name', 'FBL_p50m');
    % The blue points in this plot are the fixed pivot points and
    % the red points are the moving pivot points
    subplot(2,2,[1,2])
    plot(matrix(:,1), matrix(:,2), 'bx', matrix(:,3), matrix(:,4), 'rx')
```

```
    axis([c_1(1) c_4(1) c_1(2) c_2(2)])
    xlabel('Sitztiefe in mm');
    ylabel('Sitzhöhe in mm');
    title('gestellfeste und bewegliche Punkte')
    legend('q', 'p1', 'Location', 'southeast');

    % Only the Fixed Pivot Points
    subplot(2,2,3)
    plot(matrix(:,1), matrix(:,2), 'bx')
    axis([c_1(1) c_4(1) c_1(2) c_2(2)])
    axis equal
    xlabel('Sitztiefe in mm');
    ylabel('Sitzhöhe in mm');
    title('gestellfeste Punkte');

    % Only the Moving Pivot Points
    subplot(2,2,4)
    plot(matrix(:,3), matrix(:,4), 'rx')
    hold on
    my_color = [156 189 203]./255;
    plot(matrix_not(:,3), matrix_not(:,4),'x', 'Color', my_color)
    axis([c_1(1) c_4(1) c_1(2) c_2(2)])
    xlabel('Sitztiefe in mm');
    ylabel('Sitzhöhe in mm');
    title('bewegliche Punkte');

    % Save the Figure
    newFolder = fullfile(pwd, 'FBL');
    if ~exist(newFolder, 'dir')
        mkdir(newFolder)
    end
    saveas(f1, fullfile(newFolder, ['p50m_1', '.fig']));
    set(f1, 'PaperPositionMode','auto');
    print(f1, '-dpng', '-r100', fullfile(newFolder, ['p50m_1', '.png']));
    close(f1);

    f2=figure('NumberTitle', 'off', 'Name', 'FBL_p50m');
    for k=1:1:length(matrix)
        plot(matrix(k,1), matrix(k,2), 'bx')
        hold on
        plot(matrix(k,3), matrix(k,4), 'rx')
        hold on
        plot(matrix(k,[1,3]), matrix(k,[2,4]),  'Color', my_color)
        hold on
        axis([c_1(1) c_4(1) c_1(2) c_2(2)])
        xlabel('Sitztiefe in mm');
        ylabel('Sitzhöhe in mm');
        legend('q', 'p1', 'Location', 'southeast');
    end

    % Save the Figure
    newFolder = fullfile(pwd, 'FBL');
    if ~exist(newFolder, 'dir')
        mkdir(newFolder)
    end
    saveas(f2, fullfile(newFolder, ['p50m_2', '.fig']));
    set(f2, 'PaperPositionMode','auto');
    print(f2, '-dpng', '-r100', fullfile(newFolder, ['p50m_2', '.png']));
    close(f2);

    points=array2table(matrix, 'VariableNames', {'q_x', 'q_y', 'p1_x', 'p1_y'});
```

```
    % A q point is found in the workspace for every p value
    percentage = length(matrix)/(length(matrix_not)+length(matrix));

    save('FBL_p50m.mat', 'points', 'matrix', 'T_1', 'T_2', 'T_3', ...
        'q_ankle', 'p_knee', 'p_hip', 'alpha', 'percentage')

end

clear all
```

```
end
```

Published with MATLAB® R2016b

E. MATLAB File: Newton-Raphson Method

Evaluation of the Four Bar Linkages with the Newton Raphson Method

Here, at first two 2R Chains are combined, the Result is a Four Bar Linkage. This Four Bar Linkage can be evaluated with the Newton Raphson Method

Contents

Overview

```
%   LITERATURE:
%   McCarthy, J., Soh, G. (2010): Geometric Design of Linkages, Springer,
%   2nd Edition
%
%   Authors: Corinna Eder and Samuel Reimer
%   Created: 19th of September 2016
```

```
function [phi_hip,delta_hip,PHI] = NRM_p50m(q_A,q_B,p_A,p_B,q_ankle,p_knee,p_hip)
```

Load Necessary Informations

```
load('FBL_p50m', 'points', 'matrix', 'q_ankle', 'p_knee', 'p_hip', 'alpha')
```

Create an Empty Matrix

```
output_help=[];
```

Combination of the 2R Chains

```
for a=1:length(matrix)
    for b=1:length(matrix)
        if b>a
```

Definition of q_A, q_B, p_A and p_B

```
            if nargin == 0

                if matrix(a,3) > matrix(b,3) && matrix(a,4) > matrix(b,4)

                    q_A = [matrix(a,1); matrix(a,2)];
                    q_B = [matrix(b,1); matrix(b,2)];
                    p_A = [matrix(a,3); matrix(a,4)];
                    p_B = [matrix(b,3); matrix(b,4)];
                    q_ankle;
                    p_knee;
                    p_hip;
                    help=1;

                elseif matrix(a,3) < matrix(b,3) && matrix(a,4) > matrix(b,4)

                    q_A = [matrix(a,1); matrix(a,2)];
                    q_B = [matrix(b,1); matrix(b,2)];
                    p_A = [matrix(a,3); matrix(a,4)];
                    p_B = [matrix(b,3); matrix(b,4)];
                    q_ankle;
                    p_knee;
                    p_hip;
                    help=2;

                elseif matrix(a,3) > matrix(b,3) && matrix(a,4) < matrix(b,4)

                    q_A = [matrix(a,1); matrix(a,2)];
                    q_B = [matrix(b,1); matrix(b,2)];
                    p_A = [matrix(a,3); matrix(a,4)];
                    p_B = [matrix(b,3); matrix(b,4)];
                    q_ankle;
                    p_knee;
                    p_hip;
                    help=3;

               elseif matrix(a,3) == matrix(b,3) && matrix(a,4) > matrix(b,4)

                    q_A = [matrix(a,1); matrix(a,2)];
                    q_B = [matrix(b,1); matrix(b,2)];
                    p_A = [matrix(a,3); matrix(a,4)];
                    p_B = [matrix(b,3); matrix(b,4)];
                    q_ankle;
                    p_knee;
                    p_hip;
                    help=4;

                elseif matrix(a,3) > matrix(b,3) && matrix(a,4) == matrix(b,4)

                    q_A = [matrix(a,1); matrix(a,2)];
                    q_B = [matrix(b,1); matrix(b,2)];
                    p_A = [matrix(a,3); matrix(a,4)];
                    p_B = [matrix(b,3); matrix(b,4)];
                    q_ankle;
                    p_knee;
                    p_hip;
                    help=5;

                else
```

```
                q_A = [matrix(b,1); matrix(b,2)];
                q_B = [matrix(a,1); matrix(a,2)];
                p_A = [matrix(b,3); matrix(b,4)];
                p_B = [matrix(a,3); matrix(a,4)];
                q_ankle;
                p_knee;
                p_hip;
                help=6;

            end

        end
```

Definition of φ_c, φ_{seat} and φ_{shank}

```
        phi_c = acos(dot((p_hip-p_B),(p_A-p_B))/(norm(p_hip-p_B)*norm(p_A-p_B)));
        phi_seat = atan2((p_A(2)-p_B(2)),(p_A(1)-p_B(1)));
        phi_shank = atan2((p_knee(2)-q_ankle(2)),(p_knee(1)-q_ankle(1)));
```

Create Symbolic Variables

```
        syms l_k l_A l_m l_B l_r l_u l_v l_w
        syms phi_k phi_A phi_m phi_B phi_r phi_u phi_v
```

Calculation of Equations

p_hip - p_B

```
        A1 = [p_hip(1) 1; p_B(1) 1];
        b1 = [p_hip(2); p_B(2)];
        z1 = A1 \ b1;
        syms x
        y1 = z1(1) * x + z1(2);
```

q_A - p_A

```
        A2 = [q_A(1) 1; p_A(1) 1];
        b2 = [q_A(2); p_A(2)];
        z2 = A2 \ b2;
        syms x
        y2= z2(1) * x + z2(2);
```

q_B - p_B

```
        A3 = [q_B(1) 1; p_B(1) 1];
        b3 = [q_B(2); p_B(2)];
        z3 = A3 \ b3;
        syms x
        y3= z3(1) * x + z3(2);
```

p_B - p_A

```
A4 = [p_B(1) 1; p_A(1) 1];
b4 = [p_B(2); p_A(2)];
z4 = A4 \ b4;
syms x
y4= z4(1) * x + z4(2);
```

```
Warning: Matrix is singular to working precision.
```

```
Warning: Matrix is singular to working precision.
```

```
Warning: Matrix is singular to working precision.
```

Point of Intersection between q_A - p_A and q_B - p_B

```
outlier = solve(y2==y3, x);

if ~isempty(outlier) && outlier > q_A(1) && outlier < p_A(1)
    help_outlier = 1;
end
```

Case Differentiation

```
if (z4(1) < 0 && z1(1) < 0 && abs(z4(1)) > abs(z1(1))) || ...
        (z1(1) < 0 && z4(1) > 0) || ...
        (z4(1) > 0 && z1(1) > 0 && z1(1) > z4(1)) || ...
        p_A(1) == p_B(1) || p_A(2) == p_B(2)
```

Four non-linear Equation

```
    f1(l_k,l_A,l_m,l_B,l_r,l_u,l_v,l_w, ...
        phi_k,phi_A,phi_m,phi_B,phi_r,phi_u,phi_v) = ...
        (l_k*cos(phi_k))+(l_A*cos(phi_A))-(l_m*cos(phi_m))-(l_B*cos(phi_B));
    f2(l_k,l_A,l_m,l_B,l_r,l_u,l_v,l_w, ...
        phi_k,phi_A,phi_m,phi_B,phi_r,phi_u,phi_v) = ...
        (l_k*sin(phi_k))+(l_A*sin(phi_A))-(l_m*sin(phi_m))-(l_B*sin(phi_B));
    f3(l_k,l_A,l_m,l_B,l_r,l_u,l_v,l_w, ...
        phi_k,phi_A,phi_m,phi_B,phi_r,phi_u,phi_v) = ...
        (l_B*cos(phi_B))+(l_w*cos(phi_m+phi_c))...
        -(l_v*cos(phi_v))-(l_u*cos(phi_u))-(l_r*cos(phi_r));
    f4(l_k,l_A,l_m,l_B,l_r,l_u,l_v,l_w, ...
        phi_k,phi_A,phi_m,phi_B,phi_r,phi_u,phi_v) = ...
        (l_B*sin(phi_B))+(l_w*sin(phi_m+phi_c))...
        -(l_v*sin(phi_v))-(l_u*sin(phi_u))-(l_r*sin(phi_r));
```

Definiton of Jacobian Matrix

```
    J = [diff(f1,phi_A), diff(f1,phi_B), diff(f1,phi_m), diff(f1,phi_u);
        diff(f2,phi_A), diff(f2,phi_B), diff(f2,phi_m), diff(f2,phi_u);
```

```
        diff(f3,phi_A), diff(f3,phi_B), diff(f3,phi_m), diff(f3,phi_u);
        diff(f4,phi_A), diff(f4,phi_B), diff(f4,phi_m), diff(f4,phi_u)];
```

Help Size

```
k = J^-1 * [f1;f2;f3;f4];
```

Definition of initial Conditions

```
l_k = norm(q_A-q_B);
l_A = norm(p_A-q_A);
l_m = norm(p_A-p_B);
l_B = norm(p_B-q_B);
l_r = norm(q_B-q_ankle);
l_u = norm(p_knee-q_ankle);
l_v = norm(p_hip-p_knee);
l_w = norm(p_hip-p_B);
```

Calculation of φ_{hip}

```
j = 0;
for phi_thigh = alpha:-1:100
    j = j + 1;
    % Angles in radians
    phi_v = phi_thigh*pi/180;
    phi_u = phi_shank;
    phi_m = phi_seat;
    phi_k = atan2((q_A(2)-q_B(2)),(q_A(1)-q_B(1)));
    phi_A = atan2((p_A(2)-q_A(2)),(p_A(1)-q_A(1)));
    phi_B = atan2((p_B(2)-q_B(2)),(p_B(1)-q_B(1)));
    phi_r = atan2((q_ankle(2)-q_B(2)),(q_ankle(1)-q_B(1)));

    for i=1:7
        K = double(k(l_k,l_A,l_m,l_B,l_r,l_u,l_v,l_w,...
            phi_k,phi_A,phi_m,phi_B,phi_r,phi_u,phi_v));
        phi(:,i) = [phi_A;phi_B;phi_m;phi_u] - K; % Newton-Raphson Equation
        phi_deg(:,i) = phi(:,i)*180/pi;

        phi_A = phi(1,i); % Reset phi values for next iteration
        phi_B = phi(2,i);
        phi_m = phi(3,i);
        phi_u = phi(4,i);
    end

    % Save Output in Degrees
    phi_hip(j) = phi_thigh - (phi_m + phi_c)*180/pi;
    PHI(j,:) = [phi_thigh*pi/180,phi_A,phi_B,phi_m,phi_u].*180/pi;
end
phi_hip;
max_phi_hip = max(phi_hip);
min_phi_hip = min(phi_hip);
delta_hip = max_phi_hip-min_phi_hip;
```

```
elseif z4(1) < 0 && z1(1) < 0 && abs(z1(1)) > abs(z4(1))
```

Four non-linear Equation

```
f1(l_k,l_A,l_m,l_B,l_r,l_u,l_v,l_w, ...
    phi_k,phi_A,phi_m,phi_B,phi_r,phi_u,phi_v) = ...
    (l_k*cos(phi_k))+(l_A*cos(phi_A))-(l_m*cos(phi_m))-(l_B*cos(phi_B));
f2(l_k,l_A,l_m,l_B,l_r,l_u,l_v,l_w, ...
    phi_k,phi_A,phi_m,phi_B,phi_r,phi_u,phi_v) = ...
    (l_k*sin(phi_k))+(l_A*sin(phi_A))-(l_m*sin(phi_m))-(l_B*sin(phi_B));
f3(l_k,l_A,l_m,l_B,l_r,l_u,l_v,l_w, ...
    phi_k,phi_A,phi_m,phi_B,phi_r,phi_u,phi_v) = ...
    (l_B*cos(phi_B))+(l_w*cos(phi_m-phi_c))...
    -(l_v*cos(phi_v))-(l_u*cos(phi_u))-(l_r*cos(phi_r));
f4(l_k,l_A,l_m,l_B,l_r,l_u,l_v,l_w, ...
    phi_k,phi_A,phi_m,phi_B,phi_r,phi_u,phi_v) = ...
    (l_B*sin(phi_B))+(l_w*sin(phi_m-phi_c))...
    -(l_v*sin(phi_v))-(l_u*sin(phi_u))-(l_r*sin(phi_r));
```

Definiton of Jacobian Matrix

```
J = [diff(f1,phi_A), diff(f1,phi_B), diff(f1,phi_m), diff(f1,phi_u);
    diff(f2,phi_A), diff(f2,phi_B), diff(f2,phi_m), diff(f2,phi_u);
    diff(f3,phi_A), diff(f3,phi_B), diff(f3,phi_m), diff(f3,phi_u);
    diff(f4,phi_A), diff(f4,phi_B), diff(f4,phi_m), diff(f4,phi_u)];
```

Help Size

```
k = J^-1 * [f1;f2;f3;f4];
```

Define initial Conditions

```
l_k = norm(q_A-q_B);
l_A = norm(p_A-q_A);
l_m = norm(p_A-p_B);
l_B = norm(p_B-q_B);
l_r = norm(q_B-q_ankle);
l_u = norm(p_knee-q_ankle);
l_v = norm(p_hip-p_knee);
l_w = norm(p_hip-p_B);
```

Calculation of φ_{hip}

```
j = 0;
for phi_thigh = alpha:-1:100
    j = j + 1;
    % Angles in radians
    phi_v = phi_thigh*pi/180;
    phi_u = phi_shank;
    phi_m = phi_seat;
    phi_k = atan2((q_A(2)-q_B(2)),(q_A(1)-q_B(1)));
    phi_A = atan2((p_A(2)-q_A(2)),(p_A(1)-q_A(1)));
```

```
                phi_B = atan2((p_B(2)-q_B(2)),(p_B(1)-q_B(1)));
                phi_r = atan2((q_ankle(2)-q_B(2)),(q_ankle(1)-q_B(1)));

                for i=1:7
                    K = double(k(l_k,l_A,l_m,l_B,l_r,l_u,l_v,l_w,...
                        phi_k,phi_A,phi_m,phi_B,phi_r,phi_u,phi_v));
                    phi(:,i) = [phi_A;phi_B;phi_m;phi_u] - K; % Newton-Raphson Equation
                    phi_deg(:,i) = phi(:,i)*180/pi;

                    phi_A = phi(1,i); % Reset phi values for next iteration
                    phi_B = phi(2,i);
                    phi_m = phi(3,i);
                    phi_u = phi(4,i);
                end

                % Save Output in Degrees
                phi_hip(j) = phi_thigh - (phi_m - phi_c)*180/pi;
                PHI(j,:) = [phi_thigh*pi/180,phi_A,phi_B,phi_m,phi_u].*180/pi;
            end
            phi_hip;
            max_phi_hip = max(phi_hip);
            min_phi_hip = min(phi_hip);
            delta_hip = max_phi_hip-min_phi_hip;
```

```
        end
```

Plot

```
        if nargout == 0
            fig=figure;
            plot(PHI(:,1),phi_hip)
            if delta_hip < 20
                axis equal
            end
            grid on
            title('Change of phi_{hip} during STS Movement')
            xlabel('phi_{thigh}')
            ylabel('phi_{hip}')
            set(gca,'XDir','reverse');
        end

        name=strcat('Viergelenk', num2str(a), '.',  num2str(b));

        % Save the Figure
        newFolder = fullfile(pwd, 'NRM');
        NewFolder = fullfile(newFolder, 'p50m');
        if ~exist(NewFolder, 'dir')
            mkdir(NewFolder)
        end
        saveas(fig, fullfile(NewFolder, [(name), '.fig']));
        set(fig, 'PaperPositionMode','auto');
        print(fig, '-dpng', '-r100', fullfile(NewFolder, [name, '.png']));
        close(fig);
```

Classification of the Four Bar Linkages

In this case φ_{shank} in task position 2 and 3 are very similar to the predefined value.

```
            if PHI(floor(alpha)-130+1,5) > 67 && PHI(floor(alpha)-130+1,5) < 73 && ...
                    PHI(floor(alpha)-100+1,5) > 77 && PHI(floor(alpha)-100+1,5) < 83
```

```
                usable = 1;
```

Here φ_{shank} in task position 2 is very similar to the predefined value.

```
            elseif PHI(floor(alpha)-130+1,5) > 67 && PHI(floor(alpha)-130+1,5) < 73
```

```
                usable = 2;
```

Intersection between the two 2R Chains

```
            elseif exist('help_outlier')
```

```
                usable = -1;
                clear help_outlier
```

φ_{shank} in task position 2 and 3 are not similar to the predefined value.

```
            else
                usable = 0;
            end
```

Output of the Results

```
            output_help = [output_help; a b ...
                help phi_hip(1) phi_hip(floor(alpha)-130+1) phi_hip(floor(alpha)-100+1)...
                PHI(1,5) PHI(floor(alpha)-130+1,5) PHI(floor(alpha)-100+1,5)...
                max_phi_hip min_phi_hip delta_hip usable];

            % Sort rows
            output_help_sort = sortrows(output_help, [13 12]);

            output=array2table(output_help_sort, ...
                'VariableNames', {'a', 'b', 'help', ...
                'phi_hip_Pose1', 'phi_hip_Pose2', 'phi_hip_Pose3',...
                'phi_shank_Pose1', 'phi_shank_Pose2', 'phi_shank_Pose3',...
                'max_phi_hip', 'min_phi_hip', 'delta_hip', 'usable'});
```

```
        end
    end

    save('NRM_p50m.mat', 'output')

end
```

```
clear all
```

```
end
```

Published with MATLAB® R2016b

F. MATLAB File: Kinematic Analysis of the Lift-Assist Device

Kinematic Analysis of the Four-Bar Linkage for the Kinetostatics

This function computes the angles phi_A and phi_B with respect to the coupler angle phi_C of the chair.

Contents

Overview

```
%   Authors: Kyra Kleine and Samuel Reimer
%   Created: 28th of September 2016
```

```
function [phi_A, phi_B] = ViergelenkBerechnung(q_a,q_b,p_a,p_b,phi_S_max)
```

Load initial data if no inputs are found.

```
if nargin == 0
    q_a  = [14.5;65];
    p_a = [346;43];
    q_b  = [74.5;15];
    p_b = [371.2;17.4];
    phi_S_max = 145;
end
```

Define length of beams.

```
l_A = norm(p_a-q_a);
l_B = norm(p_b-q_b);
l_C = norm(p_b-p_a);
```

Initiate other variables.

```
x = (q_a-q_b);
alpha = atand((p_a(2)-p_b(2))/(p_a(1)-p_b(1)));
i = 1;

for phi_S = phi_S_max:1:180
```

```
    phi_C = phi_S + alpha;
```

Computation of phi_A.

Definition of q_A, q_B, p_A and p_B

```
            if nargin == 0

                if matrix(a,3) > matrix(b,3) && matrix(a,4) > matrix(b,4)

                    q_A = [matrix(a,1); matrix(a,2)];
                    q_B = [matrix(b,1); matrix(b,2)];
                    p_A = [matrix(a,3); matrix(a,4)];
                    p_B = [matrix(b,3); matrix(b,4)];
                    q_ankle;
                    p_knee;
                    p_hip;
                    help=1;

                elseif matrix(a,3) < matrix(b,3) && matrix(a,4) > matrix(b,4)

                    q_A = [matrix(a,1); matrix(a,2)];
                    q_B = [matrix(b,1); matrix(b,2)];
                    p_A = [matrix(a,3); matrix(a,4)];
                    p_B = [matrix(b,3); matrix(b,4)];
                    q_ankle;
                    p_knee;
                    p_hip;
                    help=2;

                elseif matrix(a,3) > matrix(b,3) && matrix(a,4) < matrix(b,4)

                    q_A = [matrix(a,1); matrix(a,2)];
                    q_B = [matrix(b,1); matrix(b,2)];
                    p_A = [matrix(a,3); matrix(a,4)];
                    p_B = [matrix(b,3); matrix(b,4)];
                    q_ankle;
                    p_knee;
                    p_hip;
                    help=3;

               elseif matrix(a,3) == matrix(b,3) && matrix(a,4) > matrix(b,4)

                    q_A = [matrix(a,1); matrix(a,2)];
                    q_B = [matrix(b,1); matrix(b,2)];
                    p_A = [matrix(a,3); matrix(a,4)];
                    p_B = [matrix(b,3); matrix(b,4)];
                    q_ankle;
                    p_knee;
                    p_hip;
                    help=4;

                elseif matrix(a,3) > matrix(b,3) && matrix(a,4) == matrix(b,4)

                    q_A = [matrix(a,1); matrix(a,2)];
                    q_B = [matrix(b,1); matrix(b,2)];
                    p_A = [matrix(a,3); matrix(a,4)];
                    p_B = [matrix(b,3); matrix(b,4)];
                    q_ankle;
                    p_knee;
                    p_hip;
                    help=5;

                else
```

```
                q_A = [matrix(b,1); matrix(b,2)];
                q_B = [matrix(a,1); matrix(a,2)];
                p_A = [matrix(b,3); matrix(b,4)];
                p_B = [matrix(a,3); matrix(a,4)];
                q_ankle;
                p_knee;
                p_hip;
                help=6;

            end

        end
```

Definition of φ_c, φ_{seat} and φ_{shank}

```
        phi_c = acos(dot((p_hip-p_B),(p_A-p_B))/(norm(p_hip-p_B)*norm(p_A-p_B)));
        phi_seat = atan2((p_A(2)-p_B(2)),(p_A(1)-p_B(1)));
        phi_shank = atan2((p_knee(2)-q_ankle(2)),(p_knee(1)-q_ankle(1)));
```

Create Symbolic Variables

```
        syms l_k l_A l_m l_B l_r l_u l_v l_w
        syms phi_k phi_A phi_m phi_B phi_r phi_u phi_v
```

Calculation of Equations

p_hip - p_B

```
        A1 = [p_hip(1) 1; p_B(1) 1];
        b1 = [p_hip(2); p_B(2)];
        z1 = A1 \ b1;
        syms x
        y1 = z1(1) * x + z1(2);
```

q_A - p_A

```
        A2 = [q_A(1) 1; p_A(1) 1];
        b2 = [q_A(2); p_A(2)];
        z2 = A2 \ b2;
        syms x
        y2= z2(1) * x + z2(2);
```

q_B - p_B

```
        A3 = [q_B(1) 1; p_B(1) 1];
        b3 = [q_B(2); p_B(2)];
        z3 = A3 \ b3;
        syms x
        y3= z3(1) * x + z3(2);
```

p_B - p_A

```
A4 = [p_B(1) 1; p_A(1) 1];
b4 = [p_B(2); p_A(2)];
z4 = A4 \ b4;
syms x
y4= z4(1) * x + z4(2);
```

```
Warning: Matrix is singular to working precision.
```

```
Warning: Matrix is singular to working precision.
```

```
Warning: Matrix is singular to working precision.
```

Point of Intersection between q_A - p_A and q_B - p_B

```
outlier = solve(y2==y3, x);

if ~isempty(outlier) && outlier > q_A(1) && outlier < p_A(1)
    help_outlier = 1;
end
```

Case Differentiation

```
if (z4(1) < 0 && z1(1) < 0 && abs(z4(1)) > abs(z1(1))) || ...
        (z1(1) < 0 && z4(1) > 0) || ...
        (z4(1) > 0 && z1(1) > 0 && z1(1) > z4(1)) || ...
        p_A(1) == p_B(1) || p_A(2) == p_B(2)
```

Four non-linear Equation

```
    f1(l_k,l_A,l_m,l_B,l_r,l_u,l_v,l_w, ...
        phi_k,phi_A,phi_m,phi_B,phi_r,phi_u,phi_v) = ...
        (l_k*cos(phi_k))+(l_A*cos(phi_A))-(l_m*cos(phi_m))-(l_B*cos(phi_B));
    f2(l_k,l_A,l_m,l_B,l_r,l_u,l_v,l_w, ...
        phi_k,phi_A,phi_m,phi_B,phi_r,phi_u,phi_v) = ...
        (l_k*sin(phi_k))+(l_A*sin(phi_A))-(l_m*sin(phi_m))-(l_B*sin(phi_B));
    f3(l_k,l_A,l_m,l_B,l_r,l_u,l_v,l_w, ...
        phi_k,phi_A,phi_m,phi_B,phi_r,phi_u,phi_v) = ...
        (l_B*cos(phi_B))+(l_w*cos(phi_m+phi_c))...
        -(l_v*cos(phi_v))-(l_u*cos(phi_u))-(l_r*cos(phi_r));
    f4(l_k,l_A,l_m,l_B,l_r,l_u,l_v,l_w, ...
        phi_k,phi_A,phi_m,phi_B,phi_r,phi_u,phi_v) = ...
        (l_B*sin(phi_B))+(l_w*sin(phi_m+phi_c))...
        -(l_v*sin(phi_v))-(l_u*sin(phi_u))-(l_r*sin(phi_r));
```

Definiton of Jacobian Matrix

```
    J = [diff(f1,phi_A), diff(f1,phi_B), diff(f1,phi_m), diff(f1,phi_u);
        diff(f2,phi_A), diff(f2,phi_B), diff(f2,phi_m), diff(f2,phi_u);
```

```
        diff(f3,phi_A), diff(f3,phi_B), diff(f3,phi_m), diff(f3,phi_u);
        diff(f4,phi_A), diff(f4,phi_B), diff(f4,phi_m), diff(f4,phi_u)];
```

Help Size

```
k = J^-1 * [f1;f2;f3;f4];
```

Definition of initial Conditions

```
l_k = norm(q_A-q_B);
l_A = norm(p_A-q_A);
l_m = norm(p_A-p_B);
l_B = norm(p_B-q_B);
l_r = norm(q_B-q_ankle);
l_u = norm(p_knee-q_ankle);
l_v = norm(p_hip-p_knee);
l_w = norm(p_hip-p_B);
```

Calculation of φ_{hip}

```
j = 0;
for phi_thigh = alpha:-1:100
    j = j + 1;
    % Angles in radians
    phi_v = phi_thigh*pi/180;
    phi_u = phi_shank;
    phi_m = phi_seat;
    phi_k = atan2((q_A(2)-q_B(2)),(q_A(1)-q_B(1)));
    phi_A = atan2((p_A(2)-q_A(2)),(p_A(1)-q_A(1)));
    phi_B = atan2((p_B(2)-q_B(2)),(p_B(1)-q_B(1)));
    phi_r = atan2((q_ankle(2)-q_B(2)),(q_ankle(1)-q_B(1)));

    for i=1:7
        K = double(k(l_k,l_A,l_m,l_B,l_r,l_u,l_v,l_w,...
            phi_k,phi_A,phi_m,phi_B,phi_r,phi_u,phi_v));
        phi(:,i) = [phi_A;phi_B;phi_m;phi_u] - K; % Newton-Raphson Equation
        phi_deg(:,i) = phi(:,i)*180/pi;

        phi_A = phi(1,i); % Reset phi values for next iteration
        phi_B = phi(2,i);
        phi_m = phi(3,i);
        phi_u = phi(4,i);
    end

    % Save Output in Degrees
    phi_hip(j) = phi_thigh - (phi_m + phi_c)*180/pi;
    PHI(j,:) = [phi_thigh*pi/180,phi_A,phi_B,phi_m,phi_u].*180/pi;
end
phi_hip;
max_phi_hip = max(phi_hip);
min_phi_hip = min(phi_hip);
delta_hip = max_phi_hip-min_phi_hip;
```

```
elseif z4(1) < 0 && z1(1) < 0 && abs(z1(1)) > abs(z4(1))
```

Four non-linear Equation

```
f1(l_k,l_A,l_m,l_B,l_r,l_u,l_v,l_w, ...
    phi_k,phi_A,phi_m,phi_B,phi_r,phi_u,phi_v) = ...
    (l_k*cos(phi_k))+(l_A*cos(phi_A))-(l_m*cos(phi_m))-(l_B*cos(phi_B));
f2(l_k,l_A,l_m,l_B,l_r,l_u,l_v,l_w, ...
    phi_k,phi_A,phi_m,phi_B,phi_r,phi_u,phi_v) = ...
    (l_k*sin(phi_k))+(l_A*sin(phi_A))-(l_m*sin(phi_m))-(l_B*sin(phi_B));
f3(l_k,l_A,l_m,l_B,l_r,l_u,l_v,l_w, ...
    phi_k,phi_A,phi_m,phi_B,phi_r,phi_u,phi_v) = ...
    (l_B*cos(phi_B))+(l_w*cos(phi_m-phi_c))...
    -(l_v*cos(phi_v))-(l_u*cos(phi_u))-(l_r*cos(phi_r));
f4(l_k,l_A,l_m,l_B,l_r,l_u,l_v,l_w, ...
    phi_k,phi_A,phi_m,phi_B,phi_r,phi_u,phi_v) = ...
    (l_B*sin(phi_B))+(l_w*sin(phi_m-phi_c))...
    -(l_v*sin(phi_v))-(l_u*sin(phi_u))-(l_r*sin(phi_r));
```

Definiton of Jacobian Matrix

```
J = [diff(f1,phi_A), diff(f1,phi_B), diff(f1,phi_m), diff(f1,phi_u);
    diff(f2,phi_A), diff(f2,phi_B), diff(f2,phi_m), diff(f2,phi_u);
    diff(f3,phi_A), diff(f3,phi_B), diff(f3,phi_m), diff(f3,phi_u);
    diff(f4,phi_A), diff(f4,phi_B), diff(f4,phi_m), diff(f4,phi_u)];
```

Help Size

```
k = J^-1 * [f1;f2;f3;f4];
```

Define initial Conditions

```
l_k = norm(q_A-q_B);
l_A = norm(p_A-q_A);
l_m = norm(p_A-p_B);
l_B = norm(p_B-q_B);
l_r = norm(q_B-q_ankle);
l_u = norm(p_knee-q_ankle);
l_v = norm(p_hip-p_knee);
l_w = norm(p_hip-p_B);
```

Calculation of φ_{hip}

```
j = 0;
for phi_thigh = alpha:-1:100
    j = j + 1;
    % Angles in radians
    phi_v = phi_thigh*pi/180;
    phi_u = phi_shank;
    phi_m = phi_seat;
    phi_k = atan2((q_A(2)-q_B(2)),(q_A(1)-q_B(1)));
    phi_A = atan2((p_A(2)-q_A(2)),(p_A(1)-q_A(1)));
```

```
                phi_B = atan2((p_B(2)-q_B(2)),(p_B(1)-q_B(1)));
                phi_r = atan2((q_ankle(2)-q_B(2)),(q_ankle(1)-q_B(1)));

                for i=1:7
                    K = double(k(l_k,l_A,l_m,l_B,l_r,l_u,l_v,l_w,...
                        phi_k,phi_A,phi_m,phi_B,phi_r,phi_u,phi_v));
                    phi(:,i) = [phi_A;phi_B;phi_m;phi_u] - K; % Newton-Raphson Equation
                    phi_deg(:,i) = phi(:,i)*180/pi;

                    phi_A = phi(1,i); % Reset phi values for next iteration
                    phi_B = phi(2,i);
                    phi_m = phi(3,i);
                    phi_u = phi(4,i);
                end

                % Save Output in Degrees
                phi_hip(j) = phi_thigh - (phi_m - phi_c)*180/pi;
                PHI(j,:) = [phi_thigh*pi/180,phi_A,phi_B,phi_m,phi_u].*180/pi;
            end
            phi_hip;
            max_phi_hip = max(phi_hip);
            min_phi_hip = min(phi_hip);
            delta_hip = max_phi_hip-min_phi_hip;
```

```
        end
```

Plot

```
        if nargout == 0
            fig=figure;
            plot(PHI(:,1),phi_hip)
            if delta_hip < 20
                axis equal
            end
            grid on
            title('Change of phi_{hip} during STS Movement')
            xlabel('phi_{thigh}')
            ylabel('phi_{hip}')
            set(gca,'XDir','reverse');
        end

        name=strcat('Viergelenk', num2str(a), '.',  num2str(b));

        % Save the Figure
        newFolder = fullfile(pwd, 'NRM');
        NewFolder = fullfile(newFolder, 'p50m');
        if ~exist(NewFolder, 'dir')
            mkdir(NewFolder)
        end
        saveas(fig, fullfile(NewFolder, [(name), '.fig']));
        set(fig, 'PaperPositionMode','auto');
        print(fig, '-dpng', '-r100', fullfile(NewFolder, [name, '.png']));
        close(fig);
```

Classification of the Four Bar Linkages

In this case φ_{shank} in task position 2 and 3 are very similar to the predefined value.

```
            if PHI(floor(alpha)-130+1,5) > 67 && PHI(floor(alpha)-130+1,5) < 73 && ...
                    PHI(floor(alpha)-100+1,5) > 77 && PHI(floor(alpha)-100+1,5) < 83
```

```
                usable = 1;
```

Here φ_{shank} in task position 2 is very similar to the predefined value.

```
            elseif PHI(floor(alpha)-130+1,5) > 67 && PHI(floor(alpha)-130+1,5) < 73
```

```
                usable = 2;
```

Intersection between the two 2R Chains

```
            elseif exist('help_outlier')
```

```
                usable = -1;
                clear help_outlier
```

φ_{shank} in task position 2 and 3 are not similar to the predefined value.

```
            else
                usable = 0;
            end
```

Output of the Results

```
            output_help = [output_help; a b ...
                help phi_hip(1) phi_hip(floor(alpha)-130+1) phi_hip(floor(alpha)-100+1)...
                PHI(1,5) PHI(floor(alpha)-130+1,5) PHI(floor(alpha)-100+1,5)...
                max_phi_hip min_phi_hip delta_hip usable];

            % Sort rows
            output_help_sort = sortrows(output_help, [13 12]);

            output=array2table(output_help_sort, ...
                'VariableNames', {'a', 'b', 'help', ...
                'phi_hip_Pose1', 'phi_hip_Pose2', 'phi_hip_Pose3',...
                'phi_shank_Pose1', 'phi_shank_Pose2', 'phi_shank_Pose3',...
                'max_phi_hip', 'min_phi_hip', 'delta_hip', 'usable'});
```

```
        end
    end

    save('NRM_p50m.mat', 'output')

end
```

```
clear all
```

```
end
```

Published with MATLAB® R2016b

G. MATLAB File: Kinetostatic Analysis of the Lift-Assist Device

Kinetostatics of the Lift-Assist Device

In this function the forces acting on the four-bar linkage are calculated based on the angles phi_a and phi_b found in the function 'ViergelenkBerechnung.m'. NOTE: The execution of this function works only in conjunction with 'ViergelenkBerechnung.m'.

Contents

Overview

```
%   Authors: Kyra Kleine and Samuel Reimer
%   Created: 29th of September 2016
```

```
function [F_A,F_A0,F_B,F_B0,F_P] = KraftberechnungV2
```

Initiate vectors of lift-assist device.

```
q_A  = [14.5;65];
p_A0 = [346;43];
q_B  = [74.5;15];
p_B0 = [371.2;17.4];
q_GF = [29.25;-10.8];

p_0  = [309.579;80];
p_P0 = [177.795;149.725];
p_c0 = [210.506;82.836];

phi_S_max = 145;
[phi_A,phi_B] = ViergelenkBerechnung(q_A,q_B,p_A0,p_B0,phi_S_max);
```

Weight of beam a, b and c.

```
F_a = 2.99;
F_b = 1.86;
F_c = 22.66;
```

Length of beam and other vectors.

```
l_A = norm(p_A0 - q_A);

a = norm(p_A0-p_0);
b = norm(p_B0-p_0);
c = norm(p_c0-p_0);
```

Definition of q_A, q_B, p_A and p_B

```
            if nargin == 0

                if matrix(a,3) > matrix(b,3) && matrix(a,4) > matrix(b,4)

                    q_A = [matrix(a,1); matrix(a,2)];
                    q_B = [matrix(b,1); matrix(b,2)];
                    p_A = [matrix(a,3); matrix(a,4)];
                    p_B = [matrix(b,3); matrix(b,4)];
                    q_ankle;
                    p_knee;
                    p_hip;
                    help=1;

                elseif matrix(a,3) < matrix(b,3) && matrix(a,4) > matrix(b,4)

                    q_A = [matrix(a,1); matrix(a,2)];
                    q_B = [matrix(b,1); matrix(b,2)];
                    p_A = [matrix(a,3); matrix(a,4)];
                    p_B = [matrix(b,3); matrix(b,4)];
                    q_ankle;
                    p_knee;
                    p_hip;
                    help=2;

                elseif matrix(a,3) > matrix(b,3) && matrix(a,4) < matrix(b,4)

                    q_A = [matrix(a,1); matrix(a,2)];
                    q_B = [matrix(b,1); matrix(b,2)];
                    p_A = [matrix(a,3); matrix(a,4)];
                    p_B = [matrix(b,3); matrix(b,4)];
                    q_ankle;
                    p_knee;
                    p_hip;
                    help=3;

               elseif matrix(a,3) == matrix(b,3) && matrix(a,4) > matrix(b,4)

                    q_A = [matrix(a,1); matrix(a,2)];
                    q_B = [matrix(b,1); matrix(b,2)];
                    p_A = [matrix(a,3); matrix(a,4)];
                    p_B = [matrix(b,3); matrix(b,4)];
                    q_ankle;
                    p_knee;
                    p_hip;
                    help=4;

                elseif matrix(a,3) > matrix(b,3) && matrix(a,4) == matrix(b,4)

                    q_A = [matrix(a,1); matrix(a,2)];
                    q_B = [matrix(b,1); matrix(b,2)];
                    p_A = [matrix(a,3); matrix(a,4)];
                    p_B = [matrix(b,3); matrix(b,4)];
                    q_ankle;
                    p_knee;
                    p_hip;
                    help=5;

                else
```

```
                q_A = [matrix(b,1); matrix(b,2)];
                q_B = [matrix(a,1); matrix(a,2)];
                p_A = [matrix(b,3); matrix(b,4)];
                p_B = [matrix(a,3); matrix(a,4)];
                q_ankle;
                p_knee;
                p_hip;
                help=6;

            end

        end
```

Definition of φ_c, φ_{seat} and φ_{shank}

```
        phi_c = acos(dot((p_hip-p_B),(p_A-p_B))/(norm(p_hip-p_B)*norm(p_A-p_B)));
        phi_seat = atan2((p_A(2)-p_B(2)),(p_A(1)-p_B(1)));
        phi_shank = atan2((p_knee(2)-q_ankle(2)),(p_knee(1)-q_ankle(1)));
```

Create Symbolic Variables

```
        syms l_k l_A l_m l_B l_r l_u l_v l_w
        syms phi_k phi_A phi_m phi_B phi_r phi_u phi_v
```

Calculation of Equations

p_hip - p_B

```
        A1 = [p_hip(1) 1; p_B(1) 1];
        b1 = [p_hip(2); p_B(2)];
        z1 = A1 \ b1;
        syms x
        y1 = z1(1) * x + z1(2);
```

q_A - p_A

```
        A2 = [q_A(1) 1; p_A(1) 1];
        b2 = [q_A(2); p_A(2)];
        z2 = A2 \ b2;
        syms x
        y2= z2(1) * x + z2(2);
```

q_B - p_B

```
        A3 = [q_B(1) 1; p_B(1) 1];
        b3 = [q_B(2); p_B(2)];
        z3 = A3 \ b3;
        syms x
        y3= z3(1) * x + z3(2);
```

p_B - p_A

```
A4 = [p_B(1) 1; p_A(1) 1];
b4 = [p_B(2); p_A(2)];
z4 = A4 \ b4;
syms x
y4= z4(1) * x + z4(2);
```

```
Warning: Matrix is singular to working precision.
```

```
Warning: Matrix is singular to working precision.
```

```
Warning: Matrix is singular to working precision.
```

Point of Intersection between q_A - p_A and q_B - p_B

```
outlier = solve(y2==y3, x);

if ~isempty(outlier) && outlier > q_A(1) && outlier < p_A(1)
    help_outlier = 1;
end
```

Case Differentiation

```
if (z4(1) < 0 && z1(1) < 0 && abs(z4(1)) > abs(z1(1))) || ...
        (z1(1) < 0 && z4(1) > 0) || ...
        (z4(1) > 0 && z1(1) > 0 && z1(1) > z4(1)) || ...
        p_A(1) == p_B(1) || p_A(2) == p_B(2)
```

Four non-linear Equation

```
    f1(l_k,l_A,l_m,l_B,l_r,l_u,l_v,l_w, ...
        phi_k,phi_A,phi_m,phi_B,phi_r,phi_u,phi_v) = ...
        (l_k*cos(phi_k))+(l_A*cos(phi_A))-(l_m*cos(phi_m))-(l_B*cos(phi_B));
    f2(l_k,l_A,l_m,l_B,l_r,l_u,l_v,l_w, ...
        phi_k,phi_A,phi_m,phi_B,phi_r,phi_u,phi_v) = ...
        (l_k*sin(phi_k))+(l_A*sin(phi_A))-(l_m*sin(phi_m))-(l_B*sin(phi_B));
    f3(l_k,l_A,l_m,l_B,l_r,l_u,l_v,l_w, ...
        phi_k,phi_A,phi_m,phi_B,phi_r,phi_u,phi_v) = ...
        (l_B*cos(phi_B))+(l_w*cos(phi_m+phi_c))...
        -(l_v*cos(phi_v))-(l_u*cos(phi_u))-(l_r*cos(phi_r));
    f4(l_k,l_A,l_m,l_B,l_r,l_u,l_v,l_w, ...
        phi_k,phi_A,phi_m,phi_B,phi_r,phi_u,phi_v) = ...
        (l_B*sin(phi_B))+(l_w*sin(phi_m+phi_c))...
        -(l_v*sin(phi_v))-(l_u*sin(phi_u))-(l_r*sin(phi_r));
```

Definiton of Jacobian Matrix

```
    J = [diff(f1,phi_A), diff(f1,phi_B), diff(f1,phi_m), diff(f1,phi_u);
        diff(f2,phi_A), diff(f2,phi_B), diff(f2,phi_m), diff(f2,phi_u);
```

```
        diff(f3,phi_A), diff(f3,phi_B), diff(f3,phi_m), diff(f3,phi_u);
        diff(f4,phi_A), diff(f4,phi_B), diff(f4,phi_m), diff(f4,phi_u)];
```

Help Size

```
k = J^-1 * [f1;f2;f3;f4];
```

Definition of initial Conditions

```
l_k = norm(q_A-q_B);
l_A = norm(p_A-q_A);
l_m = norm(p_A-p_B);
l_B = norm(p_B-q_B);
l_r = norm(q_B-q_ankle);
l_u = norm(p_knee-q_ankle);
l_v = norm(p_hip-p_knee);
l_w = norm(p_hip-p_B);
```

Calculation of φ_{hip}

```
j = 0;
for phi_thigh = alpha:-1:100
    j = j + 1;
    % Angles in radians
    phi_v = phi_thigh*pi/180;
    phi_u = phi_shank;
    phi_m = phi_seat;
    phi_k = atan2((q_A(2)-q_B(2)),(q_A(1)-q_B(1)));
    phi_A = atan2((p_A(2)-q_A(2)),(p_A(1)-q_A(1)));
    phi_B = atan2((p_B(2)-q_B(2)),(p_B(1)-q_B(1)));
    phi_r = atan2((q_ankle(2)-q_B(2)),(q_ankle(1)-q_B(1)));

    for i=1:7
        K = double(k(l_k,l_A,l_m,l_B,l_r,l_u,l_v,l_w,...
            phi_k,phi_A,phi_m,phi_B,phi_r,phi_u,phi_v));
        phi(:,i) = [phi_A;phi_B;phi_m;phi_u] - K; % Newton-Raphson Equation
        phi_deg(:,i) = phi(:,i)*180/pi;

        phi_A = phi(1,i); % Reset phi values for next iteration
        phi_B = phi(2,i);
        phi_m = phi(3,i);
        phi_u = phi(4,i);
    end

    % Save Output in Degrees
    phi_hip(j) = phi_thigh - (phi_m + phi_c)*180/pi;
    PHI(j,:) = [phi_thigh*pi/180,phi_A,phi_B,phi_m,phi_u].*180/pi;
end
phi_hip;
max_phi_hip = max(phi_hip);
min_phi_hip = min(phi_hip);
delta_hip = max_phi_hip-min_phi_hip;
```

```
elseif z4(1) < 0 && z1(1) < 0 && abs(z1(1)) > abs(z4(1))
```

Four non-linear Equation

```
f1(l_k,l_A,l_m,l_B,l_r,l_u,l_v,l_w, ...
    phi_k,phi_A,phi_m,phi_B,phi_r,phi_u,phi_v) = ...
    (l_k*cos(phi_k))+(l_A*cos(phi_A))-(l_m*cos(phi_m))-(l_B*cos(phi_B));
f2(l_k,l_A,l_m,l_B,l_r,l_u,l_v,l_w, ...
    phi_k,phi_A,phi_m,phi_B,phi_r,phi_u,phi_v) = ...
    (l_k*sin(phi_k))+(l_A*sin(phi_A))-(l_m*sin(phi_m))-(l_B*sin(phi_B));
f3(l_k,l_A,l_m,l_B,l_r,l_u,l_v,l_w, ...
    phi_k,phi_A,phi_m,phi_B,phi_r,phi_u,phi_v) = ...
    (l_B*cos(phi_B))+(l_w*cos(phi_m-phi_c))...
    -(l_v*cos(phi_v))-(l_u*cos(phi_u))-(l_r*cos(phi_r));
f4(l_k,l_A,l_m,l_B,l_r,l_u,l_v,l_w, ...
    phi_k,phi_A,phi_m,phi_B,phi_r,phi_u,phi_v) = ...
    (l_B*sin(phi_B))+(l_w*sin(phi_m-phi_c))...
    -(l_v*sin(phi_v))-(l_u*sin(phi_u))-(l_r*sin(phi_r));
```

Definiton of Jacobian Matrix

```
J = [diff(f1,phi_A), diff(f1,phi_B), diff(f1,phi_m), diff(f1,phi_u);
    diff(f2,phi_A), diff(f2,phi_B), diff(f2,phi_m), diff(f2,phi_u);
    diff(f3,phi_A), diff(f3,phi_B), diff(f3,phi_m), diff(f3,phi_u);
    diff(f4,phi_A), diff(f4,phi_B), diff(f4,phi_m), diff(f4,phi_u)];
```

Help Size

```
k = J^-1 * [f1;f2;f3;f4];
```

Define initial Conditions

```
l_k = norm(q_A-q_B);
l_A = norm(p_A-q_A);
l_m = norm(p_A-p_B);
l_B = norm(p_B-q_B);
l_r = norm(q_B-q_ankle);
l_u = norm(p_knee-q_ankle);
l_v = norm(p_hip-p_knee);
l_w = norm(p_hip-p_B);
```

Calculation of φ_{hip}

```
j = 0;
for phi_thigh = alpha:-1:100
    j = j + 1;
    % Angles in radians
    phi_v = phi_thigh*pi/180;
    phi_u = phi_shank;
    phi_m = phi_seat;
    phi_k = atan2((q_A(2)-q_B(2)),(q_A(1)-q_B(1)));
    phi_A = atan2((p_A(2)-q_A(2)),(p_A(1)-q_A(1)));
```

```
                phi_B = atan2((p_B(2)-q_B(2)),(p_B(1)-q_B(1)));
                phi_r = atan2((q_ankle(2)-q_B(2)),(q_ankle(1)-q_B(1)));

                for i=1:7
                    K = double(k(l_k,l_A,l_m,l_B,l_r,l_u,l_v,l_w,...
                        phi_k,phi_A,phi_m,phi_B,phi_r,phi_u,phi_v));
                    phi(:,i) = [phi_A;phi_B;phi_m;phi_u] - K; % Newton-Raphson Equation
                    phi_deg(:,i) = phi(:,i)*180/pi;

                    phi_A = phi(1,i); % Reset phi values for next iteration
                    phi_B = phi(2,i);
                    phi_m = phi(3,i);
                    phi_u = phi(4,i);
                end

                % Save Output in Degrees
                phi_hip(j) = phi_thigh - (phi_m - phi_c)*180/pi;
                PHI(j,:) = [phi_thigh*pi/180,phi_A,phi_B,phi_m,phi_u].*180/pi;
            end
            phi_hip;
            max_phi_hip = max(phi_hip);
            min_phi_hip = min(phi_hip);
            delta_hip = max_phi_hip-min_phi_hip;
```

```
        end
```

Plot

```
        if nargout == 0
            fig=figure;
            plot(PHI(:,1),phi_hip)
            if delta_hip < 20
                axis equal
            end
            grid on
            title('Change of phi_{hip} during STS Movement')
            xlabel('phi_{thigh}')
            ylabel('phi_{hip}')
            set(gca,'XDir','reverse');
        end

        name=strcat('Viergelenk', num2str(a), '.',  num2str(b));

        % Save the Figure
        newFolder = fullfile(pwd, 'NRM');
        NewFolder = fullfile(newFolder, 'p50m');
        if ~exist(NewFolder, 'dir')
            mkdir(NewFolder)
        end
        saveas(fig, fullfile(NewFolder, [(name), '.fig']));
        set(fig, 'PaperPositionMode','auto');
        print(fig, '-dpng', '-r100', fullfile(NewFolder, [name, '.png']));
        close(fig);
```

Classification of the Four Bar Linkages

In this case φ_{khank} in task position 2 and 3 are very similar to the predefined value.

```
            if PHI(floor(alpha)-130+1,5) > 67 && PHI(floor(alpha)-130+1,5) < 73 && ...
                    PHI(floor(alpha)-100+1,5) > 77 && PHI(floor(alpha)-100+1,5) < 83
```

```
                usable = 1;
```

Here φ_{shank} in task position 2 is very similar to the predefined value.

```
            elseif PHI(floor(alpha)-130+1,5) > 67 && PHI(floor(alpha)-130+1,5) < 73
```

```
                usable = 2;
```

Intersection between the two 2R Chains

```
            elseif exist('help_outlier')
```

```
                usable = -1;
                clear help_outlier
```

φ_{shank} in task position 2 and 3 are not similar to the predefined value.

```
            else
                usable = 0;
            end
```

Output of the Results

```
            output_help = [output_help; a b ...
                help phi_hip(1) phi_hip(floor(alpha)-130+1) phi_hip(floor(alpha)-100+1)...
                PHI(1,5) PHI(floor(alpha)-130+1,5) PHI(floor(alpha)-100+1,5)...
                max_phi_hip min_phi_hip delta_hip usable];

            % Sort rows
            output_help_sort = sortrows(output_help, [13 12]);

            output=array2table(output_help_sort, ...
                'VariableNames', {'a', 'b', 'help', ...
                'phi_hip_Pose1', 'phi_hip_Pose2', 'phi_hip_Pose3',...
                'phi_shank_Pose1', 'phi_shank_Pose2', 'phi_shank_Pose3',...
                'max_phi_hip', 'min_phi_hip', 'delta_hip', 'usable'});
```

```
        end
    end

    save('NRM_p50m.mat', 'output')

end
```

```
clear all
```

```
end
```

Published with MATLAB® R2016b

H. Questionnaire for the Modular Lift-Assist Prototype

Technische Universität München
Fakultät für Maschinenwesen
Lehrstuhl für Mikrotechnik und Medizingerätetechnik
Univ.-Prof. Dr. Tim C. Lüth

Datenprotokoll: Modularer Einsatz einer Aufstehhilfe

Bogennr.: Datum:

Persönliche Informationen über den Probanden:

Geschlecht: ☐ Weiblich ☐ Männlich

Name: .....

Körpergewicht: ..... kg

Körpergröße: ..... cm

Alter: ..... Jahre

☐ Gewichtsklasse I 45kg - 57kg ☐ Gewichtsklasse II 58kg – 70kg ☐ Gewichtsklasse III 71kg - 81kg ☐ Gewichtsklasse IV 82kg - 92kg

Das Hinsetzen bzw. Aufstehen erfolgt/ist grundsätzlich:
- ☐ ...ohne Schwierigkeiten.
- ☐ ...mit Schwierigkeiten aber ohne Hilfe.
- ☐ ...mit einem Hilfsmittel.
- ☐ ...mit Hilfe einer Pflegekraft.
- ☐ ...mit Hilfe einer Pflegekraft und Hilfsmittel.
- ☐ ...unmöglich.

Optimierte Einstellung der modularen Aufstehhilfe:

Korrektur der Gewichtsklasse (Betreuer): ☐ Nein ☐ Ja, Gewichtsklasse .....

Bei optimiertem Moduleinsatz ist Aufstehen möglich: ☐ ohne Hilfe ☐ mit Hilfe ☐ gar nicht

Sonstige Kommentare:

.....

.....

.....

Evaluierungsbogen: Modularer Einsatz einer Aufstehhilfe

Ihre Daten werden streng vertraulich und anonymisiert verarbeitet.

Fragen an den Probanden:

1. Sie fühlen sich bei Anwendung der Aufstehhilfe gegen seitliches Wegkippen ausreichend gesichert.

Ich stimme überhaupt nicht zu	1	2	3	4	5	Ich stimme voll zu

2. Sie werden durch die Aufstehhilfe in eine stabile Standposition gebracht.

Ich stimme überhaupt nicht zu	1	2	3	4	5	Ich stimme voll zu

3. Sie fühlen sich beim Hinsetzen beim Erreichen der Sitzposition ausreichend abgefedert.

Ich stimme überhaupt nicht zu	1	2	3	4	5	Ich stimme voll zu

4. Die Aufstehhilfe ist einfach zu bedienen.

Ich stimme überhaupt nicht zu	1	2	3	4	5	Ich stimme voll zu

5. Die Aufstehhilfe annimiert Sie öfters aufzustehen.

Ich stimme überhaupt nicht zu	1	2	3	4	5	Ich stimme voll zu

6. Die Aufstehhilfe erlaubt es Ihnen, selbstständig ohne Anwesenheit einer Pflegekraft aufzustehen.

Ich stimme überhaupt nicht zu	1	2	3	4	5	Ich stimme voll zu

7. Sie fühlen sich durch die Aufstehhilfe beim **Hinsetzen** im Vergleich zum normalen Stuhl unterstützt.

Ich stimme überhaupt nicht zu	1	2	3	4	5	Ich stimme voll zu

8. Sie fühlen sich durch die Aufstehhilfe beim **Aufstehen** im Vergleich zum normalen Stuhl unterstützt.

Ich stimme überhaupt nicht zu	1	2	3	4	5	Ich stimme voll zu

Frage an die Pflegekraft:

Die Anwendung der Aufstehhilfe führt zu einer Unterstützung bei Ihrer Pflegetätigkeit.

Ich stimme überhaupt nicht zu	1	2	3	4	5	Ich stimme voll zu

Vielen Dank für ihre Unterstützung!

Technische Universität München · Lehrstuhl für Mikrotechnik und Medizingerätetechnik (Leitung : o. Prof. Dr. Tim C. Lüth)
Boltzmannstraße 15, 85748 Garching bei München · Tel.: 089-289-15191 · Fax.: 089 289-15192 · www.mimed.de
Sekretariat: Renate Heuser (Tel.: Tel.: 089-289-15190)